The Study of Epidermal Growth Factor Receptor, ^{99m}Technetium-depreotide, and Tumour Markers in the Management of Neuroendocrine Tumours

by

Tahir H Shah

A thesis submitted to University College London for the degree of Doctor of Medicine (Res)

January 2009

Neuroendocrine Tumour Unit

&

Department of Oncology

Royal Free and University College Medical School

&

University College London

91 Riding House Street, London W1W 7B

I, Tahir H Shah, confirm that the work presented in this thesis is my own. Where information has been derived from other sources, I confirm that this has been indicated in the thesis.

ABSTRACT

Purpose: Neuroendocrine Tumours (NETs) are rare and therefore poorly understood. Their slow progression and general poor response to standard chemotherapy regimes implies that their tumour biology is significantly different from most common cancers. There have been major advances in the past few decades in the diagnosis and management of these tumours which are perceived to be associated with improvements in quality and length of life. However, since most NETs have metastasised extensively by the time of diagnosis it is a major challenge indeed to try and effect tumour regression – the ultimate goal of any anti-cancer therapy.

Chapters: 2 & 3: The epidermal growth factor receptor (EGFR) is commonly expressed in human tumours and provides an important target for therapy. Several classes of agents including small molecule inhibitors and antibodies are currently under clinical evaluation. These agents have shown interaction with chemotherapeutic agents *in vitro* and *in vivo*. However, the mechanisms of these interactions are not clearly understood, particularly in regards to NETs. The purpose of this study was to investigate the expression of EGFR in NET tissue and to determine its mechanisms of action, as well as the effects of modulation of EGFR activation.

Experimental Design (Chapter 2): Paraffin-embedded tumour tissue was available from 98 patients with NETs (39 foregut, 42 midgut, four hindgut, five paragangliomas, and four of unknown origin). Immunohistochemical evaluation was performed for the expression of EGFR, p-EGFR, p-Akt, and p-ERK1/2.

Results: Ninety-six percent of tumour samples were positive for EGFR expression; 63% were positive for activated EGFR; 76% were positive for activated Akt; and 96% were positive for activated ERK1/2. Importantly, the histological score for the activation of Akt and ERK1/2 correlated with the histological score for activated EGFR. These data provide a rationale for considering EGFR inhibitors in the treatment of NETs. Additionally, direct inhibition of Akt and ERK1/2 may provide further therapeutic options in the treatment of NETs in the future.

Experimental Design (Chapter 3): The effects of the EGFR inhibitors gefitinib and erbitux were determined in several NET cell lines. The modulation of DNA-PK activity

by these agents was quantitated using a variety of techniques including immunoprecipitations, immunoblotting, cellular fraction extractions and immunohistochemistry.

Results: Prolonged EGFR inhibition leads to reduction in DNAPK$_{CS}$ concentration in all tested NET cell lines except RIN, which displays the lowest levels of EGFR expression. This reduction in DNAPK$_{CS}$ is likely to lead to sensitisation of NET cells to ionising radiation, which causes double-strand DNA breaks, DNAPK$_{CS}$ being crucial to their repair.

There are direct EGFR/DNAPK$_{CS}$ interactions in NET cell lines, which can be enhanced by EGFR inhibition.

EGFR inhibition leads to transfer of DNAPK$_{CS}$ from the nucleus to the cytoplasm in SHP and BON cell lines but not in CRI, RIN, or NCI cell lines. This difference in the observed outcomes may be due to the lack of or mutations in intermediary proteins, though proof is needed for this hypothesis. The re-distribution of DNAPK$_{CS}$ is likely to lead to sensitisation of NET cells to ionising radiation, which causes double-strand DNA breaks, DNAPK$_{CS}$ being crucial to their repair.

Chapter 4: Surgery is at present the only therapy with the possibility of achieving a cure. Therefore optimising diagnostic modalities in order to discover the tumours early or to discover all the tumour lesions prior to surgery would be of use. The purpose of this project was to assess the role of ^{99m}Tc-depreotide in patients with negative or weakly positive OctreoScan® (Krenning score ≤ 1; measured on a scale range 0-4). To determine the usefulness of ^{99m}Tc-depreotide scintigraphy for highlighting lesions that may be missed by OctreoScan® and/or CT/MRI imaging.

Experimental Design: Prospective analysis of 25 NET patients, with negative or weakly positive ^{111}In-pentetreotide scans, who were consecutively enrolled to undergo ^{111}In-pentetreotide and ^{99m}Tc-depreotide imaging. The results were compared with either CT or MRI scans.

Results: Histology was available for 20 of 25 patients: of these 40% had high grade tumours (cellular proliferation marker Ki67 score > 20%), a further 35% had intermediate grade tumours (Ki67 2-20%), and the remainder 25% had low grade tumours (Ki67<2%). 52% of patients had completely negative and 48% had weakly positive OctreoScan®. 32% of these same patients had significantly positive [99m]mTc-

depreotide scans (Krenning score ≥ 2), with the histology demonstrating intermediate or high grade tumours.

Chapter 5: Some NETs follow an indolent course compared to others which display a rapidly progressive course with only short-lived response to therapy. Being able to confidently predict the long-term prognosis is obviously desirable. The aims of this project were to determine the diagnostic and prognostic value of serum alpha-fetoprotein (AFP) and human chorionic gonadotrophin beta (hCGβ) in NETs.

Patients and methods: a database containing biochemical, histological, and survival data on 360 NET patients was constructed. This data was statistically assessed, using SPSS statistics package, to determine the utility of commonly measured tumour markers with particular emphasis on AFP and hCGβ.

Results: AFP and hCGβ were raised in 9.5% and 12.3% of patients respectively, and jointly raised in 9.1% of patients in whom it was measured. AFP levels associated strongly and positively with tumour grade, serum CgA, hCGβ levels and worse survival. hCGβ levels also associated strongly and positively with serum CgA, AFP levels and worsening survival.

ACKNOWLEDGEMENTS

COMMUNICATIONS

PRESENTATIONS

European Neuroendocrine Tumour Society annual conference 2006: Effect of cisplatin and ionizing radiation on epidermal growth factor receptor in neuroendocrine tumor cell lines.

PUBLICATIONS

T. Shah, M. E. Caplin et al. The role of alpha fetoprotein and β-human chorionic gonadotrophin as tumour markers in neuroendocrine tumours. Br J Cancer. 2008; 99: 72-7.

T Shah, D Hochhauser, R Frow, A Quaglia, A Dhillon, M Caplin.
EGFR expression and activation in neuroendocrine tumours. J Neuroendocrinology 2006: 18; 355 – 360.

T. Shah, J. Buscombe, D Hochhauser, M. Caplin. The role of ^{99}Tc-depreotide in neuroendocrine tumour imaging. Nuclear Medicine Communications 2008 May;29(5):436-40.

B J Friedmann, M Caplin, B Savic, **T Shah,** C J Lord, A Ashworth, J A Hartley, D Hochhauser.Interaction of the epidermal growth factor receptor and the DNA-dependant protein kinase pathway following gefitinib treatment.
Molecular Cancer Therapeutics 2006: 5(2); 209 – 217.

AWAITING SUBMISSION

Expression of ErbB family of receptors in neuroendocrine tumour tissue.
Srirajaskanthan R, **Shah T**, Caplin ME.

Consequences of EGFR activation and their relation to survival outcomes in neuroendocrine tumour patients. **Shah T**, Srirajaskanthan R, Caplin ME.

TABLE OF CONTENTS

INDEX OF FIGURES

INDEX OF TABLES

ABBREVIATIONS

ATP	Adenosine Triphosphate
BSA	Bovine Serum Albumin
CDK	Cyclin-Dependent Kinase
DMSO	Dimethylsulphoxide
DNA	Deoxyribonucleic Acid
DNA-PK	DNA Protein Kinase
DNA-PK$_{CS}$	DNA Protein Kinase Catalytic Subunit
DSB	Double Strand Break
DTT	Dithiothreitol
ECACC	European Collection of Cell Cultures
ECL	Enhanced Chemoilluminescence
EDTA	Ethylenediaminesulphate Tetra-acetic acid
EGF	Epidermal Growth Factor
EGFR	Epidermal Growth Factor Receptor
EtBr	Ethidium Bromide
FCS	Foetal Calf Serum
FITC	Fluorescein Iothiocyanate
HR	Homologous Recombination
IMS	Industrial methylated spirit
kDa	kiloDaltons
MAb	Monoclonal antibody
MAPK	Mitogen Activated Protein Kinase
MMR	Mismatch Repair
NER	Nucleotide Excision Repair
NET	Neuroendocrine Tumour
NHEJ	Non-Homologous End Joining
NSCLC	Non Small Cell Lung Cancer
OD	Optical Density
PBS	Phosphate Buffered Saline
PI	Propidium Iodide
PI3K	Phosphatidylinositol 3-Kinase
PKC	Protein Kinase C

RTK	Receptor Tyrosine Kinase
SDS	Sodium Dodecylsulphate
SRB	Sulphorhodamine B
SSB	Single Strand Break
STAT	Signal Transducer and Activator of Transcription
TBE	Tris-borate-EDTA
TBS	Tris buffered saline
TBS-T	Tris buffered saline Tween
TCR	Transcription Coupled Repair
TE	Tris-EDTA
TEMED	Tetramethylethylenediamine
TKI	Tyrosine Kinase Inhibitor
VEGF	Vascular Endothelial Growth Factor

CHAPTER 1

INTRODUCTION

1.1   *Neuroendocrine Tumours (NETs)*

The neuroendocrine system consists of neuronal cells in the central and peripheral nervous system, endocrine cells disseminated in the mucosa of hollow organs, and endocrine cells in the classical endocrine glands. Greater than a dozen neuroendocrine cells have been described in humans, sharing common morphological, biochemical, and ultra-structural features. Malignant transformation of these cells may give rise to a variety of tumours (fig 1.1) (Hofsli E 2006).
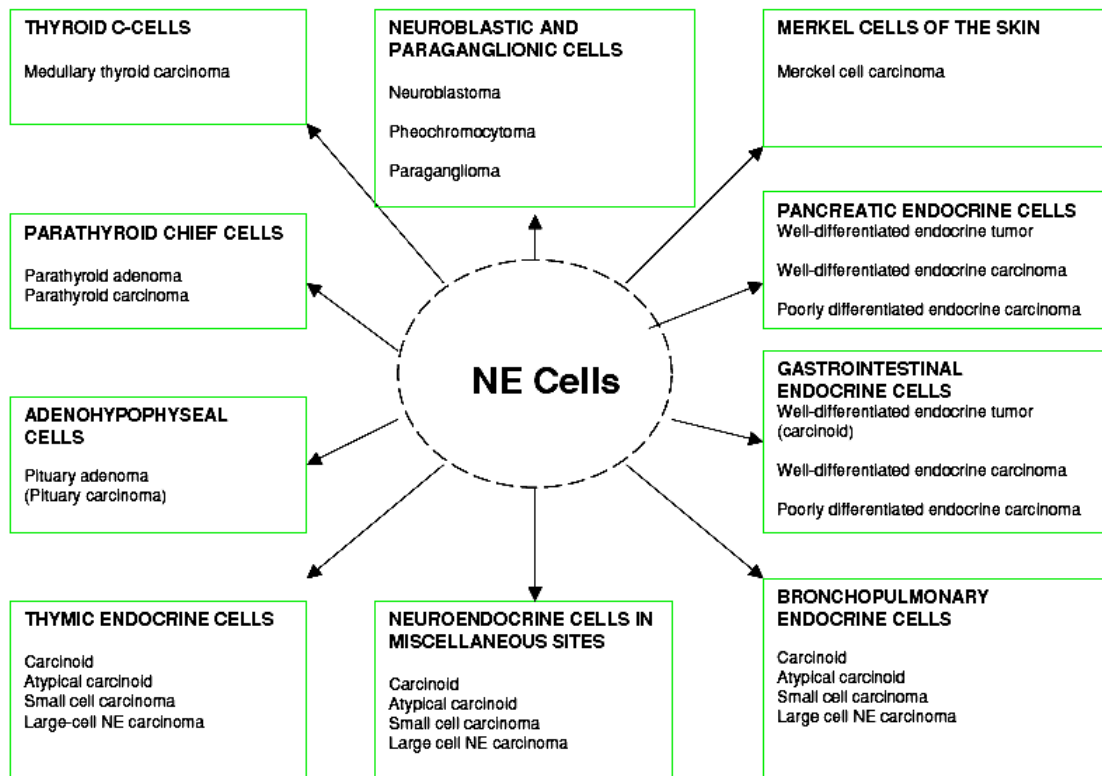
Figure 1.1: Malignant transformation of the body's neuroendocrine cells can give rise to a variety of neuroendocrine tumours.

Despite the low incidence of NETs, their prevalence is relatively high, reflecting their lower malignant potential compared to the common epithelial cancers, a higher grade of differentiation, and a slower growth rate (Hofsli E 2006).

Diagnosis of neuroendocrine tumours is often delayed as their presentation is similar to common conditions such as irritable bowel syndrome. Diagnosis is rarely made clinically and usually requires sophisticated laboratory and imaging techniques. In some cases, multiple peptides or hormones are responsible for symptoms or syndromic features, and several organs and/or multiple tumours may be involved in the disease state, confounding the clinical diagnosis. However, the secretory products these tumours

make, and the clinical syndromes that are subsequently produced, can be used to classify these gastroenteropancreatic or neuroendocrine tumours (table 1.1).

Table 1.1
Classification and leading symptoms of the most frequent endocrine tumours of the gastrointestinal tract. (Arnold R[a] 2005)

Name (syndrome)	Leading symptoms	Hormone responsible	Other hormones in the tumour	Malignancy (%)	Localisation of primary	Extra-pancreatic localization
Insulinoma	Hypoglycaemia	Insulin	Glucagon, PP	5–10	Pancreas	Very rare
Gastrinoma (Zollinger–Ellison syndrome)	Peptic ulcers, diarrhoea, reflux disease	Gastrin	Insulin, PP, glucagon, ACTH, somatostatin, chromogranin A	>90	Pancreas	Duodenum, stomach, mesentery
Carcinoid syndrome	Flushing, diarrhoea, bronchial obstruction	Serotonin	Tachykinins, prostaglandins, chromogranin A	100	Ileum	Pancreas (rare)
VIPoma (Verner-Morrison syndrome), pancreatic cholera	Intractable diarrhoea, hypokalaemia	VIP, PHI	PP, glucagon, somatostatin, chromogranin A	75	Pancreas	
Glucagonoma	Erythema necrolyticans migrans, diabetes	Glucagon	PP, insulin, somatostatin, chromogranin A	50	Pancreas	Rare
Somato-statinoma	Diabetes, steatorrhoea, gallstones	Somatostatin	PP, insulin, calcitonin	50	Pancreas	Duodenum

ACTH - Adrenocorticotrophic hormone;
CRH - corticotrophin-releasing hormone;
GHRH - growth hormone-releasing hormone;
PHI - peptide histidine isoleucine;
PP - pancreatic peptide;
VIP - vasoactive intestinal polypeptide.

1.1.1 Incidence and Mortality

The data from 6 European countries and USA demonstrates that neuroendocrine tumours (table 1.2) are rare with an incidence of 2 to 4 per 100,000, with the lowest incidence in Italy, the region of Tuscany, and the highest in the USA, especially among the black population. In Europe, there is slightly increased preponderance of women, although this may just reflect the increased use of laparoscopy for pelvic conditions leading to increased discovery of NETs (table 1.2). (Taal BG 2004)

Year of publication	Study period	Country	Men	Women
1994 [5]	1979–1987 1980–1989	UK and Scotland	0.71	0.87
1995 [6]	1978–1981	Denmark	1.1	1.1
1997 [7]	1985–1991	Italy (Tuscany)	0.65	0.65
2000 [8]	1974–1997	Switzerland (Vaud)	2.24	2.65
2001 [9]	1989–1996	Netherlands	1.8	1.9
2001 [10]	1983–1998	Sweden	2.0	2.4
2003 [11]	1973–1994	USA (SEER study)	2.47 white 4.18 black	2.58 black 3.98 white

Table 1.2: Age-standardised incidence of neuroendocrine tumours per 100,000 inhabitants (Taal BG 2004)

Site	Loco-regional	Distant metastases	Unknown	Total number	Percent-age
Head and neck	17	1	5	23	1
Stomach	69	9	26	104	4
Small bowel	197	90	62	349	15
Appendix	575	10	69	654	27
Colon	81	44	10	135	6
Rectum	118	10	8	136	6
Pancreas	28	29	11	68	3
Other gastrointestinal	23	10	13	46	2
Lung/mediastinum	467	26	49	542	23
Urogenital	21	4	2	27	1
Other sites	16	2	0	18	1
Unknown	0	289	0	289	12
All sites	1,612	524	255	2,391	

Table 1.3. Primary site and stage of carcinoid tumours in the Netherlands, 1989-1996 (Taal BG 2004)

Carcinoid tumours account for more than half the incidence of NETs (figure 1.2). They also account for 13 – 34% of all tumours of the small bowel and 17 – 46% of all malignant tumours of the small bowel. They derive from primitive stem cells known as enterochromaffin cells which are generally found in the gut wall. Carcinoids may also occur in the bronchus, pancreas, rectum, ovary, lung, and elsewhere. They frequently metastasize to the regional lymph nodes, liver, and less commonly, to the bones. The likelihood of metastases is related to the size of the tumour so that the incidence of metastases is less than 15% for tumours smaller than 1cm but rises to 95% for tumours greater than 2cm (Vinik AI et al).
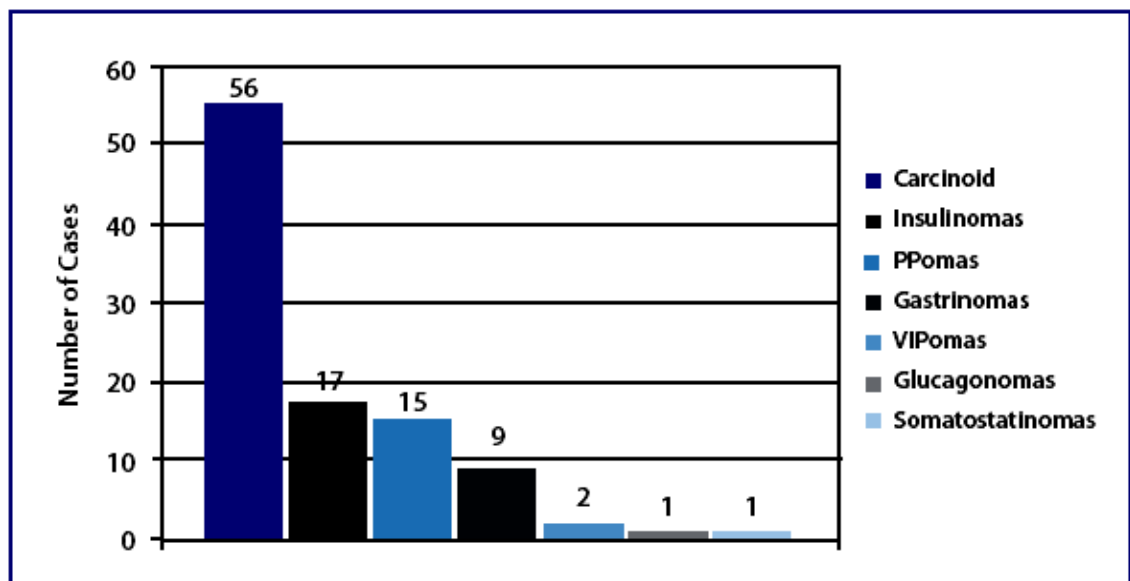
Figure 1.2 Neuroendocrine tumours of the gastrointestinal tract: Annual incidence 10 cases per million (from Vinik AI et al. Neoplasms of the gastroenteropancreatic endocrine system. In: Holland JF, Bast JR Jr, Morton DL et al, eds. Cancer Medicine, Vol 1, 4th ed. Baltimore: Williams and Wilkins; 1997: 1605-41.)

Carcinoid patients invariably have a long history of vague abdominal symptoms. These symptoms persist with a median latency to correct diagnosis of greater than 9 years by which time the tumour has metastasized, causing flushing and diarrhoea and slow but relentless progression to the patient's death (fig 1.3).
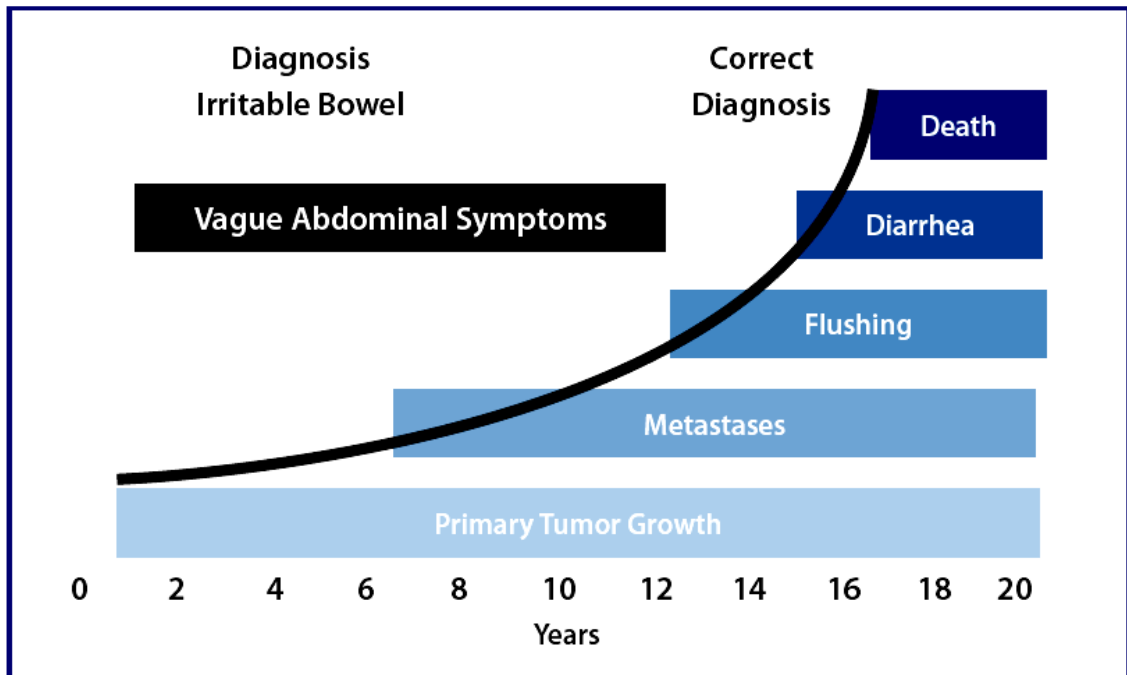
Figure 1.3: Natural history of carcinoid tumours (from Vinik AI et al. Use of somatostatin analog in the management of carcinoid syndrome. Am J Dig Dis Sci. 34: 14-27, 1989.)

In general, the 5-year survival from neuroendocrine tumours is superior to that from metastatic adenocarcinoma, and has significantly improved in recent years. In the Netherlands, patients treated from 1992 onwards fared better than those treated between 1980 and 1991. This may be due to the wide availability of octreotide since 1992, whereas the continued positive trend (fig. 1.4) may be related to better supportive care.
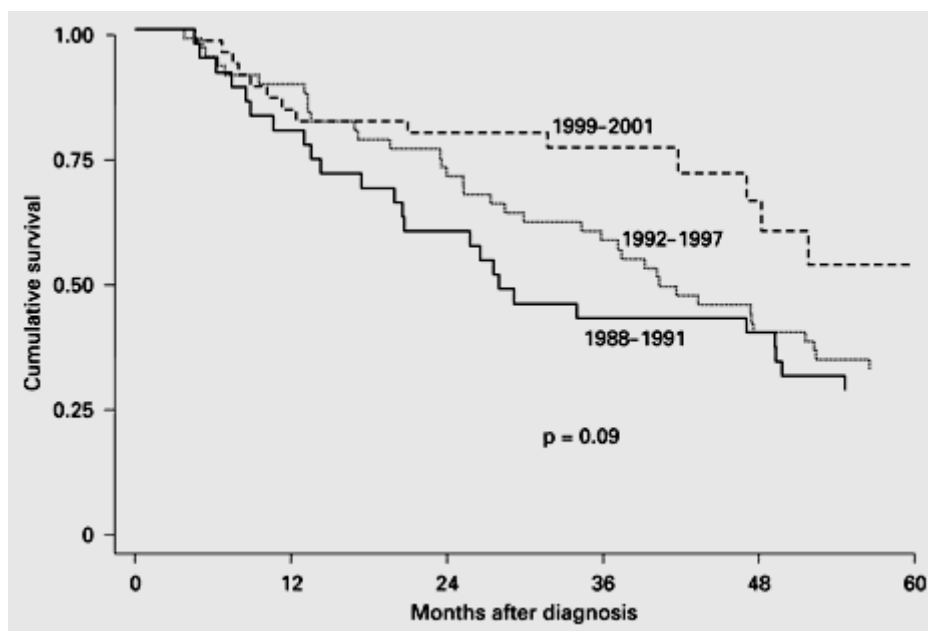
Fig. 1.4: Survival in the Netherlands of patients with metastatic carcinoid tumours according to year of diagnosis. (Vinik AI et al)

1.2 Diagnosis

1.2.1 Tumour markers

A firm diagnosis of NET is dependent on the results from a combination of tests. The initial investigations tend to be biochemical in nature; divided into general and specific tests and ectopic hormones. The general tests for NETs include: serum chromogranins and urinary 5 Hydroxy Indole Acetic Acid. In addition some centres test for neurokinin-A, hCGβ (human chorionic gonadotrophin-β), ACTH and GHRH. Specific peptides for NETs include: serum gastrin, insulin/C-peptide, glucagons, vasoactive vasointestinal peptide, pancreatic polypeptide, and somatostatin.

Measurement of circulating peptides and amines in patients with NETs is helpful on three counts.

1. In making the initial diagnosis.
2. In the assessment of treatment.
3. For prognosticating.

There is evidence to suggest that CgA and neurokinin-A have prognostic significance. However, the value of measuring other tumour markers, such as α-fetoprotein and hCGβ is not clear *(Turner et al 2006)*

We developed and subsequently analyzed a large database of Royal Free patients in order to clarify the prognostic potential of these latter tumour markers.

1.2.2 Imaging

The optimum imaging modality depends on whether it is to be used in detecting disease in a patient suspected of a NET or for assessing the extent of disease in a known case.

1.2.2.1 Imaging in suspected primary

Gastric, duodenal, chest, and colonic primary sites are easier to find as they are likely to be discovered at endoscopy or CT scanning. Barium series and CT scans may be normal but will show larger lesions (for example midgut carcinoid changes including fixation, separation, thickening, and angulation, and often calcification at the centre of a "starburst" appearance of the desmoplastic reaction). SSRS (somatostatin receptor scintigraphy, usually octreoscan®) may be useful in tumours greater than 1cm diameter

and expressing SSTR2 (see 1.2.2.2) mesenteric angiography may also be useful. A small primary, such as an intestinal NET, may not be seen on imaging and thus a patient with abdominal pain and change in bowel habit over many years is often labelled as having irritable bowel syndrome.

The so called non-functioning pancreatic NETs which do not have an associated syndrome, due to over-secretion of a hormone such as insulin or gastrin, are usually detected late in the course of the disease and seen on CT, MRI, or SSRS. Functioning pancreatic NETs may be identified earlier, due to their associated syndromes such as repeated episodes of hypoglycaemia and Zollinger Elison syndrome. The potential for surgical cure necessitates accurate localisation which may be performed using CT, MRI, endoscopic ultrasound, often together with SSRS, and in some centres digital subtraction angiography with intra-arterial calcium stimulation.

1.2.2.2 Imaging for detecting the primary tumour when the patient has already presented with metastases

Investigations for localising the primary site may include: ultrasound scans of the abdomen, testes, and ovaries; endoscopic ultrasound; CT scan of the chest (bronchial carcinoid), abdomen, and pelvis; endoscopy-colonoscopy and gastroscopy; barium studies; and nuclear medicine functional imaging. In one series, primary tumours were localised in 81–96% of cases using radiological and/or nuclear medicine imaging, although opinion is divided on whether locating the primary in the setting of metastatic disease changes prognosis. Endoscopic ultrasound is a useful diagnostic investigation in a patient with a suspected pancreatic NET. Its sensitivity may be less with extrapancreatic gastrinomas (80% of gastrinomas in MEN1 are found in the duodenum) for which an upper gastrointestinal endoscopy and CT or MRI should be performed first.

Neuroendocrine tumours express somatostatin receptors (SSTR) and this has led to the development of radiolabelled somatostatin analogues for diagnostic imaging (somatostatin receptor scintigraphy – SSRS). There are five receptor subtypes, of which only subtype 2 and 5 are targeted for imaging by Octreoscan®. With the exception of insulinomas (with only 50% of this tumour group expressing SSTR2), SSRS plays a central role in locating and assessing the tumour site in gastroenteropancreatic NETs

with reported sensitivity of up to 90%. The sensitivity could be further enhanced by the use of single positron emission computed tomography and fusion imaging with CT.

Unfortunately, a negative octreoscan not only reduces diagnostic efficiency but also limits treatment options based on somatostatin analogues as at least moderately positive SSTR imaging is required for SSTR targeted radiotherapy, an important modality of anti-NET therapy.

Hence there is a need for improving the sensitivity of SSTR scintigraphy.

1.3 Management

As with other cancers, such as breast or colon, the best chances of cure are when the disease is diagnosed at an early stage and is surgically removed in its entirety. Once distant metastases have developed, the chances of a cure, surgical or otherwise are remote. Treatment is then aimed at providing symptom palliation, and if possible, prolonging survival. There is, therefore, a need to understand the biology of these tumours in order to decide on the best treatment regimens, from those currently available to patients with other tumours, as well as to develop novel therapies specific for NET patients.

When the tumour is un-resectable the treatment has two objectives:

1) To control symptoms, produced by hormone secretion, and thereby improve quality of life;

2) To extend survival by effecting tumour reduction or limiting tumour growth.

Chemotherapy has shown efficacy in managing NETs of foregut, including pancreatic origin, but is of limited benefit in mid-gut and hind-gut carcinoid tumours [4-6]. This has led to the search for novel agents capable of slowing the progress of NETs as well as providing symptom control. With the exception of pancreatic and high grade NETs, the majority of NETs are relatively insensitive to chemotherapeutic agents. The main aim of anti-NET therapy in these cases, until recently, has been to provide symptom control using somatostatin analogues. In the last 2 decades there has been a significant expansion in the available options of anti-tumour therapy, but as with other cancers there continues to be a great need for new and more potent treatments.

Current treatment options for metastatic NETs are (also see figure 1.5):

1) Surgery: removal of the primary, tumour debulking, and in rare cases liver transplantation.

2) Monitoring only: if tumour is inoperable, asymptomatic and observed to be radiologically, biologically, and clinically stable.

3) Biotherapy: Somatostatin analogue and/or interferon therapy – if tumour is symptomatic, due to hormone production, but radiologically stable. It can temporarily stabilise the tumour in majority of patients treated and may even cause tumour regression in a small minority.

4) Chemotherapy: in a subgroup of progressive NETs known to be sensitive to this form of therapy.

5) Intravenously administered targeted radiotherapy for chemo-resistant NETs: using either radiolabelled-mIBG or radiolabelled somatostatin analogues.

6) Intra-arterially administered selective internal radiotherapy (SIRT; considered experimental and only available in specialist centres): using radiolabelled somatostatin analogues, usually when the bulk of the tumour is confined to the liver.

7) Ablative methods: trans-arterial chemoembolisation, radiofrequency ablation, ethanol ablation.
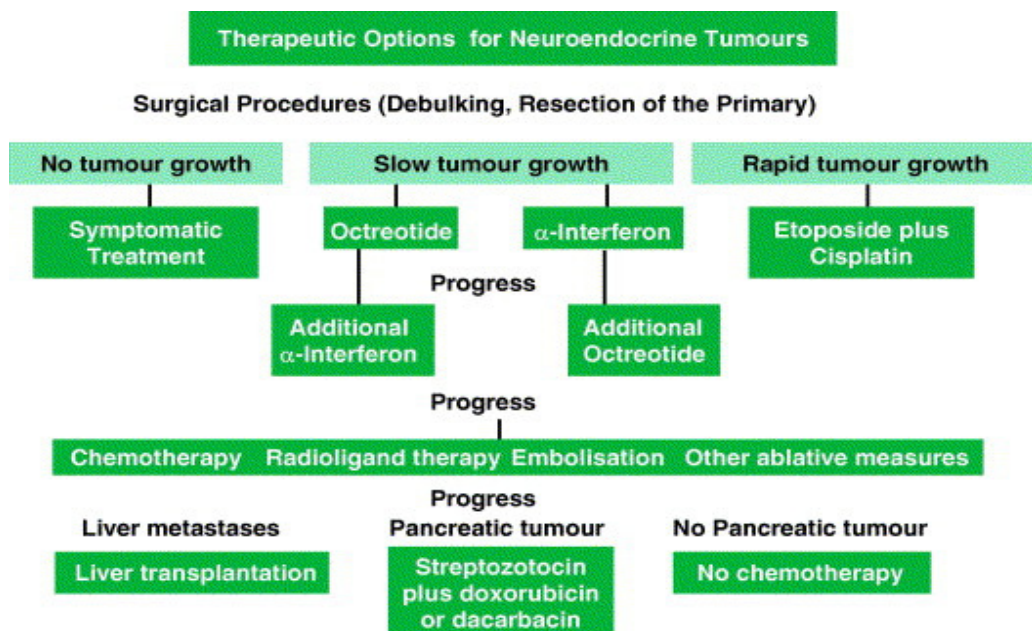
Figure 1.5: An algorhythmn for treating neuroendocrine tumours (Arnold R[a] 2005)

1.3.1 Biotherapy:

1.3.1.1 Somatostatin analogues

Somatostatin (SS) is a natural polypeptide which circulates as physiologically active somatostatin-14 and somatostatin-28. It is a powerful inhibitor of endocrine and exocrine function affecting, amongst others, the release of insulin, gastrin, glucagon, gastric secretions, and pancreatic secretions. These inhibitory effects are the core basis for the role of somatostatin and its analogues in providing symptom control in NET patients. SS has also been shown to have apoptotic and cytostatic effects on various tumour cell types [Chen C 1992, Buscail L et al 1994, Buscail L et al 1995, Liebmann C 2001].

SS acts through G-protein linked cell surface somatostatin receptors, of which there are five subtypes, 1-5. Both SS14 and SS28 are known to bind to all somatostatin receptor (SSTR) subtypes with high affinity. Binding to SSTR1 increases mitogen activated protein kinase (MAPK) activity, which would be expected to lead to cellular proliferation, but the final outcome is anti-proliferative due to induction of cell-cycle arrest. SSTR2 stimulation leads to activation of SHP-1 followed by trans-inactivation of EGFR and decrease in MAPK activity. SHP-1 also appears to be responsible for inducing cell-cycle arrest in response to SSTR2 activation. SSTR3 induces apoptosis by increasing the p53 level. SSTR4 is unusual in that its activation leads to cellular proliferation, achieved via activation of MAPK. SSTR5 mediates cell-cycle arrest by activation of a protein tyrosine phosphatase [Chen C 1992, Buscail L et al 1994, Buscail L et al 1995, Liebmann C 2001].

SS and its analogues (octreotide™ and lanreotide™) have been shown to exert an indirect antiproliferative effect on various normal and cancerous cells, both *in vitro* and *in vivo*, through numerous mechanisms: by the inhibition of release of growth factors and trophic hormones (GH, IGF-1, insulin, gastrin, EGF); inhibition of angiogenic processes (endothelial cell proliferation, VEGF release, monocyte activity), and immunomodulatory effect (lymphocyte proliferation, interleukin or cytokine release, natural killer cell activity) [Buscail L et al 2002].

The use of radio-labelled somatostatin analogues for imaging and detection of mRNA expression with in-situ hybridisation or reverse transcription-polymerase chain reaction has allowed the characterisation of the expression of somatostatin receptors in a large variety of human tumours, including NETs. Full range of SSTR subtypes can be

expressed by tumours but SSTR2 appears to be the most prevalent, with 80-90% of NETs expressing SSTR2 [Jonas S et al 1995, Benali N et al 2000, Nilsson O et al 1998, Shi W et al 1998, Reubi JC et al 1987, Thulin L et al 1978].

The beneficial effect of SS in symptom control was initially described in the late 1970s. However, it has a half life of two minutes thereby necessitating a continuous infusion which, together with the occurrence of rebound symptoms upon treatment cessation, made it impractical for clinical use in the outpatient setting. Over the last two decades the availability of longer acting SS analogues has greatly facilitated their use for the control of symptoms in patients with carcinoid syndrome and other functioning NETs. Inhibition of tumour growth and occasional decrease in tumour size has also been reported [Saltz L et al 1993, Arnold R et al 1996].

1.3.1.2 IFN alpha treatment in NETs

Interferons (IFNs) are biological response modulating agents which have been shown to have an effect in a number of tumour types, including melanoma and lymphoma. IFN-α is produced by a subset of cells in human peripheral blood in response to various viruses and bacteria and has a variety of biological functions. IFNs exert their anti-tumour effects through the modulation of multiple cellular mechanisms, including proliferation, differentiation, apoptosis, and angiogenesis. There are a number of types of interferon, three of which (alpha, beta, and gamma) have been extensively clinically investigated. IFNs were initially obtained from human leukocytes which limited their availability. Later recombinant interferon alpha became available thereby allowing its use in larger numbers of patients. IFNs have been used alone or in combination with chemotherapy and somatostatin analogues in mainly carcinoid subgroup of NETs.

Analysis of pooled data, from published studies, indicates median symptomatic and biochemical response   rates of 40 – 70% and 44% respectively, with median tumour response rate of 11%. Disease stabilisation is reported in median 35% of patients, with tumour progression in 15 – 20%. Median duration of response is 32 months [Oberg K 1991]. There is no clear dose/response relationship as shown by the lack of improved response by high dose interferon [Moertel CG et al 1989]. The recommended doses of recombinant IFNα are 3 – 9MIU every day or every other day, median 5MIU every other day, by sub-cutaneous injection. However, the dose should be titrated according to

the sex, age, and weight of the patient [Eriksson B 1993, Oberg K 1992]. The leukocyte count can also be used to titrate IFN dose, by aiming to reduce the leukocyte count to <3.0 x 10^9 / litre. This approach does not increase the risk of infection [Oberg K 2000].

IFN therapy is commonly associated with flu-like symptoms which tend to be short lived, lasting for a week or so, and can be treated with paracetamol. Chronic fatigue syndrome and depression, of various grades, can develop in up to 50% of patients. These side-effects are more difficult to manage and may lead to cessation of treatment. Serotonin uptake inhibitors have shown efficacy in treating IFN associated depression and therefore may help improve compliance [Benedetti F et al 2004]. Autoimmune manifestations are seen in 15 – 20% of patients, with majority developing thyroid dysfunction, which in turn may contribute to fatigue. More severe autoimmune reactions include the SLE syndrome and polymyositis. 1/3rd of patients develop mild derangement of liver enzymes which only occasionally require treatment withdrawal [Oberg K 2000].

1.3.2 Chemotherapy

NETs have usually metastasized to the lymph nodes, liver, bone, brain, and other sites by the time of diagnosis. Tumour progression is related to the degree of differentiation: well differentiated NETs display slow progression and prolonged survival; and poorly differentiated NETs display rapid progression and short survival. Systemic chemotherapy would be expected to play a major role in the management of metastatic NETs. However, experience has shown that chemotherapy is only effective in a subgroup of NET patients, mainly: well differentiated NETs of the pancreas, and poorly differentiated NETs of any origin (Arnold R 2005).

1.3.2.1 Well differentiated neuroendocrine tumours of the pancreas

Many chemotherapeutic substances have been trialled in NET patients. Amongst these are carboplatin, chlorozotocin, DTIC, doxorubicin, etoposide, streptozocin (STZ), and paclitaxel. Objective response rates have generally been low apart from for treatment with STZ.

Streptozocin was isolated from Streptomyces organisms in 1956 and was shown to have anti-microbial and anti-tumour activity. During pre-clinical toxicology studies, it was

discovered to cause hyperglycaemia in rats and dogs. This was subsequently shown to be due to rapid islet-cell degranulation by STZ, leading to permanent diabetes mellitus. These findings led to the focus of STZ use in patients with pancreatic islet cell tumours. STZ was first used to treat patients with multiple hormone producing metastatic islet cell tumours producing clinical effects including hypoglycaemic episodes (Varva JJ et al 1959, Rakieten N et al 1963, Evans JS et al 1965). STZ displayed a beneficial effect on the clinical symptoms of hypoglycaemia as well as demonstrating objective tumour response. Later studies confirmed monotherapy with STZ to be equally effective in functioning and non-functioning tumours, with a response rate of about 36% (Moertel CG et al 1980).

Streptozocin combinations: STZ in combination with 5-fluorouracil (5-FU) showed significantly improved response rate as compared to STZ alone. An overall response rate of 63% v 36% was observed (with complete response rate of 33% v 12%) for combination v mono-therapy respectively. The response was similar for functioning and non-functioning tumours (Moertel CG et al 1980). STZ is also given in combination with doxorubicin and has been shown to produce the best response rates, although associated with severe side-effects including long-lasting nausea and vomiting, haematological toxicity, and heart failure, which limit its use (Moertel CG et al 1992).

1.3.2.2 Well differentiated tumours of the gastrointestinal tract

The sensitivity of gastrointestinal neuroendocrine tumours to chemotherapeutic agents is low. The median reported response rate to therapies such as actinomycin D, carboplatin, cisplatin, doxorubicin, DTIC, etoposide, mitomycin C, paclitaxel, STZ, STZ + 5-FU, STZ + cyclophosphamide, STZ + doxorubicin, 5-FU + doxorubicin + cisplatin, dacarbazine + 5-FU, and others is 17%. Chemotherapy, therefore, is not recommended for the treatment of these patients at present (Jensen RT 2001).

1.3.2.3 Poorly differentiated tumours of the gastrointestinal tract

A small group of patients with poorly differentiated neuroendocrine tumours of the gastrointestinal tract were treated with a combination of etoposide + cisplatin. In 12 of 18 patients, with anaplastic NETs, objective tumour regression was seen, with disease stabilisation for a median of 11 months (Moertel CG 1986).

1.3.3 Somatostatin receptor targeted radionuclide therapy

Radiotherapy is an established form of treatment for many tumour types including gastrointestinal cancers. Radiation causes DNA and cell-membrane damage leading to activation of various pathways that end in activation of executioner caspases and cell apoptosis (figure 1.6).

Figure 1.6: Radiation induced apoptosis occurs via multiple pathways, some of which are energy dependant. ATP dependant steps are indicated by the stars. SAPK – stress activated protein kinase pathway. cs – ceramide synthase. MRN – Mre11-Rad50-Nbs1. (Hunter A et al 2006).
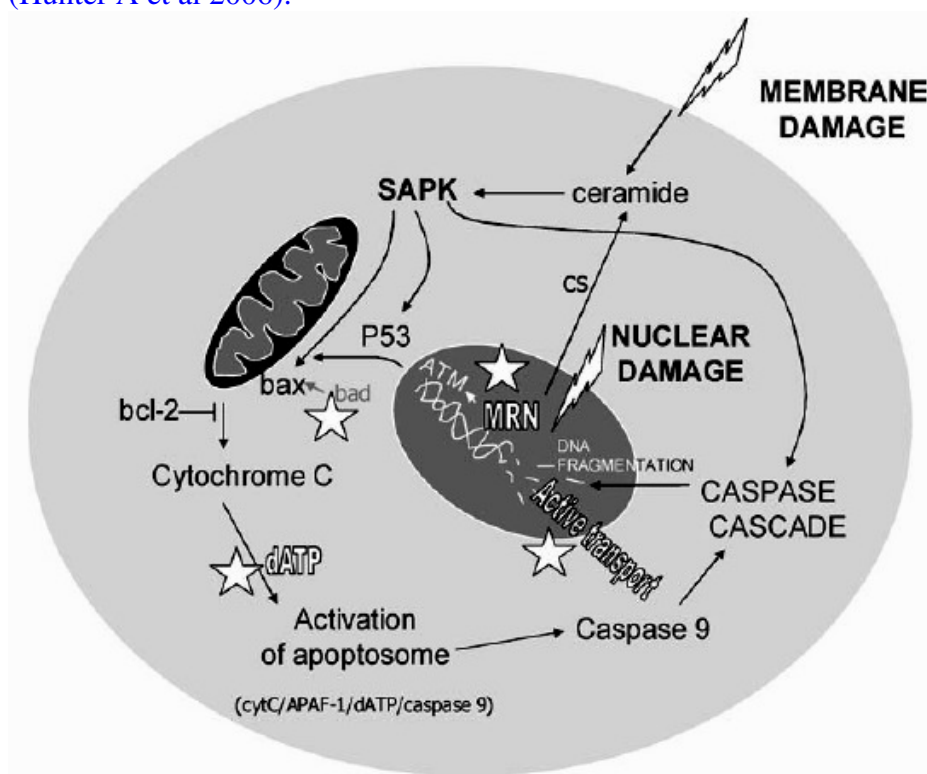
The majority of neroendocrine tumours express SSTRs with SSTR2 being the most frequently expressed subtype. In patients with un-resectable neuroendocrine tumours of the gastrointestinal tract, there is now reasonable evidence to support SSTR targeted radiotherapy. This "magic bullet" form of treatment has been rapidly developing over the past 2 decades.

SSTR targeted radiotherapy was developed from SSTR targeted scintigraphy by increasing the radiation dose of the administered radiolabelled somatostatin analogue in an attempt to cause tumour shrinkage. Since then, several radiolabelled SSTR targeting agents have been developed using a range of radionuclides with variable physical

30

characteristics (^{111}In, ^{90}Y, ^{177}Lu being the commonest), chelating agents (such as DTPA and DOTA) and somatostatin analogues (such as octreotide, octreotate, and lanreotide). These components, variously combined, give a range of affinities for SSTRs, though they all bind preferentially to SSTR2 as opposed to other SSTR subtypes (table 1.4).

Table 1.4: Affinity profile (IC50) for human somatostatin receptors hSSTR1-5 of a series of somatostatin analogues (Jaap J.M et al 2005).

Peptides	hSSTR1	hSSTR2	hSSTR3	hSSTR4	hSSTR5
Somatostatin-28	5.2 ± 0.3 (19)	2.7 ± 0.3 (19)	7.7 ± 0.9 (19)	5.6 ± 0.4 (19)	4.0 ± 0.3 (19)
Octreotide	>10,000 (5)	2.0 ± 0.7 (5)	187 ± 55 (3)	>1,000 (5)	22 ± 6 (5)
DTPA-octreotide	>10,000 (6)	12 ± 2 (5)	376 ± 84 (5)	>1,000 (5)	299 ± 50 (6)
[111]In-octreotide	>10,000 (5)	22 ± 3.6 (5)	182 ± 13 (5)	>1,000 (5)	237 ± 52 (5)
DOTATOC	>10,000 (7)	14 ± 2.6 (6)	880 ± 324 (4)	>1,000 (6)	393 ± 84 (6)
[90]Y- DOTATOC	>10,000 (4)	11 ± 1.7 (6)	389 ± 135 (5)	>10,000 (5)	114 ± 29 (5)
DOTALAN	>10,000 (7)	26 ± 3.4 (6)	771 ± 229 (6)	>10,000 (4)	73 ± 12 (6)
^{90}Y-DOTALAN	>10,000 (3)	23 ± 5 (4)	290 ± 105 (4)	>10,000 (4)	16 ± 3.4 (4)
DOTA-OC	>10,000 (3)	14 ± 3 (4)	27 ± 9 (4)	>1,000 (4)	103 ± 39 (3)
^{90}Y-DOTA-OC	>10,000 (5)	20 ± 2 (5)	27 ± 8 (4)	>10,000 (4)	57 ± 22 (4)
DTPA-Tyr[3]-octreotate	>10,000 (4)	3.9 ± 1 (4)	>10,000 (4)	>1,000 (4)	>1,000 (4)
^{111}In-DTPA-Tyr[3]-octreotate	>10,000 (3)	1.3 ± 0.2 (3)	>10,000 (3)	433 ± 16 (3)	>1,000 (3)
DOTA-Tyr[3]-octreotate	>10,000 (3)	1.5 ± 0.4 (3)	>1,000 (3)	453 ± 176 (3)	547 ± 160 (3)
^{90}Y-DOTA-Tyr[3]-octreotate	>10,000 (3)	1.6 ± 0.4 (3)	>1,000 (3)	523 ± 239 (3)	187 ± 50 (3)

Modified from Reubi et al.[26]
    [a] All values are $IC_{50} \pm SEM$ in nM. The number of experiments is in parentheses.

[^{90}Y-DOTA-Tyr3]octreotide for instance has been shown to be effective in treating moderate to large metastases (≥ 1 cm[2]; 7-9cm[2]), in rat models, as ^{90}Y emits high energy β-particles which have a maximum tissue penetration range of 12mm and can therefore seriously damage approximately 600 cells surrounding the index cell, hopefully leading to cell apoptosis (table 1.5).

[^{177}Lu-DOTA0-Tyr3]octreotate has an order of magnitude greater binding affinity for SSTR2. This agent has shown good results in the treatment of smaller tumours (≤ 1 cm2) as radiation from ^{177}Lu has a shorter tissue penetration range (2mm; 100 cells) than [90]Y (table 1.5).

[^{90}Y-DOTA]lanreotide shows high affinity for SSTR2 and SSTR5. It has been shown to be as effective as [^{90}Y-DOTA-Tyr3]octreotide in the treatment of metastatic gastrointestinal neuroendocrine tumours. This reagent may become important in treating

31

patients whose tumours either do not express SSTR2, or have lost SSTR2 expression during progression from a low-grade tumour to high-grade tumour, but continue to express SSTR5 (Virgolini I et al 2002).

Table 1.5: Physical characteristics of the radionuclides used in peptide receptor radionuclide therapy (Jaap J.M et al 2005).

Radionuclides	Emitted particle	Particle energy (mean keV)	Maximum tissue penetration range (approximate number of cells[a])	Half-life (days)
Indium (^{111}In)	Auger electrons	3 and 19 keV	10 μm (<1)	2.8
	γ-radiation	171 and 245 keV		
Yttrium (^{90}Y)	β-radiation	935 keV	12 mm (approximately 600)	2.7
Lutetium (^{177}Lu)	β-radiation	130 keV	2 mm (approximately 100)	6.7
	γ-radiation	113 and 208 keV		

[a] Number of cells based on an average tumour cell size of 20 μm.

All these reagents are useful in controlling tumour progression, but treatment rarely leads to cure.

Failure of radiotherapy induced DNA damage to cause apoptosis is an important mechanism for limiting disease response.

Encouraging radiotherapy induced apoptosis by blocking anti-apoptosis / cell-repair pathways should therefore improve response rates. Discovery of relevant cell repair mechanisms, which could be suitable for pharmacological manipulation, is part of the remit of this research thesis.

1.3.4 Chemoembolisation of liver metastases

Neuroendocrine tumour patients usually have liver metastases by the time of diagnosis. Often the bulk of tumour burden lies in the liver. When possible, surgery is the best form of treatment for liver metastases. However, a high proportion of patients have diffuse bi-lobar disease not amenable to surgery. Systemic chemotherapy can be given in these cases, especially when the disease is progressive and/or symptomatic, and shows reasonable results in patients with pancreatic primaries. Patients with liver metastases from midgut primaries, however, do not respond well to chemotherapy and their 5-year survival rate is reported to be 0-40%. Liver metastases can be responsible for endocrine hyperfunction resulting in symptoms, such as carcinoid syndrome, which

can be difficult to control. Somatostatin analogues may be efficacious in controlling these symptoms but their effect tends to wear out usually with time, due either to tachyphylaxis or tumour progression.

Vascular occlusion aiming at selective ischaemia induction of hepatic metastases has been in use for some time. This initially consisted of surgical ligation of hepatic artery to produce transient or intermittent hepatic ischaemia. These methods were commonly associated with severe complications as well as high treatment associated mortality.

1.3.5 Sequential hepatic artery embolization

A percutaneous technique, for radiologically guided hepatic artery embolization, has been developed. Portal vein patency has to be demonstrated and tumour vasculature visualised. Selective catheterization of hepatic artery branches is achieved followed by contrast injection and embolization of fragments of absorbable gelatine sponge. This technique has been efficacious in neuroendocrine tumour metastases to the liver, as well as advanced non-resectable hepatocellular carcinoma and liver metastases from colorectal cancer. (O'Toole & Ruszniewski 2005).

1.3.6 Trans-catheter arterial chemoembolization (TACE)

This employs the same technique as hepatic artery embolisation, but in addition an emulsion made from a cytotoxic drug (e.g. adriamycin 50mg/m2 or STZ 1.5g/m2) dissolved in 10ml of normal saline and combined with 10ml of iodized oil (Lipoidol®) is injected prior to embolization with gelatine sponge 2-3mm particles or microspheres (Embospher®). Patients need to be pre-medicated with intravenous hydration and antibiotics, somatostatin analogues (in cases of carcinoid syndrome in order to prevent carcinoid crises), anti-emetics, and analgesia. STZ administration requires a general anaesthetic because of the severe pain associated with the administration of this acidic agent. The results from various studies are encouraging (O'Toole & Ruszniewski 2005; table 1.6).

Table 1.6: Symptoms and hormonal secretion (O'Toole & Ruszniewski 2005).

References	N/type	Chemotherapy	Sustained relief (%) (in symptomatic pts)	5-HIAA decrease > 50% (results only for MGC)
26	23/CT	DOX	100	91
32	18/CT, 5/ICC	DOX	73	57
34	14/CT[a]	DOX	90	69
33	10/CT	CDDP, MMC, DOX[b]	100	–
35	8/CT, 7/ICC	STZ (1.5 g/m^2)	67	50
27	10/CT, 4/other	DOX	70	75

ICC, islet cell tumour; CT, patients with carcinoid syndrome mostly from midgut origin; DOX, doxorubicin; MMC, mitomycin; CDDP, cisplatin.
[a] Mostly CT; all 14 tumours were functionally active.
[b] Sequential intra-arterial 5-fluorouracil also administered.

1.4 Promising fields for study in the management of NETs: Modulation of DNA-damage repair mechanisms through better understanding of EGFR/DNA-PK$_{CS}$ interactions

1.4.1 Intrinsic causes of DNA Damage

The integrity of genomic DNA is constantly under threat. DNA damage can result from the action of endogenous reactive oxygen species (ROS) such as hydroxyl radicals, hydrogen peroxide or superoxide anions. Errors in replication and recombination as well as environmental agents such as ultraviolet (UV) light from the sun, ionising radiation and genotoxins such as cigarette smoke, can also result in DNA damage in the form of single-strand (SSB's) or double-strand breaks (DSB's) (Norbury & Zhivotovsky 2004). If for any reason the DNA cannot be repaired, mutations may result and the risk of cancer increases (Hoeijmakers 2001).

1.4.2 DNA-Interactive Chemotherapeutic Agents

While unicellular organisms respond to the presence of DNA lesions by activating cell cycle checkpoint and repair mechanisms, multicellular animals have the additional possibility of eliminating the damaged cells by triggering programmed cell death or "apoptosis".

Anti-cancer agents targeting DNA are some of the most potent treatments in clinical practice. They have improved patient survival particularly when used in combination with drugs employing differing mechanisms for their anti-tumour activity. They act by relatively selectively targeting cells types with a rapid turnover such as cancer cells, bone marrow and the gut lining. These chemotherapeutic agents can be classed according to the nature of their molecular interactions with DNA and the subsequent modifications they induce. Figure 1.7 summarises these different interactions namely, DNA strand crosslinking, intercalation, DNA strand breaking and code reading molecules (Hurley 2002).
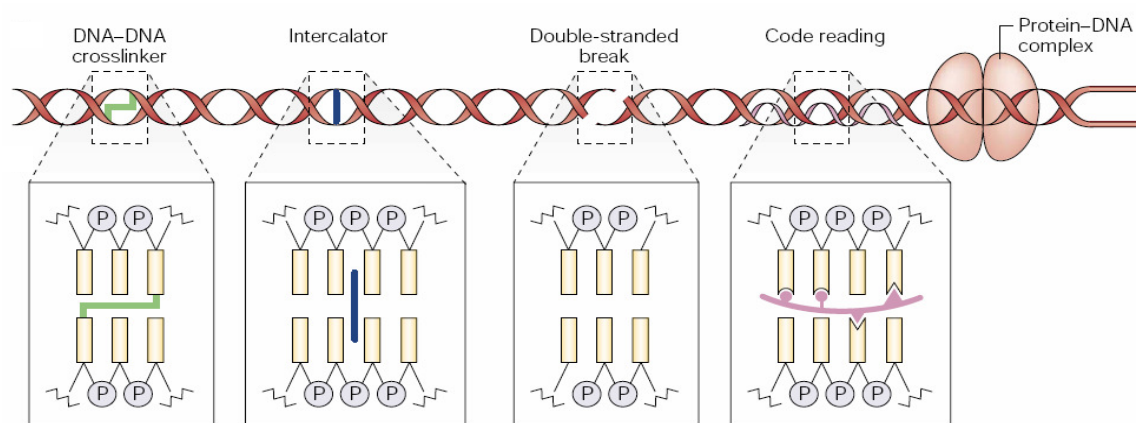
Figure 1.7: Classes of DNA-interactive agents and their molecular interactions with DNA.

Source: Adapted from L. Hurley, Nature Reviews Cancer, 2002.

1.4.3   Cellular Response to DNA Damage

The cell-cycle infrastructure is able to detect DNA damage at specific checkpoints in G_1, S, G_2 and M phases allowing repair of lesions before they become permanent (Zhou & Elledge 2000). If the damage is too severe, apoptosis will be initiated at the expense of the whole cell.

Short-term damage to DNA as a result of disrupted DNA metabolism and longer-term effects by way of irreversible mutations contributing to oncogenesis and cannot be reversed by way of a single repair process. No one system can cope with the variety of lesions and so at least four main damage repair systems are known to exist (Hoeijmakers 2001). These are: Nucleotide Excision Repair, Base Excision Repair, Homologous Recombination and Non-Homologous End Joining.

35

Common damage detection and signal transduction mechanisms are shared between pathways governing DNA repair, cell cycle checkpoint activation and apoptosis. By allowing the survival and proliferation of cells with damaged DNA, failure of these processes contributes to tumourigenesis and resistance to cancer therapies (Igney and Krammer 2002).

1.4.4 DNA-Dependent Protein Kinase (DNA-PK) and its role in NHEJ

DNA-PK is a nuclear serine/threonine kinase with a molecular mass of ~460 kDa that is involved in non-homologous end-joining (NHEJ) of DNA double-strand breaks, and therefore is a key player in DNA damage repair. It is made up of a regulatory subunit, containing the Ku70/80 subunits, and a catalytic subunit, DNA-PK$_{CS}$ (Smith & Jackson 1999; Collis *et al*. 2005). Electron microscopy shows that DNA-PK$_{CS}$ is divided into two large regions, labelled as 'head' and 'palm' connected by a third region labelled 'arm' (Figure 1.8B) (Brewerton *et al*. 2004).

DNA-DNA-PK$_{CS}$ binding to DNA greatly stimulates DNA-PK$_{CS}$ activity with the phosphorylation of one of its natural substrates, the XRCC4 protein. This indicates that DNA interaction is functionally relevant to DNA-PK$_{CS}$ (Boskovic *et al*. 2003; Collis *et al*. 2005).

DNA binding to DNA-PK$_{CS}$ induces conformational changes causing the palm domain to bend, coming into contact with the head and exposing a small channel able to accommodate double-stranded DNA. These structural movements are likely to play a role in the activation of DNA-PK$_{CS}$ kinase activity upon DNA binding (Martensson & Hammarsten 2002).
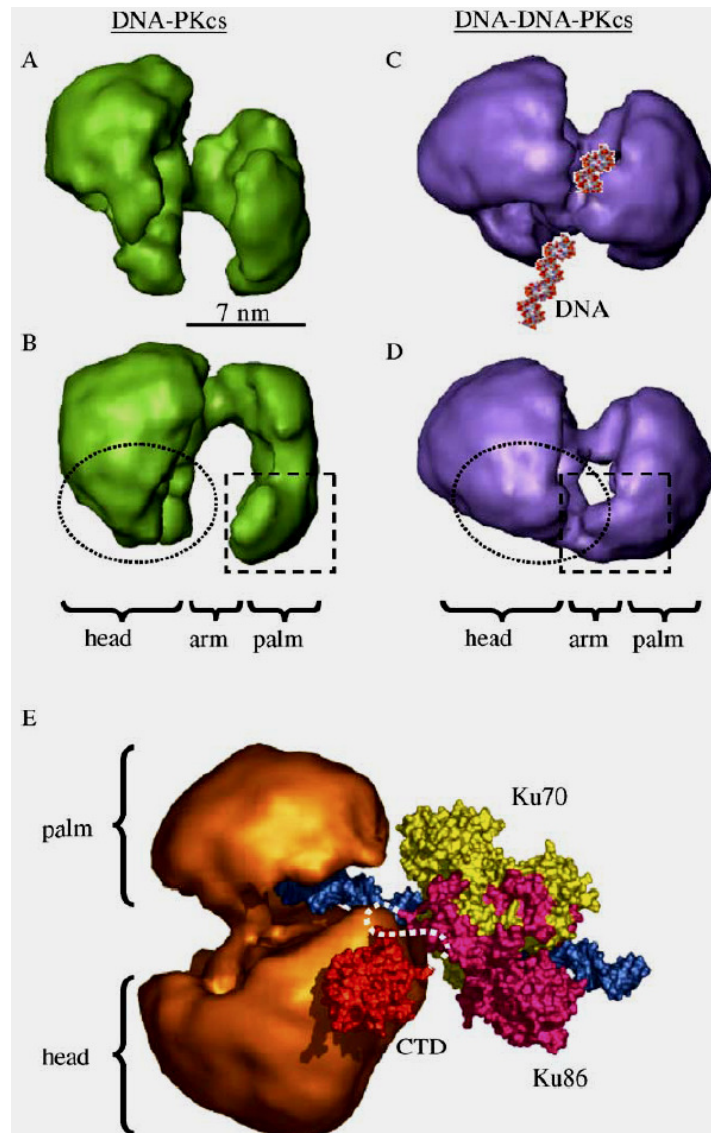
Figure 1.8: 3D structure of DNA-PK$_{CS}$ and its DNA-bound complex.

Source: O. Llorca & L.H. Pearl, Micron, 2004.

DNA-PK$_{CS}$ may also act as a scaffold protein to aid the localisation of DNA repair proteins to the site of damage (Collis *et al*. 2005). DNA-PK$_{CS}$, as well as Ku, is found at the ends of chromosomes, suggesting a further role for DNA-PK$_{CS}$ in the maintenance of telomeric stability and the prevention of chromosomal end fusion (Espejel 2004; Rebuzzini *et al*. 2004).

DNA-PK$_{CS}$ and the Ku subunits associate directly with each other even in the absence of DNA, and can each bind DNA end structures independently (Lieber *et al*. 2003). It has been suggested that the Ku component of DNA-PK is probably the initial DNA double strand breaks (DSBs) sensor *in vivo* (Collis *et al*. 2005). It is proposed that Ku binds to DNA termini generated at the site of damage to recruit DNA-PK$_{CS}$, which is

activated upon DNA binding although the key target for phosphorylation by DNA-PK$_{CS}$ is unclear (Llorca & Pearl 2004). Proteins phosphorylated by DNA-PK$_{CS}$ include regulators of the cellular DNA damage response such as p53, as well as other components of the NHEJ complex such as Artemis, XRCC4 and Ku, as well as DNA-PK$_{CS}$ itself (Lieber *et al*. 2003). Once the catalytic subunit of DNA-PK is supporting the DNA, Ku then moves to a more internal position where the DNA-PK$_{CS}$ probably contributes to hold the two DNA ends together (DeFazio *et al*. 2002). To finish, the XRCC4-DNA-ligase-IV complex is recruited by DNA-PK and ligation is achieved (figure 1.9).
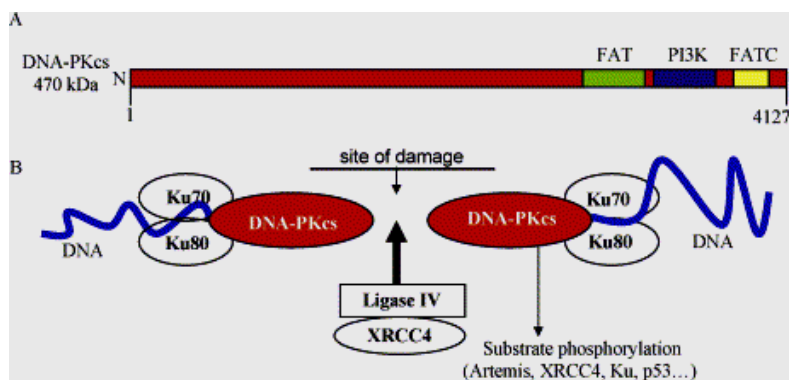
Fig. 1.9: Model for non-homologous recombination DNA repair (NHEJ). (A) The catalytic subunit of the DNA-dependent protein kinase (DNA-PKcs) is the major orchestrator of NHEJ repair in mammalian cells. DNA-PKcs is a large molecule with a C-terminal region containing conserved domains named as FAT, FATC and the region with homology to the kinase of domain of PI3-kinases (PI3K). It has been postulated that the N-terminal portion of DNA-PKcs consists of helical repeats with a low degree of conservation. (B) Present models propose that the two Ku subunits are among the first proteins to recognise damaged DNA and help recruit DNA-PKcs to the site of damage, which in turn acts as scaffolding for other repair factors, included the XRCC4/ligase IV complex. DNA-PKcs kinase is activated upon DNA binding and phosphorylates substrates that participate in the adequate progression of DNA repair.

Source: O. Llorca & L.H. Pearl, Micron, 2004.

Role of DNA-PK in DNA repair mechanisms in Neuroendocrine Tumours

No significant body of work has been published in this field, to date.

1.5 Epidermal Growth Factor Receptor (EGFR)

EGFR was the 1st cell surface receptor to be linked directly to cancer. The finding that EGFR is ligand-dependant tyrosine kinase and that the product of the v-erbB oncogene from avian erythroblastosis virus is a truncated form of EGFR, revolutionised both growth factor and cancer biology. Many cancers are promoted by EGFR activation, which can result from mutations of the receptor (leading to constituitive activation), EGFR over expression, or from EGFR stimulation through autocrine loops.

EGFR is a member of the ErbB family of receptors which include: EGFR itself, ErbB2 (HER2/Neu), ErbB3 (HER3) and ErbB4 (HER4). Since its discovery more than 40 years ago (Cohen 1960), EGFR ligand epidermal growth factor (EGF) has provided numerous puzzles for scientists. Recently, major advances in understanding of EGF action have come from crystallographic studies of EGFR family of receptor, yielding several surprises. A dramatic conformational transition was shown to occur upon ligand binding; a receptor-mediated mode of dimerization was identified; and a "preactivated" state was defined for the ErbB2 monomer. By combining the information gained from the recent structural studies, models for the allosteric regulation of EGFR family members have been developed. These models have greatly improved our understanding of ErbB receptor signaling and have created opportunities for the design of new anticancer agents.

1.5.1 ErbB receptors are activated by ligand-induced dimerization

It is well established that growth factor binding to the extracellular region of EGFR promotes dimerization of the monomeric receptor and increases the tyrosine kinase activity of its intracellular domain (Schlessinger 2000). Receptor molecules in the ligand-induced EGFR dimer become tyrosine autophosphorylated. The resulting phosphotyrosines recruit the SH2 domains of multiple downstream signalling molecules, thus initiating an array of intracellular signalling pathways (Schlessinger 2000). Biological activity of EGFR family members is modulated by receptor display, ligand availability, ligand/receptor affinity, and competency. EGFR appears to exist in two different affinity classes at the cell surface (Ullrich and Schlessinger 1990), with 2%–5% of receptors binding EGF with high affinity (K_D < 0.1 nM) and 95%–98% binding with lower affinity (K_D 6–12 nM). The affinity classes are thought to represent different receptor conformations and/or oligomers.

1.5.2 Growth Factor Ligands that Regulate the Four ErbB Receptors

EGFR is regulated by a family of at least seven distinct peptide ligands (Groenen et al. 1994 and Harris et al. 2003), including EGF, transforming growth factor-α (TGF-α), amphiregulin, betacellulin, epigen, epiregulin, and heparin binding EGF-like growth factor (HB-EGF). ErbB2 has no known direct activating ligand (Citri et al. 2003), while ErbB3 and/or ErbB4 function as receptors for the four known neuregulins (NRGs) (Falls 2003). All EGFR ligands are expressed as type I integral membrane proteins (Harris et al. 2003) and are proteolytically processed to yield the 49–85 amino acid mature growth factor that consists largely of the EGF-like domain (Harris et al. 2003). The bioactive core of mature NRG isoforms is also their EGF-like domain (Falls 2003).

1.5.3 Domain Organisation and Relationships with the ErbB Receptor Family

The four ErbB receptors are closely related single-chain modular glycoproteins with an extracellular ligand binding region (620 residues), a single transmembrane domain (23 residues), and an intracellular tyrosine kinase domain (260 residues) that is flanked by juxta-membrane (40 residues) and C-terminal (232 residues) regulatory regions (Figure 1.10). It is intriguing that this family includes an orphan receptor that nonetheless has robust tyrosine kinase activity (ErbB2) and a demonstrated NRG receptor (ErbB3) that lacks tyrosine kinase activity (Guy et al. 1994). Each ErbB receptor is thought to have a distinct physiological role, which can be modified by ligand-induced formation of ErbB receptor hetero-oligomers that are capable of generating unique signalling responses (Holbro et al. 2003 and Yarden and Sliwkowski 2001). Thus, the signalling characteristics of the 4 ErbB receptors are strongly interdependent.
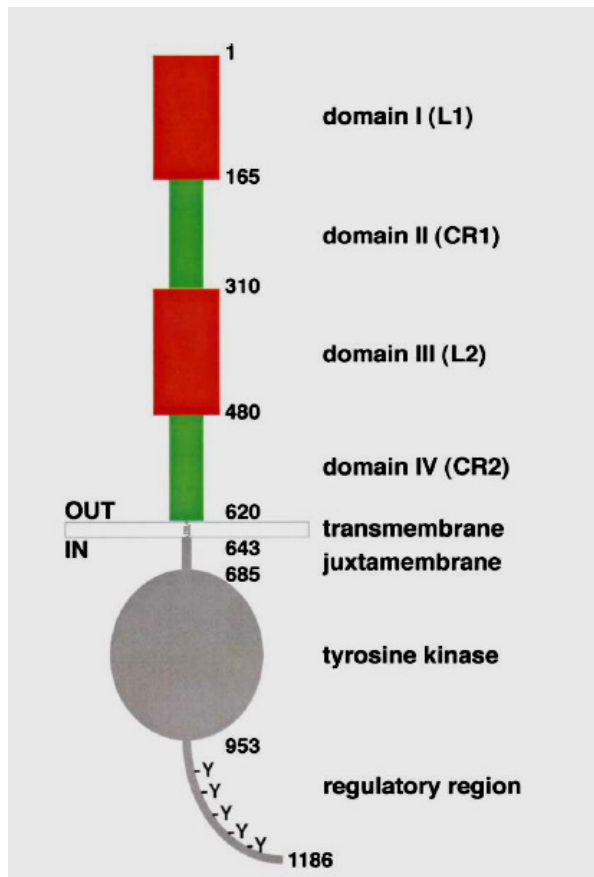
Figure 1.10: Domain Organization of ErbB Receptors.

1.5.4 ErbB Receptor Signalling

A bow-tie structure of the ErbB signalling is presented in Figure 1.11. The input of multiple growth factors that function through eight potential receptor hetero- or homodimers activates common signalling cascades. This results in the specific activation of transcription factors that lead to the selected cell fate. The ligands consist of 13 growth factors that directly bind to three receptors, ErbB1, ErbB3 and ErbB4. The specificity of ligand–receptor interactions displays remarkable redundancy. For example, betacellulin binds to and activates both ErbB1 and ErbB4, whereas epiregulin binds to ErbB1, ErbB3 and ErbB4. The multiplicity of ErbB ligands feeds into the combinatorial nature of the ErbB network, in which homo- or hetero-dimeric receptors can be formed, thereby establishing a high level of complexity. Biochemical evidence attributes to each ligand-driven receptor dimer distinct functional properties in terms of binding affinity, endocytic routing and effector activation (Citri A, and Yarden Y 2006).

41
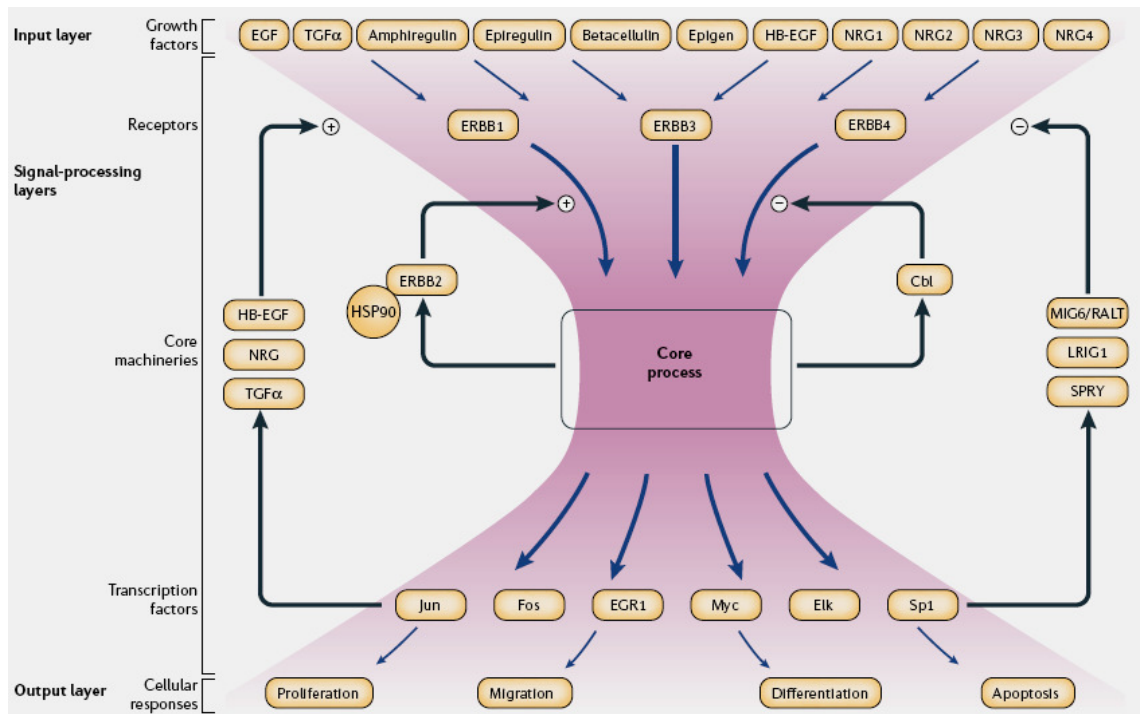
Figure 1.11: A reductionist view of the bow-tie-architectured signalling network is represented. The heart of the system is a collection of biochemical interactions, which are tightly coupled to each other and interface with two sets of components: three input modules, each comprising an ErbB receptor tyrosine kinase; and a large group of partly redundant ligand growth factors. The output of the core process is translated to gene expression through multiple transcription factors. Depending on the exact combination of transcription factors and the cellular context, the output of the network regulates cell behaviour. The system maintains two steady states, for which inter-conversions depend on ligand binding. The fail-safe action of the system is conferred by structural modularity and functional redundancy, along with rich and stringent system controls. An important positive regulator is ErbB2, a co-receptor. Heterodimerization between ErbB2 and any of the three ErbB input modules enhances and prolongs the respective output. ErbB2 is chaperoned and catalytically suppressed by heat-shock protein-90 (HSP90). On the other hand, a ubiquitin ligase that is involved in receptor degradation, Cbl, controls an important negative-feedback loop. Several activation-dependent control loops fine-tune. These include transcription of ErbB ligands (positive regulation) and newly synthesized negative regulators such as mitogen-inducible gene-6 (MIG6)/receptor-associated late transducer (RALT), sprouty (SPRY) and leucine-rich repeats and immunoglobulin-like domains-1 (LRIG1).
EGF - epidermal growth factor; EGR1 - early growth response-1; NRG1/2/3/4, neuregulin-1/2/3/4; TGFα - transforming growth factor-α.
(Citri A, and Yarden Y 2006).

1.5.5 System Controls of the ErbB Signalling Network

The ErbB network has evolved positive- and negative-feedback circuits in order to dynamically control the amplitude, kinetics and frequency of output signals,

1.5.5.1 Positive-feedback loops.

Positive-feedback loops enhance the amplitude and prolong the active state of signalling pathways. In the case of ErbB, the output of the main switch, namely binding of the ligand to the primary receptor, is tuned by the identity of the secondary receptor. ErbB2 can be considered as an important positive regulator; it functions as the preferred secondary receptor, and ErbB2-containing heterodimers evade negative regulation (Baulida J et al 1996, Worthylake R 1999, Lenferink AE *et al* 1998).

Another important mechanism of positive feedback is based on autocrine and paracrine loops, in which EGF-like ligands, as well as angiogenic factors, are produced following receptor activation. ErbB-mediated activation of the Ras–MAPK pathway strongly induces the transcription of multiple ErbB ligands, including TGFα and HB-EGF (Schulze A et al 2001). Similarly, transactivation of ErbB1/EGFR by G-protein-coupled receptors occurs through the stimulation of surface proteinases, generating mature, active HB-EGF (Schafer B 2004).

1.5.5.2 Negative-feedback loops.

Multiple molecular mechanisms, including post-translational modifications, compartmentalization, catalytic inactivation and steric hindrance, lead to signal attenuation. It is useful to distinguish between general attenuation, which functions at the level of the ligand–receptor complex, and pathway-specific inactivation such as inactivation of SOS through phosphorylation by the downstream MAPK. Furthermore, negative regulators either pre-exist, or they are newly synthesized following stimulation of ErbBs by their respective ligands.

Pre-existing attenuators primarily control receptor dephosphorylation and degradation. Receptor internalization coupled to degradation is considered the most effective, irreversible process that robustly attenuates signalling by targeting surface receptors for degradation in lysosomes (see below, and Wiley HS 2003). Another general mechanism of signal attenuation that functions at the receptor level is instigated by tyrosine

phosphatases such as density-enhanced phosphatase-1, which dephosphorylates ErbB1 as well as other RTKs (Berset TA et al 2005), and protein tyrosine phosphatase-1B, which dephosphorylates RTKs in endosomes (Haj FG 2002).

Unlike pre-existing attenuators, the level of expression of newly synthesized attenuators rises after stimulation, reaching a peak within an hour of the initial stimulation and thereby defining the window of active signalling. Transcriptional up-regulation of this group of attenuators affects multiple processes. For example, EGF treatment induces expression of the suppressor of cytokine signalling-5 (SOCS5) that leads to a marked reduction in the levels of the receptor by promoting ErbB1 degradation (Kario E *et al 2005).* A further example of a negative-feedback loop that functions downstream of the receptor and is common to many mitogens, including ErbB ligands, involves the inducible expression of dual-specificity phosphatases of MAPKs, which thereby defines the time frame of MAPK activation.

1.5.6 Loss of System Control

Several pathological conditions (for example, cancer, psoriasis and atherosclerosis) harness the ErbB network by de-regulating its essential hubs. Gain-of-function perturbations may incapacitate system controls in diverse malignancies (see below and Figure 12; Box 3).

1.5.6.1 Kinase-domain mutations and deletions.

Certain heterozygous, somatically acquired ErbB1 mutations in lung cancer correlate with clinical responses to ErbB1-specific kinase inhibitors (Lynch TJ et al 2004, Paez JG et al 2004, Pao W. et al 2004*).* These aberrations, which include deletions, insertions and missense point mutations that stabilize interactions with ATP and kinase inhibitors, concentrate in regulatory regions that surround the ATP-binding cleft of ErbB1.

ErbB1 mutants have been associated with enhanced autophosphorylation and cell survival; this finding provides an explanation as to why kinase inhibitors selectively induce the apoptosis of mutant-expressing cells (Tracy S et al 2004, Sordella R et al 2004). Along with pathway-selective activation, ligand-induced downregulation of ErbB1 mutants seems impaired (Lynch TJ et al 2004, and the association with ErbB3

seems enhanced (Engelman JA et al2005), which is in line with multiple mechanisms of network dysregulation. Although occurring significantly less frequently, cancer-associated kinase-domain mutations have also been reported in ErbB2 (Shigematsu H et al 2005). Consistent with the importance of receptor heterodimers, mutations in ErbB1 and ErbB2 have not been detected in the same tumours.

1.5.6.2 Large deletions in ErbB1.

Brain tumours, especially gliomas, display multiple rearrangements within the ErbB1 gene, including large deletions, point mutations and insertional mutations (Ekstrand A J et al 1992). Up to 20% of glioblastomas show ErbB1 rearrangements and up to 40% of glioma tumours over-express the ErbB1 receptor (Ekstrand AJ et al 1991, Liu L et al 2005). The most frequent mutant, EGFRvIII, lacks the dimerization arm and an essential part of the ligand-binding domain (Ekstrand A J et al 1992), yet this mutant is constitutively active at the plasma membrane and evades downregulation (Huang HS et al1997), thereby bypassing system controls.

1.5.6.3 Receptor over-expression.

ErbB1 over-expression due to gene amplification or increased translation has been reported in diverse tumours, such as lung, pancreas and breast lesions (Nicholson RI et al 2001). In head and neck cancer, ErbB1 over-expression is observed in at least 80% of tumours (Ford AC & Grandis JR 2003), and correlates with a reduction in patient survival rates. Likewise, over-expression of ErbB2 has been reported in breast, lung, pancreas, colon, endometrium and ovarian cancer (Ross JS et al 2003), and it has been associated with a poor prognosis for breast and ovarian cancer patients (Slamon D J et al 1989). Along with high basal auto-phosphorylation, receptor over-expression delays ligand-induced degradation because of the limited capacity of clathrin-mediated endocytosis.

1.5.6.4 Autocrine mechanisms.

Co-expression of an ErbB protein and one or more of its ligands might establish an autocrine loop that drives uncontrolled cell growth. In cancer patients, the autocrine production of TGFα or EGF is associated with reduced survival (Hirai T et al 1998, Tateishi M et al 1990).
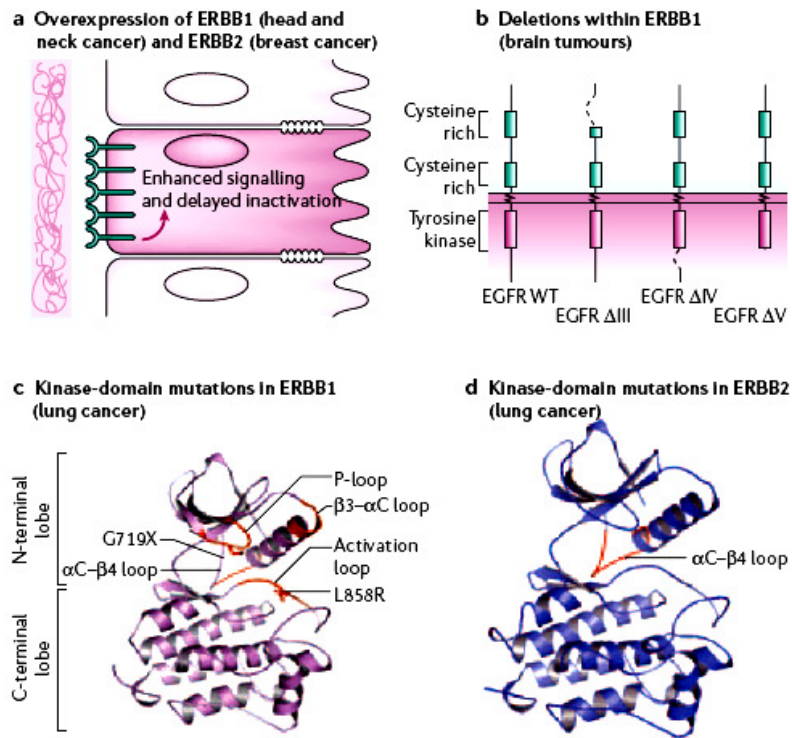
Figure 1.12: Mutiple pathways to oncogenesis. **a** | Over-expression of ErbB receptors, owing primarily to gene amplification, results in the exaggerated activation of signalling pathways and delayed endocytosis. ErbB1 over-expression has been observed in 80% of head and neck tumours (Ford AC & Grandis JR 2003); it correlates with poor prognosis and resistance to therapy. ErbB2 over-expression has been found in breast, lung, pancreas, colon, endometrial and ovarian cancer and it has been frequently associated with an adverse prognostic value (Ross JS et al 2003, Slamon D J et al1989). **b** | Large deletions within ErbB1 that are commonly found in brain tumours create constitutively active protein products that lack parts of the ligand-binding domain, or the C-terminal tail (Shigematsu H *et al* 2005, Ekstrand A J et al 1992). **c** | Multiple short deletions within the 3–αC loop of the ErbB1 kinase domain, as well as within the activation loop, P-loop and αC–4 loop (all marked in red) have been observed in lung cancer. Likewise, mutations of Gly719 and Leu858 are common. These aberrations affect regulatory regions and result in enhanced kinase activity, or altered substrate specificity. The presence of these diverse mutations predicts significant clinical responses to specific kinase inhibitors (Lynch TJ et al 2004, Paez JG et al 2004). **d** | Small duplications within the kinase domain of ErbB2 have been detected in lung cancer and other malignancies. This is an infrequent event of unclear functionality (Shigematsu H *et al* 2005). However, all the mutations that have been identified reside within the αC–4 loop.

1.5.7 Various clinically useful options are now available to target the ErbB system:
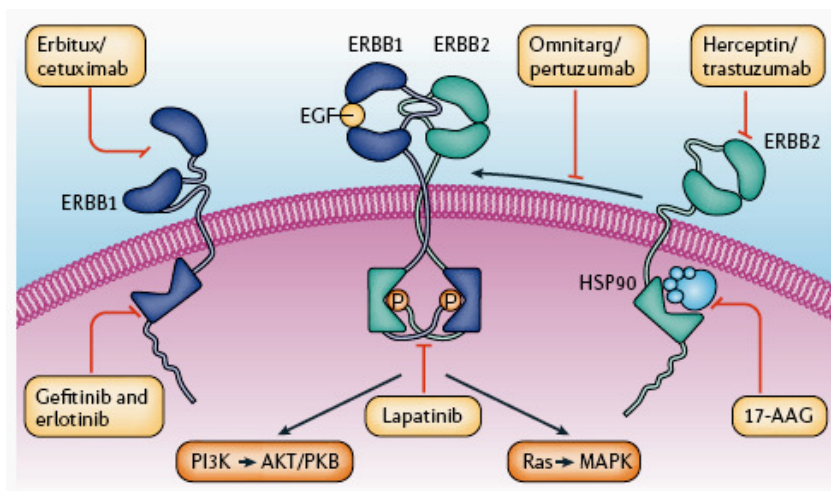
Figure 1.13: The ErbB system can be targeted through multiple means. AKT/PKB, AKT/protein kinase B; EGF, epidermal growth factor; MAPK, mitogen-activated protein kinase; P, phosphate; PI3K, phosphatidylinositol 3-kinase (Citri A, and Yarden Y 2006).

1.5.7.1 Monoclonal antibodies

Therapeutic antibodies function by recruiting cytotoxic lymphocytes (Clynes RA et al 2000), as well as through direct effects on signalling in the target tumour cell (Nagata Y et al 2004). Antibodies in use at present are trastuzumab (Herceptin; Genentech; which targets ErbB2) for treatment of breast tumours, and cetuximab (Erbitux; Bristol Myers Squibb (BMS)/ImClone; which targets ErbB1) for treatment of colorectal cancer. Novel experimental therapeutic approaches target the heterodimerization of ErbB2 (Omnitarg/pertuzumab), or use antibody combinations (Spiridon CI et al 2002) to promote receptor degradation (Friedman LM et al 2005).

1.5.7.2 Tyrosine-kinase inhibitors

These small molecules block the nucleotide-binding pocket of ErbB proteins. Two ErbB1-specific drugs, gefitinib (Iressa; AstraZeneca) and erlotinib (Tarceva; Genentech/OSI), were recently approved for the treatment of non-small-cell lung cancer, and have been shown to be effective against tumours that express catalytically hyperactive ErbB1 mutants (Lynch TJ et al 2004, Paez JG et al 2004). A more effective strategy may be to use dual-specificity inhibitors, such as Lapatinib (GlaxoSmithKline),

CI-1033 (Pfizer) and EKB-569 (Wyeth-Ayerst Research), thereby targeting both ErbB1 and ErbB2 (Xia W *et al* 2002).

1.5.7.3 Inhibitors of heat-shock protein-90 (HSP90)

ErbB2 is strictly dependent on the HSP90 chaperone complex for maintenance of its stability, identifying an Achilles heel of the ErbB system (Neckers L & Ivy SP 2003). The clinical efficacy of HSP90 inhibitors, such as 17-N-allylamino-17-demethoxygeldanamycin (17-AAG), is under evaluation. However, a novel approach for the specific targeting of ErbB2 for proteasomal degradation involves the use of kinase inhibitors that dissociate HSP90 from ErbB2 (Citri A *et al* 2002).

1.5.7.4 Drug combination

Genetic heterogeneity and cellular dynamics are thought to underlie tumour resistance to drugs, but combinations of non-cross-resistant treatment regimens might prevent its recurrence (Goldie JH & Coldman AJ 1979). Therapeutic strategies that target various components of the ErbB signalling network might be beneficial (Ye D et al 1999). Integration of anti-ErbB drugs with conventional anti-cancer chemotherapy and radiotherapy have been shown to improve outcome (Slamon DJ et al 2001) and overcome drug resistance (Shou J et al 2004).

1.6 Epidermal growth factor receptor and DNA double strand break repair

Cancer management often includes radiotherapy which, though effective, rarely leads to cure on its own. Combined treatment with two DNA-damaging agents, physical (ionising radiation) and chemical (e.g. alkylating agent), enhances the lethal effect in cancer cells but at the same time considerably increases the adverse effects due to damage to normal tissues. An efficacious and better tolerated option may be to combine X-ray therapy with drugs of low general toxicity that would specifically enhance the lethal effect of local irradiation. Of special interest is the relationship between cellular signalling and DSB (DNA double strand break) repair, which may be amenable to manipulation in order to improve radio-sensitivity of tumours in vivo (Schmidt-Ullrich RK 2000). Numerous reports point to a high efficiency of radio-sensitisation by

inhibition of growth factor-dependent receptor tyrosine kinases (RTKs) (Szumiel I 2006).

These kinases appear to be suitable targets for therapy, as most aggressive and invasive human cancers over-express them (e.g. Nagane M et al 2001, Ohgaki H 2005). In monotherapy of cancers with over-expressed RTKs, improvement in outcomes is achieved by using specific receptor antibodies and RTK inhibitors (RTKI; e.g. Raben D et al 2004, Barker FG et al 2nd 2001], Chinnaiyan P et al 2005). RTKs, of special interest include the receptor kinases of the ErbB family, including EGFR, which form homo- or heterodimers after binding ligands (Ohgaki H 2005).

EGFR activation by ionising radiation is an important part of the radioprotective cellular defence system. One effect of reactive oxygen species generated by ionising radiation is inactivation of a redox-sensitive, cysteine-based protein-tyrosine phosphatase. This causes a shift in the equilibrium between the phosphorylated and dephosphorylated forms of EGFR and stimulates the kinase activity of the receptor in a ligand-independent manner. The same mechanism operates in the case of UV-A, UV-B, UV-C, hydrogen peroxide (Knebel A 1996) and pro-oxidant chemical agents, e.g. menadione (Abdelmohsen K et al 2003).

Another possible mechanism of EGFR activation in the irradiated cell is by upregulation of autocrine/paracrine secretion of EGFR ligands (Dent P et al 2003) and Shvartsman SY et al 2002.

After exposure to X- or γ-ray doses 1–5 Gy (a dose range used in cancer radiotherapy), multiple signalling pathways are activated; among them, EGFR activation and increased signalling through the Ras–MAPK pathway take place (review in (Dent P et al 2003). This EGFR initiated signalling is the source of anti-apoptotic (survival) signals and of increased cellular radioresistance, as measured by survival or chromosomal aberration frequency. The latter end-point very often is applied to estimate the response to irradiation and it shows the cell's ability to repair DNA.

In concert with the initiation of signalling pathways and EGFR internalisation, nuclear translocation of DSB repair proteins, including DNA-PK$_{CS}$ from the cytoplasmic stores takes place. This ensures an immediate increase in activity of the main repair system

necessary after X-irradiation, NHEJ. Efficiency of such defence may vary between cell types, depending on the status of EGFR, on how many supplementary DNA-PK subunits are stored for use under stress conditions, to what extent does the cell rely on D-NHEJ for DSB repair (this also depends on position in the cell cycle) and how effective is the translocation machinery. Figure 1.14 presents a diagram of the events that are believed to take place in the X-irradiated cell and involve EGFR and DNA-PK actions and interactions.
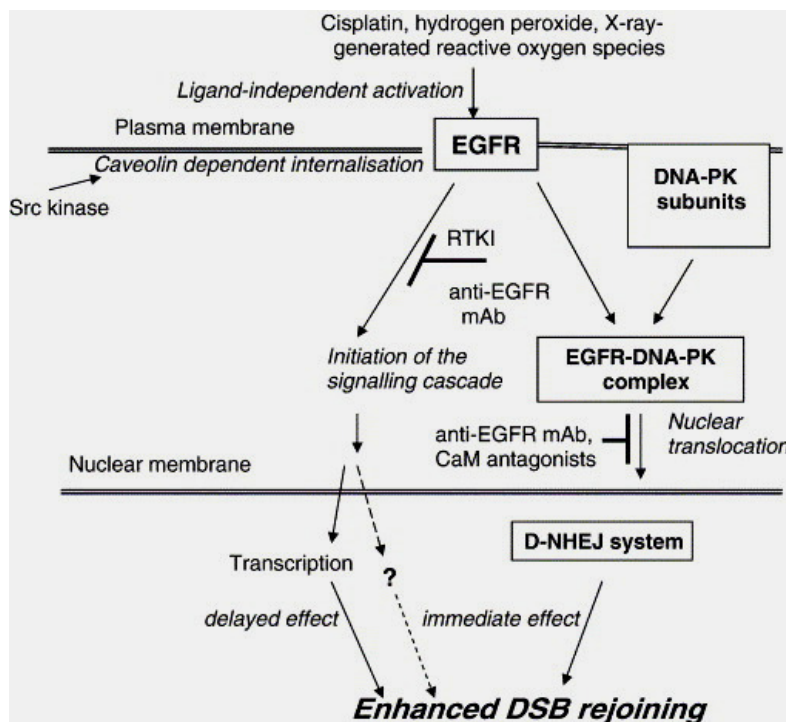
Figure 1.14: Diagram representing the hypothetical relations between EGFR activation and DSB repair (Szumiel I 2006).

Although there is evidence to support the existence of direct and indirect EGFR/DNA-PK interactions modulating DNA double strand break repair, much further work is needed to confirm the reported observations and to define the pre-requirements for EGFR–DNA-PK interaction. Furthermore, very little is known about DNA damage repair in neuroendocrine tumours or cell lines.

Understanding the mechanism of action of EGFR inhibitors is important in devising a rationale for combined radio- and chemotherapy since these inhibitors are being increasingly applied in combination with DNA-damaging agents. It may be expected that their efficiency can be enhanced by a suitable drug combination, thus representing a significant contribution to cancer therapy.

1.7 EGFR and Neuroendocrine Tumours

EGFR has been shown to be expressed by neuroendocrine tumours, in various small scale studies (see chapter 2). Furthermore, a recent study of neuroendocrine tumour cell lines has demonstrated promising effects of EGFR inhibition using the EGFR-specific tyrosine kinase inhibitor gefitinib. In human insulinoma (CM) cells, in human pancreatic carcinoid (BON) cells and in NE tumour cells of the gut (STC-1), gefitinib induced a time- and dose-dependent growth inhibition by almost 100%. The anti-proliferative potency of gefitinib correlated with the proliferation rate of the tumour cells. The IC(50) value of gefitinib was 4.7+/-0.6 microM in the fast-growing CM cells, still 16.8+/-0.4 microM in the moderate-growing BON cells, and up to 31.5+/-2.5 microM in the slow-growing STC-1 cells. Similarly, the induction of apoptosis and cell-cycle arrest by gefitinib differed according to growth characteristics: fast-growing CM cells displayed a strong G0/G1 arrest in response to gefitinib, while no significant cell-cycle alterations were seen in the slow-growing STC-1. Conversely, the proapoptotic effects of gefitinib, as determined by caspase-3 activation and DNA fragmentation, were most pronounced in the slow-growing STC-1 cells. Thus, EGFR-TK inhibition appears to be a promising novel approach for the treatment of NE tumour disease. (Höpfner M et al 2003)

1.7.1 Rationale for studying EGFR in NETs

Current options for treatment of NET patients, such as targeted radiotherapy and chemo-embolisation, should theoretically lead to marked reductions in tumour lesions and prolonged disease control. However, their efficacy is curtailed by dose limiting side effects and emergence of therapy resistant tumour clones.

The general aim of anti-tumour therapies is to induce sufficient tumour cell damage to activate tumour apoptosis pathways. However, not all severely damaged tumour cells follow this pathway. Some tumour cells are able to circumvent apoptosis through the activation of powerful signals which lead to cell repair and survival. Many studies point to EGFR activation, through ligand-dependent as well as ligand-independent means, to be a key factor in cell repair and survival. These insights are further reinforced by phase III clinical trials demonstrating improvements in tumour response rates and survival when anti-EGFR therapy is combined with chemotherapy or radiotherapy. Furthermore,

combination therapy does not lead to potentiation of chemotherapy/radiotherapy-associated side effects, although it can be responsible for the development of severe acne in some patients.

EGFR has been shown to be over-expressed in most tumour-types, when tested for. Moreover, its over-expression is related to impaired survival. EGFR, therefore, seems to be an excellent subject for further study in relation to NETs.

1.8   Aims of this thesis

1) Determine the role of EGFR expression and activation in neuroendocrine tumours by analysing histological samples from NET patients.

2) Study the molecular pathways mediating the effects of EGFR activation, using neuroendocrine tumour cell lines.

3) Improve sensitivity of somatostatin receptor targeted scintigraphy imaging.

4) Determine prognostic value of alpha-fetoprotein, hCGβ, and other commonly measured tumour markers in neuroendocrine tumours.

Chapter 2:

Epidermal growth factor receptor expression and activation in neuroendocrine tumours

EGFR is over-expressed by most tumour types in which it has been tested. Furthermore, it is suggested that expression is related to worse prognosis. Using cell lines with neuroendocrine differentiation EGFR has been demonstrated to act through cellular activation pathways in which Akt and ERK1/2 activation forms a key step. This chapter details the immunohistochemical study of neuroendocrine tumour tissue. Consecutive tumour slides from 96 patients were used to determine the expression of EGFR, its activation, and the activation of Akt and ERK1/2, molecules involved in the downstream signalling following EGFR activation.

Furthermore, the effects of EGFR expression, its activation, and the activation of Akt and ERK1/2 were correlated with survival.

Chapter 3:

Effects of EGFR inhibition on EGFR/DNA-PK$_{CS}$ interactions in neuroendocrine tumour cell lines

EGFR inhibition has been shown to impair survival and proliferation in cell lines with neuroendocrine differentiation. This chapter details experiments performed to determine the molecular mechanisms for these effects. In particular the effects of EGFR inhibition and the subsequent EGFR/DNA-PK interactions were studied using immunoprecipitation and western blotting techniques. Also, the effects of EGFR inhibition and the subsequent effect on DNA-PK protein expression and localisation were studied using immunoblotting, immunofluorescence as well as nuclear fractionation and western blotting techniques.

Chapter 4:

The role of ^{99m}Technetium-depreotide in the management of neuroendocrine tumours

This chapter details the role of ^{99m}Technetium-depreotide, a somatostatin analogue, in imaging neuroendocrine tumours which are negative with 'standard' ^{111}In-pentetreotide (OctreoScan®) scintigraphy. There are 5 somatostatin receptor subtypes (1-5) with SSTR2 being the most widely expressed in NETs and commonly utilised for diagnostic and treatment purposes. However OctreoScan® is not always positive highlighting the lack of SSTR2 by some NETs. ^{99m}Technetium-depreotide has an expanded SSTR subtype affinity, through binding SSTR sub-types 2/3/5, and may be positive in OctreoScan® negative cases. We examined the frequency, strength, and pattern of positivity of ^{99m}Technetium-depreotide scans in OctreoScan® negative patients in order to determine the utility of ^{99m}Technetium-depreotide in improving the sensitivity of SSTR scintigraphy as an imaging modality.

Chapter 5:

The role of alpha-fetoprotein and hCGβ as prognostic tumour markers in neuroendocrine tumours.

Many generalised and specific serum and urinary biochemical markers are measured in NET patients. Some of these markers, such as CgA, 5HIAA gastrin, insulin etc, are helpful in arriving at the diagnosis of NET. They may also alert the physician to changes in tumour biology, as well as informing on the efficacy of any given anti-

tumour therapy. CgA and neurokinin-A in particular may also provide prognostic information.

Current internationally accepted guidelines for the management of NETs also recommend the measurement of serum alpha fetoprotein and human chorionic gonadotrophin-β. However their role and value in NET management is not clear. We have analysed, using the large Royal Free Hospital NET database, the prognostic significance of these two tumour markers.

Chapter 6:
Discussion and conclusion

CHAPTER 2

Epidermal growth factor receptor expression and activation in neuroendocrine tumours

Published as paper in:

Tahir Shah, Daniel Hochhauser, Richard Frow, Alberto Quaglia, Amar Paul Dhillon, Martyn Caplin

2.1 Introduction

Epidermal growth factor receptor (EGFR), the first ErbB receptor family member to be described and sequenced (Ullrich A et al 2004), is a large (175kDa) membrane glycoprotein with a trans-membrane lipophilic segment and a cytoplasmic tyrosine kinase segment flanked by regulatory segments (Lazarides E 1984, Schlessinger J 1998, Yarden Y 2001, Groenen LC et al 1994). The ErbB receptor family comprise 3 other related receptors: ErbB2 (HER2/neu); ErbB3 and ErbB4 (Yarden Y 2001). EGFR ligands, such as EGF and TGFα, are synthesised as membrane-anchored precursor forms which are shed by metalloproteinase-cleavage to generate soluble ligands. Both the membrane anchored isoforms and the soluble growth factors may act as biologically active ligands, thereby inducing: juxtacrine, autocrine, paracrine, and/or endocrine signalling (Singh AB 2005). Ligand binding leads to receptor activation and auto-phosphorylation of tyrosine residues located in the carboxyl region of the receptor, and results in the recruitment and phosphorylation of several intracellular substrates (Ullrich A et al 2004, Cochet C et al 1988, Heldin CH 1995, Schlessinger J 1992, Pazin MJ 1992, Ullrich A 1990).

Two major pathways mediating EGFR signalling require the activation of intracellular signalling molecules ERK1/2 and PKB/Akt, leading to enhanced: cell survival; proliferation; transformation and motility (Schlessinger J 2000). Over-expression of EGFR and its natural ligands results in activation of these receptors through autocrine stimulation, leading to increased cell growth signalling in many types of cancer (Rusch V et al 1996, Hirono Y et al 1995). This is likely to be the reason for the association of EGFR over-expression with early recurrence, metastasis, and significantly lower patient survival (Lei W et al 1995).

EGFR inhibition, by either humanised anti-EGFR antibodies or orally active small molecule ATP-competitive inhibitors of the receptor tyrosine kinase (tyrosine kinase inhibitors [TKIs]), is now possible. This approach was successful *in vitro*, using tumour cell lines, and *in-vivo*, using human tumour cells grafted into athymic mice (Shintani S et al 2003, Friedmann B et al 2004). Subsequent clinical studies have been promising. In particular cetuximab, a humanised anti-EGFR antibody, in combination with radiotherapy for locoregionally advanced head and neck cancer and in combination with irinotecan in colon cancer, has provided improved response and survival rates. Meanwhile the small molecule receptor TKIs, gefitinib and erlotinib, have demonstrated

activity in non-small cell lung cancer (Bonner JA et al 2004, Cunningham D et al 2004, Lynch TJ et al 2004, Paez JG et al 2004)**.**

Neuroendocrine tumours (NETs) are an often slowly progressing heterogeneous group of tumours that have been postulated to originate from a common precursor cell population (Rindi G et al 2001). NETs can be subdivided, according to the site of origin, into tumours of the foregut (medullary thyroid cancer, bronchus, pancreas, stomach, proximal duodenum), midgut (distal duodenum, jejunum, ileum, appendix, and proximal colon), and hindgut (distal colon and rectum). They tend to be diagnosed fairly late in the course of the disease often having already metastasised (Perry RR 1995, Gibril F et al 1995). Somatostatin analogues are the mainstay of symptomatic treatment, but these agents have minor anti-tumour effect. Chemotherapy has shown efficacy in managing NETs of foregut, including pancreatic, origin but is of limited benefit in mid-gut and hindgut carcinoid tumours (Modlin IM 1997, Oberg K et al 1987, Moertel CG et al 1992). Often treatments such as alpha interferon and radionuclide therapy (i.e.^{131}I-mIBG and ^{90}Y-DOTA octreotide) may be useful, but objective response rates are disappointing. When the tumour is unresectable, treatment is aimed at extending survival by affecting tumour reduction or limiting tumour growth. Thus there is need for new agents capable of reversing or slowing the progress of NETs.

EGFR has been shown, in small studies, to be expressed by NETs. Further work with neuroendocrine tumour cell lines has shown that inhibition of EGFR or interference with the intracellular transduction of EGFR-activation related signalling causes potent anti-tumour effects related to inhibition of the downstream signalling molecules ERK and Akt (Hopfner M et al 2003, Song C et al 2002, Peghini PL et al 2002).

The aim of this study was to assess EGFR expression in tumour tissue from NET patients and to determine the activation of the downstream signalling molecules ERK1/2 and Akt, which are mediators of cell survival and proliferation signals.

2.2   Patients and Methods

Human breast cancer tissue was used to determine the optimum pre-treatment conditions and to determine optimum antibody concentrations for use. Human breast cancer tissue was also used for control purposes as it is known to express EGFR and is easily available *(figure 2.1).* Consecutive samples of formalin fixed paraffin embedded

tumour tissue were available from 98 patients with a histologically confirmed diagnosis of neuroendocrine tumour. Tumour tissue was available from 77 patients who had undergone an operation and tumour resection with a further 21 samples from tumour biopsies. All major NET subtypes were represented: foregut – 39 patients; midgut – 42 patients; hindgut – 4 patients; paraganglioma – 5 patients; and NETs of unknown origin – 4 patients.

The study was performed under the auspices of the Royal Free Hospital Pathology Department ethics recommendations for studies on archive histology samples. 3μm sections of tumour tissue were de-waxed in xylene for 10 minutes, dehydrated in alcohol and then rinsed in distilled water for 5 minutes. Endogenous peroxidase activity was blocked by incubation in 1% hydrogen peroxide, diluted in acetone, for 10 minutes. Pre-treatment: slides were placed in a plastic rack, immersed fully in pre-heated citrate buffer and micro-waved at full power for 5 minutes (for EGFR IHC), 5 minutes (for ERK IHC) and 10 minutes (for p-EGFR IHC). No pre-treatment was necessary for Akt IHC. Sections were sequentially incubated with avidin and biotin solutions for 10 minutes each in order to block avidin binding protein. Non-specific binding was minimised by incubating the sections with 10% normal goat serum, in phosphate buffered saline (PBS), for 30 minutes. PBS was used for washing the sections between each stage.

Primary antibodies:

1] anti-phospho-AKT antibody ab8932, specific for S473 phosphorylated AKT, was purchased from Abcam Ltd Cambridge, UK.

2] anti-EGFR rabbit polyclonal antibody ab2430 (immunogen: synthetic peptide EDMDDVVDADEY, corresponding to C terminal amino acids 1005 – 1016 of EGFR) was purchased from Abcam Ltd, Cambridge, UK.

3] anti-phospho-EGFR mouse monoclonal antibody 1H12, specific for Tyr1068 phosphorylated EGFR and manufactured by Cell Signalling Technology, was purchased from New England Biolabs UK Ltd, Hitchin, UK.

4] anti-diphosphorylatedERK1&2 mouse monoclonal antibody (M9692) was obtained from Sigma-Aldridge Co Ltd, Gillingham, UK.

Antibodies were used at 1 in 100 dilutions in PBS, except for anti-phosphoEGFR, which was used at 1 in 500 dilution. All primary antibodies were incubated overnight at 4°C. Biotinylated 2° antibody (DAKO StreptABComplex / HRP Duet, mouse / rabbit;

DK – 2600 Glostrup, Denmark) was used at 1 in 100 dilution, with the slides being incubated for 30 minutes. The antibody binding was visualised by using DAB peroxidase substrate kit from Vector Laboratories Inc. The sections were counterstained with Mayer's haematoxylin for 5 minutes.

Breast carcinoma stained strongly positive for all four antibodies and was therefore used for optimising the pre-treatment and staining methods and subsequently used as control tissue for all four antibodies. The negative controls consisted of i) omitting the primary antibody; ii) using species and sub-type matched, but non-specific, control antibodies. Cytotoxicity of drugs alone or in combination was determined by the Sulphorhodamine B (SRB) proliferation assay as described in Section 2.4.1. Experiments were largely carried out on MCF-7 cells. This is a human breast adenocarcinoma cell line established from a pleural effusion from a 69 year female Caucasian (Soule *et al.*, 1973). The line exhibits some features of differentiated mammary epithelium including oestradiol synthesis and may carry B or C type retrovirus (Zhang *et al.*, 1993). Cells express the wild-type and variant oestrogen receptors as well as the progesterone receptor (ECACC, 86012803). MCF-7 cells express functional EGFR of a magnitude of approximately 250,000 EGF binding sites per cell (Ciardiello *et al.*, 1999).

2.2.1 Histological Interpretation

Tumours were classified according to their site of origin, level of differentiation, and their mitotic index. Two examiners (Richard Frow [trainee histopathologist] and Tahir Shah) performed the interpretation of immunohistochemical staining for EGFR, p-EGFR, p-Akt, and p-ERK1/2. The examiners were blinded to the identity of the samples, and their findings were compared for the level of concordance. Any discordant results were then reviewed to reach agreement or determine an average value for the disputed sections. Quality control advice was provided by Professor Dhillon (histopathologist). The intensity of staining was compared to the intensity of staining of positive controls for each protein tested. Slides were graded for the density of staining: 0 = negative; 1 = weak staining; 2 = moderate staining; 3 = strong staining. The percentage of tumour cells staining positive were determined by randomly selecting 10 high power fields per slide, when possible, and determining the average percentage of positive staining cells. The extent of tumour staining was scored as follows: 1 = <25% cells staining positive; 2 = 25-75% of cells positive; 3 = >75% positive. The product of

the density of staining and the percentage of tumour cells staining positive was used as the histological score giving final values of 0, 1, 2, 3, 4, 6, and 9 (Iddon J et al 2000 32).

2.3   Results

Tumour tissue was available from 98 patients with histologically confirmed diagnosis of NET. 94 of 98 (96%) patients were positive for EGFR expression. The staining was predominantly cytoplasmic and perinuclear in the tumour cells. Vascular endothelial cells also stained positive and acted as additional internal positive controls.62 of 98 (63%) patients were positive for p-EGFR expression. The staining was primarily cytoplasmic, with strong positive staining of vascular endothelium.74 of 98 (76%) were positive for p-Akt. The tumour cells displayed positive cytoplasmic staining, together with strong positive staining of vascular endothelium. 94 of 98 (96%) were positive for p-ERK1/2. The tumour cells displayed nuclear as well as cytoplasmic staining together with positive staining of vascular endothelium *(figure 2.2).*

Staining for all 4 markers tested was generally restricted to tumour cells. However, strong positive staining was seen in blood vessels throughout the tissue samples, including in areas of normal tissue. Tumour grade could be assessed for 76 of 98 patients who had tissue available for MIB-1 staining. Of these 47 were classified as low grade; 9 as intermediate grade; and, 20 as high grade. Multi-variant statistical analysis did not show any correlation between tumour grade, EGFR expression, EGFR activation and either Akt activation or ERK1/2 activation.

Results for the 4 markers were subdivided according to histological scores for purposes of statistical comparisons *(figure 2.3).* This revealed correlations between the histological scores (i.e. the strength and extent of extent) for activated EGFR and activated forms of Akt as well as ERK1/2:

p-EGFR and p-Akt – correlation coefficient = 0.386, p = > 0.0001

p-EGFR and p-ERK1/2 – correlation coefficient = 0.322, p value = 0.001

Furthermore, there was correlation between the histological score for p-Akt and p-ERK1/2, with correlation coefficient of 0.466 and p value of > 0.0001.

There was no correlation between the immunostaining data and tumour grade.

The majority of tissue samples were less than 4 years old, and statistically there was no deterioration in the quality of staining of the samples greater than 4 years old as compared to the newer samples.
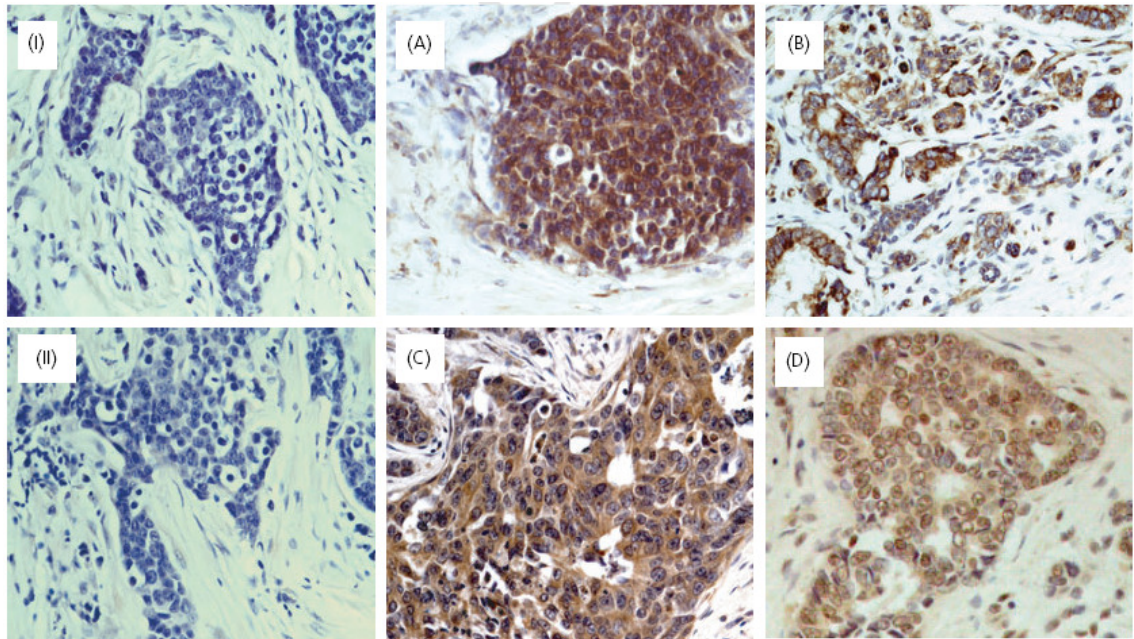
Figure 2.1: Immunohistochemical staining of breast carcinoma as controls, 200X magnification. Representative negative controls: I- with the omission of primary antibody; and II - with non-specific antibody used as the primary. Representative positive controls: A – EGFR; B – pEGFR; C – pAkt; D – pERK1/2.
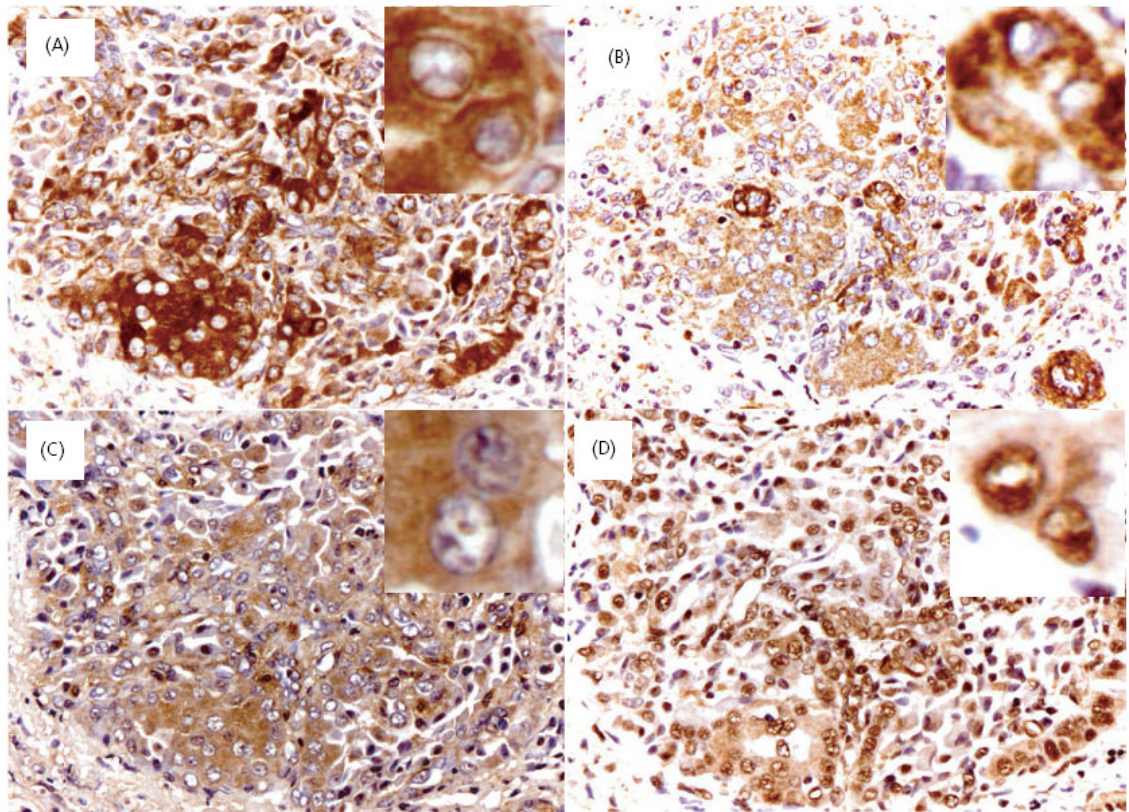
Figure 2.2: Immunohistochemical staining images, 200X magnification with close ups (insets) to demonstrate staining patterns. Consecutive tumour tissue slides, from the same field, of a pancreatic neuroendocrine tumour liver metastasis: A – EGFR: cytoplasmic and perinuclear staining; B – p-EGFR: cytoplasmic and perinuclear staining; C – p-Akt: cytoplasmic staining; D – p-ERK1/2: nuclear and cytoplasmic staining.
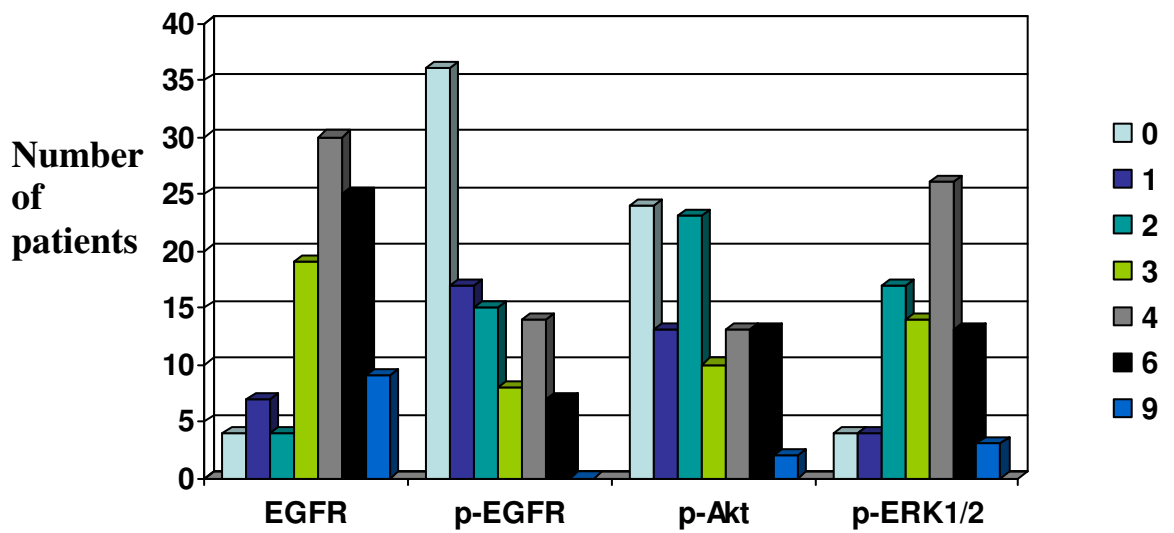
Figure 2.3: Breakdown of tumour samples according to the overall score for the immunohistochemical staining. The method of scoring for immunohistochemical staining is described in the methods. IHC score – immunohistochemical score

2.4   Discussion

EGFR plays an important role in regulating cellular processes such as proliferation, differentiation, and survival and is central to the maintenance of normal epidermal tissues where its expression is highly regulated. When its function becomes deregulated, leading to increased signalling through molecules such as Akt and ERK1/2, it contributes to the growth and survival of cancer cells and as such is recognised as an important target for cancer therapy. Indeed EGFR is prominently expressed in a variety of human solid tumours, including colorectal cancer, head and neck squamous cell cancer and non-small cell lung cancer (Grandis et al 1996, Goldstein 2001, V. Rusch et al 1997). Although the relationship between EGFR status and prognosis is not completely understood, EGFR expression in tumours is usually associated with more aggressive disease, increased resistance to chemotherapy and radiotherapy, increased metastasis, poor clinical prognosis and decreased survival (Neskovic-Konstantinovic et al 1999, Nicholson et al 2001, Ang et al 2002).

We undertook a large-scale immunohistochemical study of the expression of EGFR in order to assess the EGFR associated cellular activation pathways, in tumour tissue from 98 NET patients.

Tumour samples were available either from primary sites or from a site of metastasis. Paired tissue samples from primary site as well as from synchronous metastases were not usually available, which prevented a comparative study of EGFR expression in primary versus secondary sites. Immunostaining demonstrated expression of EGFR in a high proportion of the NET tissue samples studied, as well as its activation in the majority of these cases, with the pattern of EGFR expression being perinuclear and cytoplasmic. Although EGFR is classically reported to have a membranous distribution, its expression has been shown to be mainly cytoplasmic in a previous immunohistochemical staining study of lung neuroendocrine tumour tissue (Rusch VW et al 1996). Also, recent data on patterns of EGFR expression in A549 human bronchial carcinoma cells has demonstrated a perinuclear distribution during unstressed growth conditions (Dittmann K et al 2005).

The modulation of EGFR signalling pathways by gefitinib has been shown to lead to dephosphorylation and transcriptional down-regulation of ERK1/2 in NET cell lines (Hopfner M et al 2003). Furthermore, disruption of EGFR signalling can significantly

64

attenuate EGFR mediated activation of ERK1/2 and Akt in cell lines (Song C et al 2002). This study demonstrates the activation of Akt and ERK1/2 in NET tissue, and shows this activation to be related to activation of EGFR. Thus providing evidence for similar cellular activation mechanisms in NETs to those previously reported in dynamic studies using neuroendocrine tumour cell lines (Hopfner M et al 2003, Song C et al 2002). We also assessed the degree of correlation, between the histological score for p-EGFR and the activated forms of downstream signalling molecules, p-Akt and p-ERK1/2. This demonstrated a moderate but highly statistically significant linkage. The moderate nature can be explained by the fact that these intracellular signalling molecules are mediators of messages from multiple origins including, but not exclusive to, EGFR. Furthermore, the higher correlation coefficient between the activated forms of Akt and ERK1/2 can be taken as evidence that EGFR activation leads to the simultaneous activation of the two separate signalling pathways involving Akt and ERK1/2, as predicted from dynamic studies of EGFR activation pathways using cellular models (Song C et al 2002). Additionally, a recent IHC study of EGFR expression and activation in NET tissue has demonstrated that the presence of EGFR in its activated form is a predictor for poor prognosis, not the overall expression of EGFR (Papouchado et al 2005). These findings, together with our large-scale study demonstrating downstream signalling following EGFR activation, highlight the importance of EGFR signalling in NETs as well as confirming the importance of EGFR as target for anti-tumour therapy. This work also highlights Akt/PKB and ERK1/2, two molecules well known to be involved in tumour cell survival and proliferation, as future targets for anti-tumour therapy in NET patients.

EGFR expression and activity, and therefore its influence on cancer cell survival, can be amplified by a number of mechanisms other than increased receptor expression (C.L. Arteaga 2002). These include an increase in ligand expression, interaction with human epidermal receptor-2 (HER2) to form highly stable and potent EGFR–HER2 heterodimers, and the expression of constitutively activated mutant EGFRs. Further work is under way by our group to characterise the expression of the entire EGFR family of receptors and their relationship to tumour characteristics as well as patient survival.

Further advances in EGFR targeted anti-tumour therapy may follow the full characterisation of EGFR mutations, including the commonly occurring EGFRvIII deletion mutation, which can determine tumour behaviour as well as response to anti-EGFR therapy. Assessment for the presence of a number of mutations occurring at the region encoding for the ATP binding site of EGFR, which result in enhanced EGFR activation as well as a higher susceptibility to TKIs (Lynch TJ et al 2004, Paez JG et al 2004), has also been carried out. These ATP binding site mutations, however, have been shown not to occur in neuroendocrine tumours (Gilbert JA et al 2005), whereas the role of EGFRvIII in neuroendocrine tumours is yet to be determined.

Small molecule inhibitors of Akt and ERK1/2 are also currently under development. The demonstration of activated Akt in a majority of NET samples and activated ERK1/2 in virtually all the NET tissue samples signals a promising future for the role of Akt and ERK1/2 inhibitors in the treatment of NET patients.

In conclusion we have demonstrated expression of EGFR by NET tissue, the presence of activated EGFR and the subsequent activation of intracellular signalling pathways as demonstrated by the immunostaining for p-Akt and p-ERK1/2 in our NET tissue samples. This data provides a basis for the trial of anti-EGFR therapy in NET patients. Furthermore, the availability of specific inhibitors of ERK1/2 and Akt makes them attractive targets for assessment in neuroendocrine tumours.

Rationale for using immunohistochemistry:

Several standard techniques are available for the detection of EGFR expression in tumours, including protein expression assays (e.g., IHC, Western blot analysis, enzyme-linked immunosorbent assay (ELISA), fluorescence-activated cell sorting (FACS), RNA transcript assays (e.g., Northern blot analysis, reverse transcriptase polymerase chain reaction (RT-PCR) and DNA assays (e.g., quantitative PCR, Southern blot analysis and fluorescence *in situ* hybridisation (FISH). However these methods have their drawbacks such as loss of tumour architecture, technically difficult and requiring specialist equipment, or not being able to measure the protein product directly.

IHC is the most commonly used method for determining EGFR expression, which has been used in the majority of published studies for EGFR expression in human tumours. Its widespread use is mainly due to it being a relatively quick technique that utilises commonly available reagents and equipment. Unlike extractive methods, IHC also has

the benefit of preserving cellular morphology and tissue integrity and this can provide additional, important information regarding the distribution of the target molecule within the tissue sample.

CHAPTER 3

GEFITINIB AND EGFR/DNA-PK$_{CS}$ INTERACTIONS IN NEUROENDOCRINE TUMOUR CELL LINES

3.1 Introduction

Combined treatment with DNA-damaging agents, physical (ionising radiation) and chemical (e.g. alkylating agent), enhances their lethal effect in cancer cells but at the expense of considerably increased adverse effects due to damage to the normal tissues. A possible improvement in outcomes of combined therapy may be achieved by combining X-rays treatment with drugs of low general toxicity that would specifically enhance the lethal effect of local irradiation without significantly increasing side-effects. Of particular interest is the relationship between cellular signalling and DSB (DNA double strand break) repair, because they might be applied for modulating radiosensitivity in vivo (Schmidt-Ullrich RK et al 2000). Numerous reports (Harari PM 2000 & 2001, Friedmann B et al 2004, Raben D et al 2004) point to enhanced radiosensitisation by inhibition of growth factor-dependent receptor tyrosine kinases (RTKs) such as those of the ErbB family.

The DNA-dependent protein kinase (DNA-PK) is a serine/threonine kinase that consists of a 350-kDa catalytic subunit and a heterodimeric regulatory complex Ku70/80 and can *in vitro* phosphorylate a number of transcription factors and DNA binding proteins, including p53, the RNA polymerase II carboxyl-terminal domain, replication factor A, and the Ku (Carter T et al 1990, Jackson SP 1995, Weaver DT 1995, Reeves WH 1997). DNA-PK is believed to play a major role in repairing double strand DNA breaks and V(D)J recombination, as mutations of DNA-PK$_{CS}$ (catalytic subunit) cause both x-ray sensitivity and defective V(D)J recombination (Baselga J et al 1993, Reeves WH 1997). Since efficient DNA repair may require growth factor signaling (John Mendelsohn 1997, Haimovitz-Friedman A 1991), it became of interest to explore any linkage between EGFR-mediated signaling and DNA-PK pathway.

3.1.1 Stimulation of EGFR by DNA damage

The model of how cells are killed by ionising radiation and their association with events at the plasma membrane are of great interest (Perry RR 1995). In light of the recent experimental data, EGFR activation by ionising radiation is considered to be an important part of the radioprotective cellular defence system.

One effect of reactive oxygen species generated by ionising radiation is inactivation of a redox-sensitive, cysteine-based protein-tyrosine phosphatase. Inactivation of phosphatase causes a shift in the equilibrium between the phosphorylated and dephosphorylated forms of EGFR and stimulates the kinase activity of the receptor in a ligand-independent manner (Chiarugi P 2003). Another possible mechanism of EGFR activation in the irradiated cell is by upregulation of autocrine/paracrine secretion of EGFR ligands (Dent P 2003, Shvartsman SY 2002).

3.1.2 Initiation of the Signalling Kinase Cascade

Exposure to DNA damaging therapies leads to activation of multiple signalling pathways; among them, are EGFR activation and increased signalling through the Ras–MAPK pathway (Dent P 2003). Other EGFR/ERBB downstream signalling pathways involved include:

• phosphatidylinositol 3-OH kinase–protein kinase B (PI3K–PKB) (Shah T et al 2006)

• phospholipase C (PLC) γ-calmodulin-dependent kinase (CaMK) – protein kinase C (PKC)

• janus-activated kinase 2 – signal transducer and activator of transcription (JAK–STAT).

Stimulated signalling results in enhanced proliferation of cells surviving despite cytotoxic treatment, clonogenic cells, and consequently tumour repopulation–an important cause of treatment failure – becomes accelerated. The same signalling initiated by EGFR is the source of anti-apoptotic (survival) signals and of increased cellular radio-resistance, as measured by survival.

There are several methods to interfere with the signalling initiated by EGFR, following DNA damage, leading to decreased cellular radio-resistance. The most clinically advanced methods are:

(a) blockade of the extracellular part of the receptor molecule with monoclonal antibody against the ligand-binding domain, which prevent ligand binding and receptor activation, e.g. chimeric antibody cetuximab (Lammering G et al 2003)

(b) inhibition of the receptor kinase, using small molecule tyrosine kinase inhibitors that compete with ATP e.g. gefitinib (Harari PM 2004)

The addition of gefitinib has been shown to increase inhibition of proliferation, induce apoptosis, and increase antitumor activity *in vitro* and *in vivo* when combined with a variety of chemotherapeutic agents. Similarly, combination with radiation synergistically increases inhibition of proliferation and pro-apoptotic effects *in vitro* and increases tumour growth delay in the treatment of human tumour xenografts (Bianco *et al* 2002; Solomon *et al* 2003; Giocanti *et al* 2004).

3.1.3   EGFR / DNA-PK$_{CS}$ Interactions

The study of EGFR/DNA-PK$_{CS}$ interactions has been a very active field of research leading to numerous insights into tumour biology. The initial study of EGFR inhibition with mAb 225 showed direct binding of DNA-PK$_{CS}$ to EGFR, leading to sequestration of DNA-PK$_{CS}$ in the cytoplasm thereby reducing intra-nuclear DNA-PK$_{CS}$. This reduction in the level of DNA-PK$_{CS}$ in the nucleus is important, as it implies a direct role of EGFR-signalling in maintenance of the nuclear levels of DNA-PK$_{CS}$, and interference in EGFR signalling may result in the impairment of DNA repair activity in the nuclei of anti-EGFR mAb-225 treated cells. (Bandyopadhyay D et al 1998)

Since then there have been many published studies not only on the mechanisms of EGFR/DNA-PK$_{CS}$ interactions, under varying circumstances, but also into EGFR's various other roles including as a transcription factor. Two recent publications from our lab detail the effects of EGFR inhibition, using a small molecule tyrosine kinase inhibitor gefitinib, on EGFR / DNA-PK$_{CS}$ interactions and the downstream effects on DNA damage repair, cellular proliferation and survival. The first study revealed a synergistic effect on growth inhibition when gefitinib treatment was given in combination with cisplatin or etoposide. There was delayed repair of DNA strand breaks after treatment with etoposide combined with gefitinib, and repair of DNA

interstrand crosslinks produced by cisplatin was delayed when concomitantly treated with gefitinib. Immunoprecipation of cell extracts demonstrated that after exposure to gefitinib, there was increased association between EGFR and DNA-PK$_{CS}$ (Friedmann B et al 2004).

The second study specifically investigated the effects of EGFR inhibition by gefitinib on functional activity of DNA-PK$_{CS}$ in cancer cell lines and the interaction between EGFR and DNA-PK$_{CS}$. DNA-PK$_{CS}$ activity was quantitated and expression measured by immunoblotting following gefitinib treatment. Immunoprecipation experiments were done with and without gefitinib in breast carcinoma MCF-7 cells, the AR42J pancreas cell line with high EGFR, and human MDA-453 breast cancer cell line with low EGFR expression. Nuclear and cytoplasmic extracts were immunoblotted with antibody to DNA-PK$_{CS}$ to determine if gefitinib treatment altered cellular expression. Gefitinib treatment reduced DNA-PK$_{CS}$ activity in MCF-7 and AR42J but not MDA-453 cells. Immunoprecipation experiments showed interactions between EGFR and DNA-PK$_{CS}$ in a dose dependent and time dependent manner following gefitinib treatment in MCF-7 and AR42J but not MDA-453 cells. Gefitinib treatment reduced nuclear expression and increased cytosolic expression of DNA-PK$_{CS}$ MCF-7 and AR42J but not MDA-453 cells. Thus the study concluded that gefitinib treatment modulates EGFR and DNA-PK$_{CS}$ association leading to decreased function of DNA-PK$_{CS}$. This is likely to be an important factor in sensitising cancer to chemo and radiotherapy following treatment with inhibitors of the EGFR pathway. (Friedmann BJ et al 2006)

3.1.4   Study of EGFR / DNA-PK$_{CS}$ Interactions in NET cell lines

Neuroendocrine tumours (NETs) are a heterogeneous and rare group of tumours and hence their tumour biology is poorly understood. They tend to be diagnosed fairly late in the course of the disease often having already metastasised (Perry RR 1995, Modlin IM 1997). Treatments such as alpha interferon and radionuclide therapy (i.e.[131]I-mIBG and ^{90}Y-DOTA octreotide) may be useful, but objective response rates are disappointing. When the tumour is unresectable treatment is aimed at extending survival by effecting tumour reduction or limiting tumour growth. Thus there is need for new agents capable of reversing or slowing the progress of NETs.

Our large IHC study demonstrating expression of EGFR, its activation, and the

activation of molecules known to be key members of downstream signalling pathways, namely PKB/Akt and ERK1/2, together with recent publication of an IHC study using tumour tissue from NET patients confirming the poor prognosis associated with EGFR activation, has placed the spotlight on EGFR as a likely target for therapy in NETs. Preliminary work in our laboratory with neuroendocrine tumour cell lines showed that gefitinib could sensitise the cells to the effects of chemotherapy. The promising results with MCF-7 and AR42J cell lines encouraged us to look at EGFR related pathways in these neuroendocrine tumour cell lines in order to gain new insights into the role of EGFR in NETs.

This chapter details work to:

1.   Determine the expression of EGFR in neuroendocrine tumour cell lines.
2.   Determine the expression of DNA-PK$_{CS}$ in neuroendocrine tumour cell lines.
3.   Determine the effects of gefitinib on EGFR activation in neuroendocrine tumour cell lines.
4.   Determine the effect of gefitinib and cetuximab on EGFR / DNA-PK$_{CS}$ interactions in neuroendocrine tumour cell lines.
5.   Determine the effect of EGFR inhibition on DNA-PK$_{CS}$.

3.2   MATERIALS

3.2.1   Chemical Reagents and Drug Source

All reagents and disposables were obtained from Sigma Chemical Co., Poole, UK or VWR International Ltd., Poole, UK unless otherwise stated.

Cytotoxic drugs (Table 3.1) were prepared as stocks in advance, or as fresh prior to individual experiments depending on stability and activity in solution as well as experimental parameters. The concentration ranges used for experiments were modified based on previous personal communications on the cytotoxicity of individual agents where necessary.

Table 3.1: Drugs used in this study.

Drug	Chemical Structure	Stock Solution	Solvent	Supplier
Gefitinib (Iressa[TM], ZD1839)		10mM	DMSO	AstraZeneca
Cetuximab				Merck Pharmaceuticals
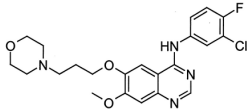
3.2.2 Experimental Cell Lines

African green monkey kidney cell line Cos-7 cells were grown in Dulbecco's MEM (DMEM).

Cell lines used were obtained as shown in Table 3.2. All tissue culture media were supplied by Autogen Bioclear, Calne, UK and were supplemented with 10% Foetal calf serum (FCS) (previously heat-inactivated for 30 minutes at 57°C) and 1% glutamine. The growth medium described for the routine propagation of exponentially growing cell lines is referred to as complete growth medium throughout. Antibodies used are listed in table 3.3.

Cell Line	Origin	Culture Conditions	Supplier
MCF-7	Human Breast Adenocarcinoma – Pleural effusion with hormone receptors. 69 year old Caucasian female.	Dulbecco's Minimal Essential Medium (DMEM)	Cancer Research UK London Research Institute.
A431	Human epithelial carcinoma cell line	DMEM & 10% FBS	Cancer Research UK London Research Institute.
NCI-H727	Pulmonary carcinoid tumour	RPMI + glutamine + 10% FCS	Cancer Research UK London Research Institute.
SHP-77	Pulmonary carcinoid tumour	RPMI + glutamine + 10% FCS	Cancer Research UK London Research Institute.
CRI-G1	Rat islet-cell tumour	DMEM + 10%FCS	Cancer Research UK London Research Institute.
RIN-5F	Rat islet-cell tumour	RPMI + 10%FCS	Cancer Research UK London Research Institute.
BON	Human pancreatic carcinoid	DMEM/F12K + 10%FCS	

Table 3.2: Cell lines used in this study.

Primary Antibodies					
Antibody	Description	Supplier	Antibody	Description	Supplier
EGFR 170KDa	Mouse, Monoclonal	Santa Cruz, UK	PKBα/ AKT 60KDa	Mouse, Monoclonal	Abcam, UK
EGFR 170KDa	Rabbit, Polyclonal	Abcam, UK	P-AKT (Ser-473) 70KDa	Rabbit, Polyclonal	Abcam, UK
P-EGFR (Tyr-845) 175KDa	Rabbit, Polyclonal	Cell Signaling Technology, USA	MAPK 38KDa	Mouse, Monoclonal	Abcam, UK
P-EGFR (Tyr-1045) 175KDa	Rabbit, Polyclonal	Cell Signaling Technology, USA	P-MAPK 43KDa	Rabbit, Polyclonal	Abcam, UK
P-EGFR (Tyr-1068) 175KDa	Rabbit, Polyclonal	Cell Signaling Technology, USA	Bax 22KDa	Mouse, Monoclonal	BD Biosciences, UK
P-EGFR (PY20) 175KDa	Mouse, Monoclonal	BD Biosciences, UK	Bcl-2 26KDa	Rabbit, Polyclonal	BD Biosciences, UK
DNA-PK$_{CS}$ 460KDa	Mouse, Monoclonal	Sigma, UK	Bcl$_{XL}$ 29KDa	Mouse, Monoclonal	BD Biosciences, UK
Ku70 70KDa	Goat, Monoclonal	Abcam, UK	Lamin B1 67KDa	Mouse Monoclonal	Abcam, UK
Her-2 185KDa	Mouse, Monoclonal	Abcam, UK	α-Tubulin 170KDa	Mouse, Monoclonal	Sigma, UK
Secondary Antibodies					
Antibody		Supplier	Antibody		Supplier
HRP-Conjugated Rabbit Anti-Goat		Abcam, UK	HRP-Conjugated Goat Anti-Mouse		BD Biosciences, UK
HRP-Conjugated Goat Anti-Rabbit		Abcam, UK			

Table 3.3: Primary and secondary antibodies used in this study.

3.3   METHODS

3.3.1   Tissue Culture

3.3.1.1 Maintenance of Cell Lines

All cell lines were grown in $50cm^2$ (T50) flasks and maintained at 37^oC with 5% CO_2 in dry incubators (Forma Scientific, UK). All procedures were carried out in Class II MDH biological safety cabinet (Intermed MDH, UK) using aseptic techniques. Exponentially growing cells were maintained at a cell concentration according to the European Collection of Cell Cultures (ECACC), Salisbury, UK.

Cells were routinely passaged at 90% confluence (biweekly). To this end, cells were washed with 10ml of 0.01M phosphate buffered saline (PBS) to remove serum. To detach the cells from the flask 5ml of 1X Trypsin/EDTA (Autogen Bioclear, Calne, UK) was then added for 5 minutes at 37°C. 5ml of complete growth medium was then added to inactivate the trypsin and the cell suspension was pelleted by centrifugation at 1,500rpm for 5 minutes at room temperature. Cells were then resuspended in complete growth medium and re-plated at an appropriate passage ratio for the cell line. The passage number was increased by one. Cells were discarded after approximately 25 passages and fresh cells were taken from the initial passage number used.

3.3.1.2 Cell Count

Trypsinised cells were resuspended in 10ml of complete growth medium and counted using a haemocytometer. To this end, 20μl of cell suspension was mixed with trypan blue (Sigma, UK) to exclude dead cells and the cell number was determined for each of five separate $1mm^2$ fields. The average was multiplied by $1x10^4$ to give the number of cells per ml of suspension.

3.3.1.3 Determination of Cell Doubling Time

Cells were seeded out at an initial total cell number of $1x10^5$ cells per $25cm^2$ (T25) flask containing 10ml of complete growth medium with an individual flask for every time-point. Cells were trypsinised, centrifuged, resuspended and counted using a haemocytometer as described above and the subsequent concentration used to determine the total cell count per flask. Further samples were taken every 24 hours until confluence. The doubling time of each cell line was calculated by reading off the exponential portion of the growth curve derived by plotting number of hours against total number of cells counted.

3.3.1.4 Mycoplasma Testing

Cell cultures were routinely tested for *Mycoplasma* contamination every 6 months. The human breast cancer cell line, MCF-7 cells were grown in Dulbecco's MEM (DMEM) supplemented with 10% FCS and 1% glutamine. They were maintained at 37°C with 5% CO_2. A total number of $5x10^4$ MCF-7 cells were seeded onto a sterile coverslip placed in a flat bottom Falcon tube. Cells were allowed to adhere to the coverslips for

24 hours at 37°C with 5% CO_2. Previously, the cell lines to be *Mycoplasma* tested had been set up such that the cells reached confluency concurrently with the set-up of the *Mycoplasma* test. Thus, from a flask containing a confluent cell population to be tested, 500µl of the supernatant growth medium was removed and transferred to the *Mycoplasma* testing tube. The cell-free supernatant must not contain additives such as hydrocortisone, cholera toxin or antibiotics that might interfere with *Mycoplasma* growth. The MCF-7 cells were incubated until they reached confluence after 5 days. The medium was removed and the cells washed once with 0.01M PBS. The cells were then fixed in absolute methanol for 5 minutes and subsequently washed twice with 0.01M PBS and stained with 5µg/ml of Hoechst 33258 dissolved in 0.01M PBS for 10 minutes. Following two more washes with 0.01M PBS, the coverslips were carefully removed from the *Mycoplasma* testing tube, placed cell surface upwards on a glass microscope slide and covered with a coverslip. Analysis was performed under a fluorescent microscope using a x40 objective and ultra-violet (UV) illumination. Control cells showed intense blue-white staining of the nuclei only. *Mycoplasma* infected cells would have been covered in a fine lawn of speckles all over.

3.3.1.5 EGFR ihibition with gefitinib

Cell lines were grown in 80ml flasks until approximately 70% confluent. They were then serum starved for 16 hours (overnight). Cellular inhibition was performed by adding concentrated gifitinib, from stock solution, in order to obtain the desired final concentrations (C, 1um, 5um, and 10 um etc). Cells were incubated with gefitinib for 3 hours, followed by EGF activation for 30 minutes.

3.3.2 Protein Extraction

3.3.2.1 Total Cell Lysis

Cells cultured and treated in $75cm^2$ (T75) flasks were washed twice in PBS at room temperature, drained well and placed in ice. To lyse the cells, 500µl RIPA buffer (1% deoxycholic acid, 1% Triton X-100, 0.1% SDS, 250 mM NaCl, 50 mM Tris pH 7.5, 100 µg/ml AEBSF, 17µg/ml aprotinin, 1µg/ml leupeptin, 1µg/ml pepstatin, 5µM fenvalerate, 5µM potassium bisperoxo (1,10-phenanthroline) oxovanadate (V) (BpVphen) and 1µM okadaic acid) was added to each flask for 10 minutes with occasional rocking. Cells were then scraped into a 1.5ml Eppendorf tube using a cell scraper (VWR International Ltd.) and centrifuged at 13,000rpm for 10 minutes at 4^oC. The supernatant (containing total cell protein) was then carefully transferred to a fresh tube and the pellet discarded. This is the total cell lysate and can be stored at -80^oC.

3.3.2.2 Protein Assay

To determine the protein concentration of a particular total cell lysate, the Biorad Protein Assay kit was used. Briefly, 2µl of each lysate is added to 18µl H_2O. In a separate Eppendorf, 20µl *Reagent S* is mixed with 1ml *Reagent A*. 100µl of this is added to each 20µl lysate sample mixed well with a short spin. 800µl *Reagent B* is then added to each and incubated at room temperature for 15 minutes. The optical density (O.D.) for each sample is then read on a spectrophotometer (Beam PU 8600 Series UV/Vis Single, Philips®) at 750nm and the protein concentration determined using the following formula:

$$O.D. \times 25 = [\ ]/µl \text{ (i.e. µg/µl)}$$

3.3.3 Co-Immunoprecipitation

The topic of co-immunoprecipitation (Co-IP) is best preceded by a discussion of immunoprecipitation (IP) to help frame an understanding of the principles involved. Immunoprecipitation is one of the most widely used methods for antigen detection and purification. An important characteristic of IP reactions is their potential to deliver not only the target protein but also other macromolecules that interact with the target.

The principles of immunoprecipitation (see appendix 1; page 92)

Protein G Sepharose™ 4 Fast Flow is protein G immobilised by the CNBr method to Sepharose 4 Fast Flow. Protein G binds to the Fc region of IgG from a variety of mammalian species. Protein G Sepharose 4 Fast Flow may be used to isolate and purify classes, subclasses and fragments of immunoglobulins from any biological fluid or cell culture medium. Since only the Fc region is involved in binding, the Fab region is still available for binding antigen. Hence, Protein G Sepharose 4 Fast Flow is extremely useful for isolation of immune complexes. The potential applications of protein G include almost all of the current and projected applications of protein A. Protein G and protein A, however, have different IgG binding specificities, dependent on the origin of the IgG. Compared to protein A, protein G binds more strongly to polyclonal IgG, for example, from cow, sheep and horse. Furthermore, unlike protein A, protein G binds polyclonal rat IgG, human IgG3 and mouse IgG1 (Table 3.4). In this study, only Protein G Sepharose was used.

Species	Protein G	Protein A
Human IgG$_1$	++	++
Human IgG$_2$	++	++
Human IgG$_3$	++	-
Human IgG$_4$	++	++
Rabbit	++	++
Cow	++	+
Horse	++	-
Goat	++	+
Guinea Pig	+	++
Sheep	++	-
Dog	+	++
Pig	++	++
Rat	-	-
Mouse	+	+
Chicken	-	-

Table 3.4: Relative binding strength of polyclonal IgG from various species to free protein G and protein A, as measured in a competitive ELISA test.
Source: Amersham Biosciences Instruction Manual 71-7083-00 Edition AF

Protein Sepharose G™ 4 Fast Flow (Amersham Biosciences, Sweden) beads were prepared by washing as follows: Taking the required volume of Protein Sepharose G™ the supernatant (slurry) was removed by centrifugation at 13,000rpm for 15 seconds at 4°C. The pellet was then resuspended in a volume of PBS equal to the volume of the

bead pellet for a total of 5 times. For each sample, 25 – 45µl of Protein Sepharose G^{TM} was then added to 500 – 1000µg of protein taken from the total cell lysate. (To ensure that the beads themselves were being collected, the nib of the pipette tip was cut off.) The appropriate antibody at a final concentration of 4µg was then added to each sample and then placed on a rotation wheel at 4°C and left overnight. The supernatant was removed by centrifugation at 13,000rpm for 15 seconds at 4°C and rested upright on ice for approximately 10 minutes. This lead to a level pellet at the bottom of the epindorph tube. This can be stored at -80°C for future analysis as it is still a total cell lysate with the immunoprecipitated protein depleted and is a useful control for confirming that the immunoprecipitation has purified the required protein. The pellet was washed three times by resuspending in 100µl RIPA buffer and centrifuging at 13,000rpm for 15 seconds at 4°C. The pellet contained the Protein Sepharose beads attached to the Fc segments of antibody, which in turn were bound to the purified antigen (protein) and anything else that may be associated to the antigen. This complex can be stored at -80°C for further analysis at a future date if necessary.

The antibodies used for immunoprecipitations were the rabbit polyclonal anti-EGFR antibody which cross-reacts with human, mouse and rat; and the mouse monoclonal anti-DNA-PK$_{CS}$ antibody which cross-reacts with human and rat. Both were purchased from Abcam Limited, Cambridgeshire, UK (Harlow & Lane, 1999).

3.3.3.1 Troubleshooting

Whilst the immunoprecipitation technique is well defined and allows for a clear and concise study of specific proteins and their characteristics, optimisation is variable and dependent on a number of factors such as protein of interest and antibodies used. In this study, modifications to the methodology were made to obtain the best results and were as follows:

1.   The Protein Sepharose G^{TM} beads were not originally washed in PBS prior to use. Supplied in a preservative this masked the beads activity and therefore yielded a poor protein binding affinity.

2.   The final concentration of antibodies used was increased from 2 to 4µg.

3.   Initial rotation time was 2h which did not allow for sufficient antibody-protein binding. This was then increased to16h.

4. Following rotation, pellets were initially washed once with RIPA buffer. This gave variable results due to contamination with DNA-PK which is usually present in cells at much higher concentration than EGFR. Number of washes was increased to three times giving far greater consistency.

5. Immunoprecipitates were originally resuspended in 50µl RIPA buffer. This diluted the protein concentration too much and so samples were resuspended in 15µl of RIPA/running buffer.

3.3.4 Nuclear and Cytosolic Extraction

To separate out nuclear and cytosolic components of total cell lysates, the TransFactor$^{®}$ Extraction Kit (Clontech Laboratories, UK) was used according to the manufacturer's instructions. Briefly, all steps were performed at 4°C unless otherwise specified. Reagents were pre-cooled to 4°C, and not used until fully defrosted. Cells were collected and transferred to an Eppendorf tube centrifuged at 13,000rpm for 10 minutes at 4°C and the supernatant discarded. The pellet was then washed twice in PBS and the pellet size estimated. Lysis buffer was prepared as follows: 150ml 10x Pre-lysis Buffer (Hypotonic) (100mM HEPES pH 7.9, 15mM $MgCl_2$, 100mM KCl), 15ml 0.1M DTT, 15ml Protease Inhibitor Cocktail (Aprotinin, Pepstatin A, Bestatin, trans-Epoxysuccinyl-Lleucylamido (4-guanidino) butane, and 4-(2-aminoethyl) benzenesulfonyl fluoride hydrochloride in DMSO) and 1.32ml ddH_2O. Cells were resuspended in a volume of lysis buffer equal to five times the cell pellet volume and incubated on ice for 15 minutes. Following centrifugation at 13,000rpm for 10 minutes at 4°C, the supernatant was carefully removed and the pellet resuspended in a volume of lysis buffer equal to twice the cell pellet volume.

The suspension was then slowly drawn into a syringe through a narrow-gauge (No. 27) needle and then ejected with a single rapid stroke. This was repeated ten times and centrifuged at 13,000rpm for 10 minutes at 4°C. The supernatant was then transferred to a fresh Eppendorf tube and is the cytosolic fraction. This can be snap-frozen and stored at -70°C.

Extraction Buffer was prepared as follows: 147ml Pre-extraction Buffer (20mM HEPES pH 7.9, 1.5mM $MgCl_2$, 0.42M NaCl, 0.2mM EDTA, 25% (v/v) glycerol), 1.5ml 0.1M DTT and 1.5ml Protease Inhibitor Cocktail. The crude nuclear pellet was resuspended in a volume of Extraction Buffer equal to two-thirds of the cell pellet volume. To

disrupt the nuclei, the suspension was then syringed as before and placed on a shaker at low speed for 30 min at 4$^{\text{o}}$C. The nuclear suspension was then centrifuged at 13,000rpm for 10 minutes at 4$^{\text{o}}$C. The supernatant or nuclear fraction, was transferred to a fresh Eppendorf tube and can be snap-frozen and stored at -80$^{\text{o}}$C.

For determination of the protein concentrations within both the nuclear and cytosolic extractions, the protein assay detailed in Section 2.7.2 was used.

3.3.4.1 Troubleshooting

A number of obstacles were overcome whilst performing the nuclear and cytosolic extractions:

1. Initial low protein concentrations were due to improper measurement of cell pellet volume.
2. Protein activities were at first not present because some of the proteins of interest are highly susceptible to proteolytic degradation. With practice, work efficiency decreased the time of initial purification steps whilst keeping all reagents on ice at all times.
3. There was difficulty drawing cell lysates into the syringe. This was because of a compact cell pellet and was overcome by using a pipette tip to disperse them.

3.3.5 Immunoblotting

3.3.5.1 Electrophoresis

Protein concentrations of total cell lysates were determined using the protein assay outlined in Section 2.7.2. For each sample the required volume containing 30-50μg of protein was transferred to a fresh Eppendorf tube. Loading (Laemmeli) buffer (4% SDS, 10% β-Mercaptoethanol, 20% glycerol, 0.02% bromophenol-blue and 100mM Tris HCl (pH 6.8)) was then added to each lysate before heating at 95$^{\text{o}}$C for 4 minutes to denature the proteins. Samples were then centrifuged at 13,000rpm for 10 minutes at 4$^{\text{o}}$C and the pellet discarded.

For immunoprecipitates, the whole pellet containing 500 – 100μg of protein was resuspended in loading buffer and boiled as above. Boiling allows for denaturing of and dissociation between the proteins and the antibodies and beads. Following

centrifugation, the pellet containing beads and antibody was discarded and the supernatant could be loaded for electrophoresis.

The NuPAGE® Electrophoresis System (Invitrogen, UK) was used. For analysis of proteins with a molecular weight of between 120 and 410 KDa, lysates and immunoprecipitates were loaded onto NuPAGE® Novex 3-8% Gradient Tris-Acetate Pre-Cast Gels which were placed in the XCell *SureLock*™ Mini-Cell (two gels per cell) and included an appropriate marker (Kaleidoscope pre-stained standards, BioRad, Hemel-Hempstead, UK) and a positive protein control (A431+EGF cell lysate; BD Biosciences, UK). Upper (200ml) and lower (600ml) buffer chambers were then filled with 1x NuPAGE® Tris-Acetate SDS Running Buffer (diluted from a 20x stock: 50mM Tricine, 50mM Tris base, 0.1% SDS, pH 8.24) and Mini-Cells were run at 150V constant at 4°C for approximately 1h 30min (Expected 40-55 mA/gel at start; 25-40 mA/gel at end).

For analysis of proteins with a molecular weight of between 10 and 180 KDa lysates and immunoprecipitates were loaded onto NuPAGE® Novex 4-12% Gradient Bis-Tris Pre-Cast Gels and placed in Mini-Cells as above. Upper (200ml) and lower (600ml) buffer chambers were then filled with 1x NuPAGE® MOPS SDS Running Buffer (diluted from a 20x stock: 50mM MOPS, 50mM Tris base, 0.1% SDS, pH 7.7) and Mini-Cells were run at 200V constant at 4°C for approximately 50min (Expected 100-125 mA/gel at start; 60-80 mA/gel at end).

3.3.5.2 Protein Transfer and Immunoblotting

Proteins were electrically transferred to Immobilon™ polyvinylidenedifluoride (PVDF) membranes (Millipore, UK). These extremely hydrophobic membranes will not wet in aqueous solution and so were prepared as follows: blots were immersed in 100% methanol for three seconds and then placed in H_2O for 2 minutes to elute the methanol. To equilibrate, membranes were then soaked in protein transfer buffer (diluted from a 10x stock: 3% TrisBase, 14.4% glycine and 20% methanol). Gels and prepared membranes were then placed into the X-Cell II™ Blot Module (Novex®) as illustrated in Figure 3.1.
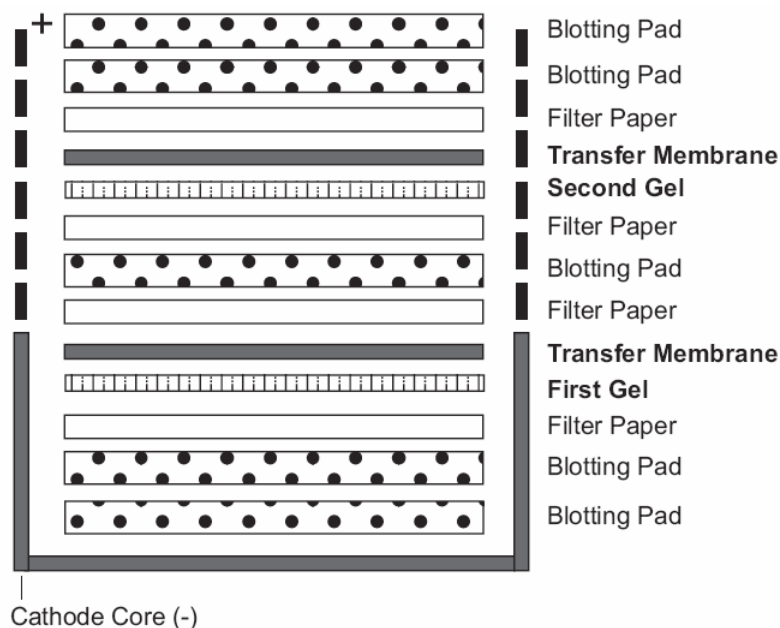
Figure 3.1: Gel/Membrane sandwich for 2 gels.

Source: NuPAGE® Technical Guide, Invitrogen, UK

Transfer was achieved at 40V for 2h using the XCell *SureLock*™ Mini-Cell (two blots per cell) and filled with protein transfer buffer as described in the NuPAGE Novex® protocol.

Membranes were then blocked in 3% casein blocking buffer [(3% skimmed milk powder (Marvel, UK) in TBS-Tween (TBS-T) (20mM TrisBase, 0.15M NaCl pH 7.5 in Elga H$_2$O with 0.1% Tween-20)] for at least 1 hour on a shaker at 4°C. Membranes being probed for phosphorylated proteins were blocked in 5% Bovine Serum Albumin (BSA) in TBS-T. This is due to the fact that milk contains a number of phosphorylated proteins which interfere with a phosphotyrosine antibody's ability to bind specific proteins of interest.

Blots were then probed with primary antibody against proteins of interest for at least 2h on a roller at room temperature. Antibodies used in this study are detailed in Table 2.5. All were diluted in a 1:1 mix of either Milk-TBS-T or BSA-TBS-T and TBS as necessary. Following this membranes were washed three times for 5 minutes in TBS-T followed by three more washes for 5 minute with TBS. Membranes were then probed with an appropriate horseradish peroxidase conjugated secondary antibody for at least 1h and washed as before.

Immunocomplexes were visualised using the enhanced chemiluminescence (ECL) system (Amersham Pharmacia, Little Chalfont, UK) by incubating the membranes in

the ECL system solution for 1 minute before wrapping the moist blots in cling film and exposing the blots to Kodak X-OMAT™LS film for varying exposure times (two seconds to 24h) (Sambrook *et al.*, 1989).

In order to remove or 'strip' pre-bound antibody, membranes were rehydrated in TBS for 5 minutes and placed in a hybridiser (Techne, UK) with 100ml of stripping buffer (100mM β-Mercaptoethanol, 2% SDS, 62.5mM Tris-HCl, pH 6.7) and left for 30 minutes at 50ºC. Membranes were then washed twice in TBS-T for ten minutes each, blocked and reprobed as described above.

3.3.6 Densitometric Analysis

To mathematically compare the intensity of particular bands produced by immunoblotting, densitometric analysis was used. Briefly, blots were placed in the imaging densitometer (Imaging Densitometer GS-670 BioRad, UK) and the bands of interest selected. Intensity was then measured by computer and the background subtracted. Data is represented as a percentage of control band intensity.

The screen-grab shown in Figure 3.2 illustrates the methodology. In this case V5 serves as a background, V1 is the control and bands V2-4 represent different drug treatments.

Volume Name	Type	Mean (OD)	Area (mm*mm)	Min (OD)	Max (OD)	Volume (OD*mm*mm)	Adj. Volume (OD*mm*mm)	% Volume	Concentration	Mol. Weig
V1	Unknown	0.534	21.48	0.144	1.093	1.1476e+1	9.1658e+0	36.46	–	–
V2	Unknown	0.229	21.48	0.142	0.358	4.9165e+0	2.6067e+0	10.37	–	–
V3	Unknown	0.215	21.48	0.135	0.375	4.6238e+0	2.3141e+0	9.21	–	–
V4	Unknown	0.622	21.48	0.123	1.146	1.3360e+1	1.1050e+1	43.96	–	–
V5	Background	0.108	21.48	0.088	0.202	2.3097e+0	–	–	–	–
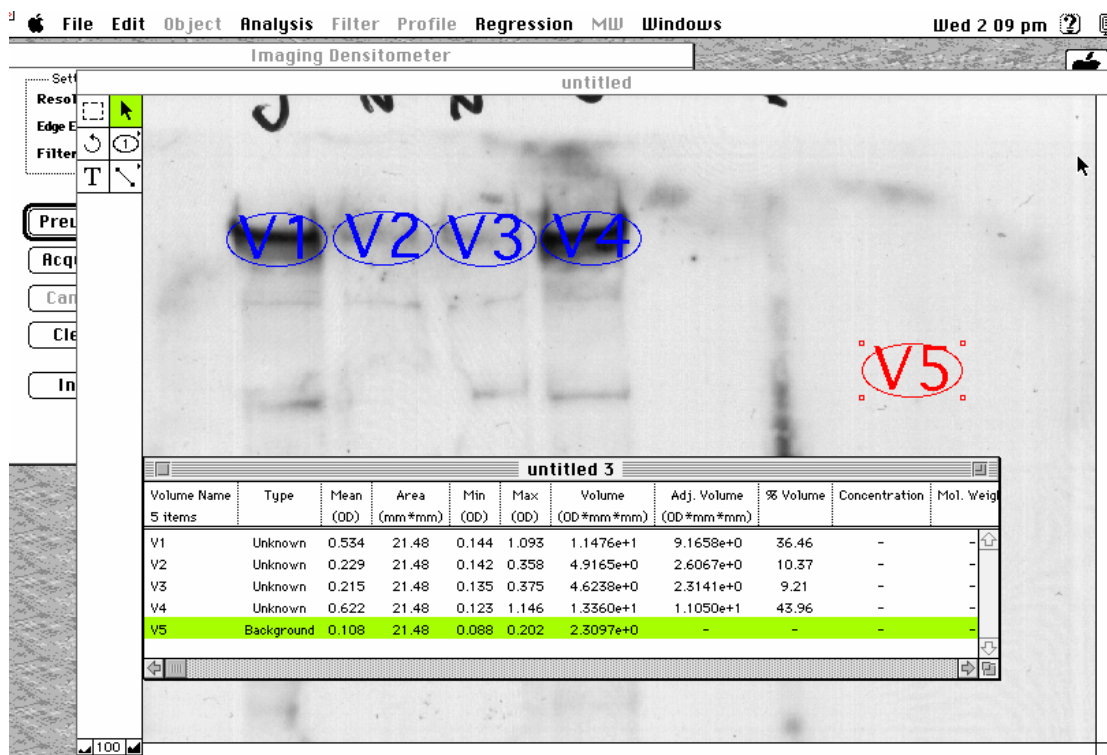
Figure 3.2: Sample screen display of densitometric analysis as seen using the BioRad Imaging Densitometer Software.

3.3.7 Immunofluorescent Staining

Exponentially growing cells were seeded at 2×10^4 cells per well on circular glass slides in 12 well plates (Nunclon™, VWR) and incubated for 24h at 37°C in 5% CO_2. Cells were then treated as required, the media subsequently removed and the cells washed twice with cold PBS. Cells were then fixed using 500µL/well of 50% methanol/50% acetone mix at 4°C for 8 minutes. Following this the slides were then washed twice with cold PBS and permeablised using 500µL/well of 0.5% TritonX-100 in PBS. Slides were then blocked in 3% casein blocking buffer [(3% skimmed milk powder (Marvel, UK) in TBS-Tween (TBS-T) (20mM TrisBase, 0.15M NaCl pH 7.5 in Elga H_2O with 0.1% Tween-20)] overnight at 4°C.

Slides were then washed 3 times in cold PBS following which the cells were incubated with anti-DNA-PK$_{CS}$ antibody for 1 hour. Slides were then washed 3 times with washing buffer (0.1% TritonX-100 in PBS) and then incubated for 1 hour at room temperature with FITC-labelled secondary antibody: Alexa fluoro® 488 goat anti-mouse IgG (green). Nuclear counterstaining was performed using 2µg/ml Propidium Iodide (blue) for 3 minutes followed by destaining with distilled water for 20 minutes.

The slides were viewed and photographed using a laser scanning confocal microscope.

3.4 RESULTS

Expression of EGFR in neuroendocrine tumour cell lines

Five cell lines, with neuroendocrine differentiation, were tested for EGFR expression. All five proved positive for EGFR expression as demonstrated below (figure 3.3). A431 was used as positive control for EGFR in cell lysates.
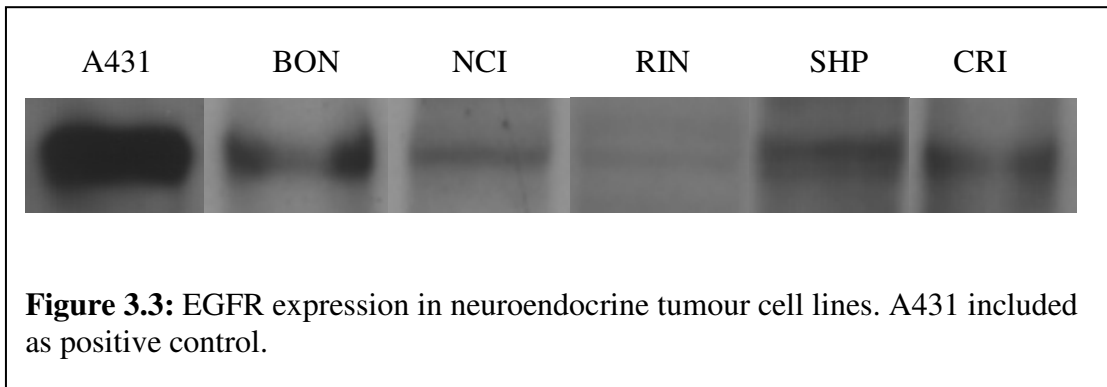
A431	BON	NCI	RIN	SHP	CRI

Figure 3.3: EGFR expression in neuroendocrine tumour cell lines. A431 included as positive control.

Expression of DNA-PK$_{CS}$ in neuroendocrine tumour cell lines

Five cell lines, with neuroendocrine differentiation, were tested for DNA-PK$_{CS}$ expression. All five proved strongly positive for DNA-PK$_{CS}$ expression as demonstrated below (figure 3.4). A431 was used as positive control for DNA-PK$_{CS}$ in cell lysates.

A431	RIN	NCI	BON	SHP	CRI

Figure 3.4: DNA-PK$_{CS}$ expression in neuroendocrine tumour cell lines. A431 included as positive control.
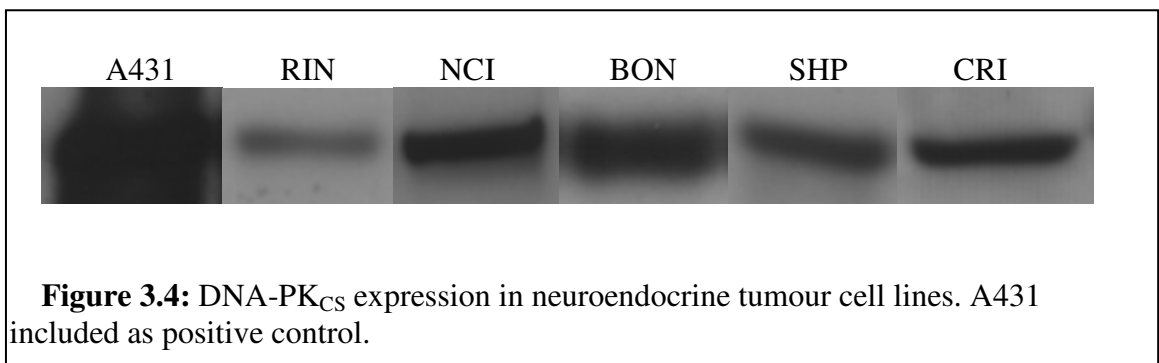
3.4.1 Gefitinib Treatments

Cytotoxicity of gefitinib was determined by the Sulphorhodamine B (SRB) proliferation assay. Experiments were carried out in NET cell lines by Dr V Kostoula, a member of Dr Caplin and Dr Hochhauser's research team. These experiments demonstrated IC_{50} values to be between 18 and 30 μM (table 3.5). Majority of EGFR inhibition experiments, however, were performed at final concentrations of gefitinib of up to 10 μM as these concentrations best represented the concentrations attainable in tumours, in-vivo.

Table 3.5

Chemotherapy drug and gefitinib IC_{50}s in μM

	SHP-77	CRI-G1	NCI-H727	RIN-5F	BON
Gefitinib	18	19	18	30	21

Table 3.5: courtesy of V. Kostoula

3.4.2 Gefitinib Treatment and EGFR/DNA-PK$_{CS}$ interactions in NET cell-lines

A431 and NET cell lines were treated with gefitinib as detailed in methods (3.3.1.5). EGFR, expressed by all cell lines, was shown to be susceptible to inhibition by gefitinib (figure 3.5). Furthermore, gefitinib treatment led to dose dependent reduction in cellular DNA-PK$_{CS}$ concentration (figure 3.6).

A431 cell-line

Gefitinib concentration   C   10μM   20μM

p-EGFR

EGFR

Figure 3.5: a representative western demonstrating the ability of gefitinib to inhibit EGFR. Arrow indicates phosphorylated EGFR, showing complete inhibition with 10 & 20μM gefitinib.
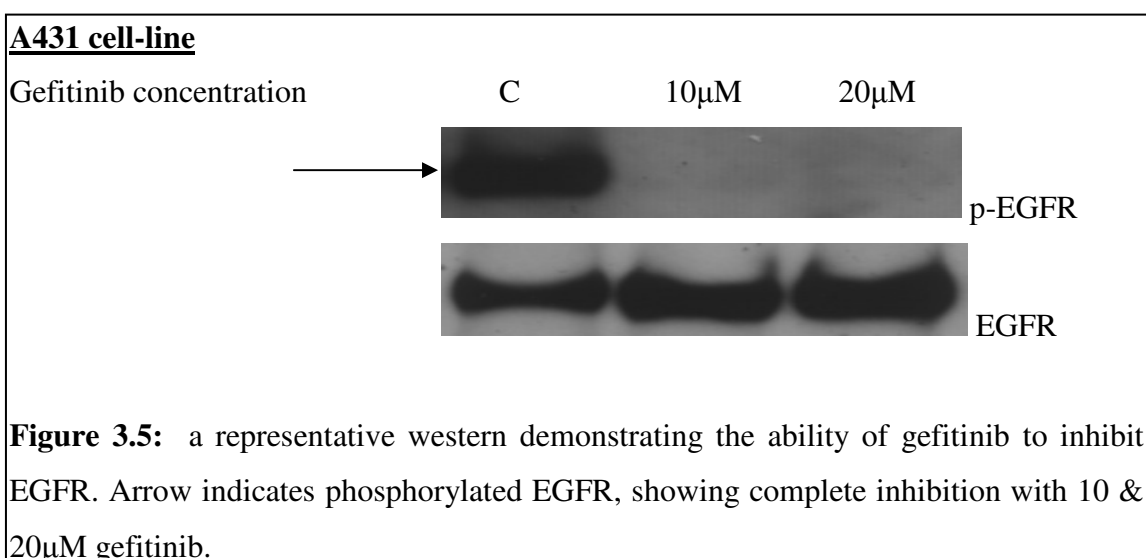
3.4.3 Effect of gefitinib treatment on cellular DNA-PK$_{CS}$ concentration

BON   C   1 μM   5 μM   10 μM gefitinib

DNA-PK$_{CS}$

α-tubulin

NCI   C   1 μM   5 μM grfitinib

DNA-PK$_{CS}$

α-tubulin

SHP   C   1 μM   5 μM   10 μM gefitinib

DNA-PK$_{CS}$

α-tubulin

CRI   C   2 μM   10 μM gefitinib

DNA-PK$_{CS}$

α-tubulin

RIN   C   1 μM   5 μM   10 μM gefitinib

DNA-PK$_{CS}$

α-tubulin
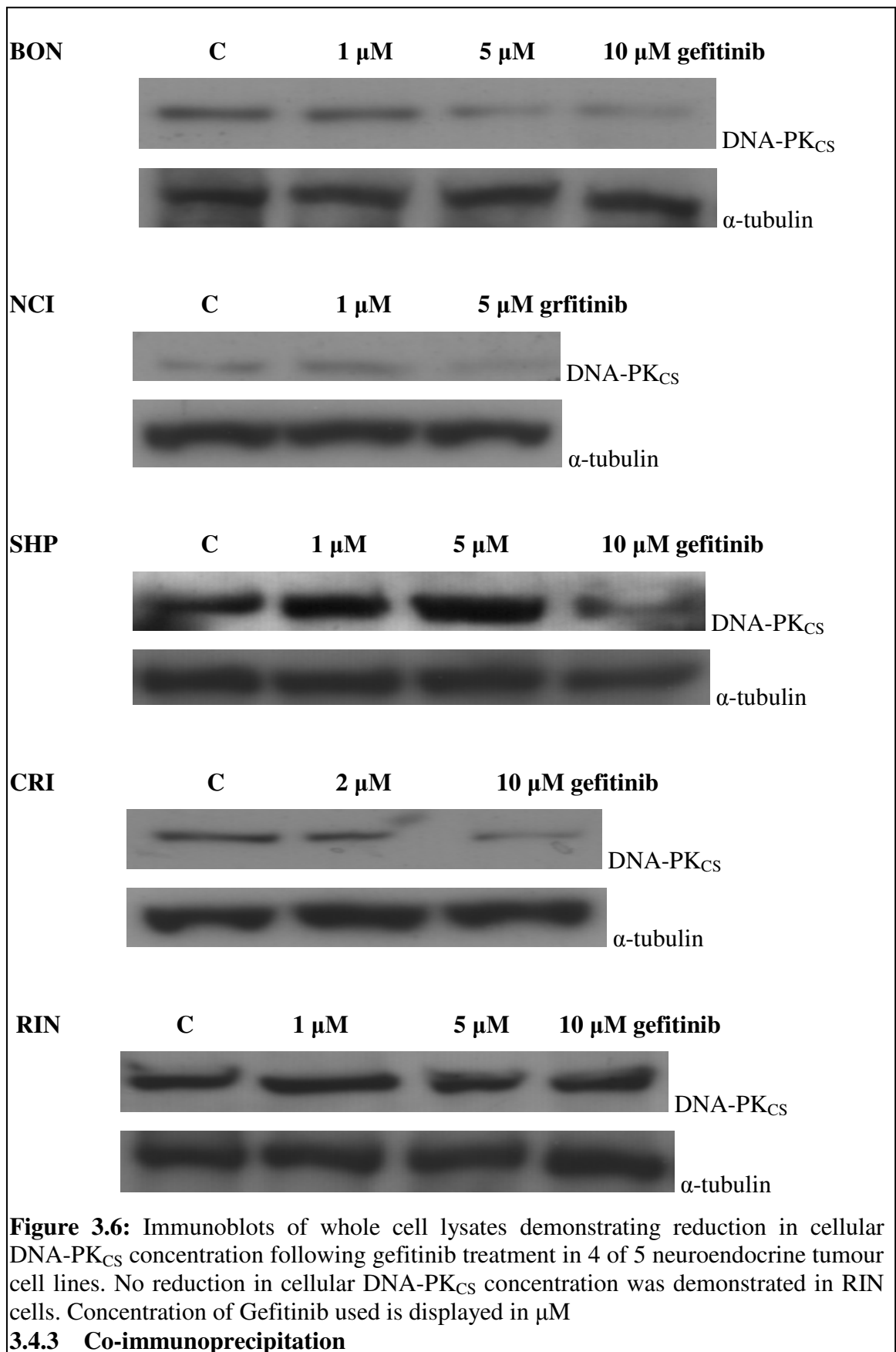
Figure 3.6: Immunoblots of whole cell lysates demonstrating reduction in cellular DNA-PK$_{CS}$ concentration following gefitinib treatment in 4 of 5 neuroendocrine tumour cell lines. No reduction in cellular DNA-PK$_{CS}$ concentration was demonstrated in RIN cells. Concentration of Gefitinib used is displayed in μM

3.4.3   Co-immunoprecipitation

Having demonstrated EGFR expression and down-regulation of cellular DNA-PK$_{CS}$ levels following EGFR inhibition with gefitinib, the next step was to look for evidence of direct interaction between EGFR and DNA-PK$_{CS}$. Immunoprecipitation technique was employed for this purpose. Whole cell lysates were incubated with anti-EGFR antibodies to selectively pull out EGFR. These IP samples were then probed for EGFR and subsequently for DNA-PK$_{CS}$ to determine whether there is a direct and strong interaction between these 2 proteins and whether EGFR inhibition, with gefitinib, modulates these interactions.

Experiments were performed under a range of conditions. The variable parameters included:

i) Concentration of gefitinib: 1 – 30µM

ii) Duration of gefitinib treatment: 3 – 24 hours

iii) With or without serum starvation, prior to gefitinib treatment, in order to stimulate EGFR expression

iv) With or without EGF stimulation

Representative results for these experiments are shown below (figures 3.6 & 3.7). These experiments demonstrated successful EGFR IP with all NET cell lines used. When the membranes were probed for DNA-PK$_{CS}$ it was found to be consistently present, suggesting its co-immunoprecipitation with EGFR. Gefitinib treatment increased DNA-PK$_{CS}$ co-immunoprecipitation in A431 (control cell-line), and NCI, while BON also demonstrated a small increase (figure 7). However there was no demonstrable increase of DNA-PK$_{CS}$ co-immunoprecipitation in CRI, RIN, and SHP cell lines (SHP displayed in figures 3.6).

Thus far we had demonstrated that EGFR inhibition leads to decreased DNA-PK$_{CS}$ levels in neuroendocrine tumour cell-lines. We had also demonstrated that there is direct interaction between EGFR, a cell surface receptor molecule, and DNA-PK$_{CS}$ which is known to reside mainly in the nucleus. Furthermore, this direct EGFR/DNA-PK$_{CS}$ interaction can be modulated, in some cell types at least, such that there are increased EGFR/DNA-PK$_{CS}$ associations upon EGFR inhibition (figure 3.8).

Figure 3.7: Co-immunoprecipitation experiments in four cell lines: gefitinib treated cells were lysed and EGFR immunoprecipitated using anti-EGFR antibody. Protein transfer embranes were immunoblotted with anti-EGFR to confirm successful EGFR immunoprecipitation, and anti-DNA-PK$_{CS}$ to look for co-iimunoprecipitation of DNA-PK$_{CS}$ with EGFR. This figure demonstrates co-immunoprecipitation of DNA-PK$_{CS}$ with EGFR as well as an increase in EGFR/DNA-PK$_{CS}$ association upon EGFR inhibition in A431, NCI, and BON cell lines, but not SHP cell line (highlighted red).
μM refers to gefitinib concentrations.

Successful inhibition of EGFR with gefitinib followed by immunoprecipitation with anti-EGFR antibodies was used to look for direct association of EGFR with DNA-PK$_{CS}$. The above results confirm that DNA-PK$_{CS}$ is co-immunoprecipitated with EGFR, thus suggesting a direct interaction between these two proteins. Furthermore, EGFR inhibition led to an increase in interactions between EGFR and DNA-PK$_{CS}$ in two of the five NET cell lines, namely NCI and BON, as well as in the control cell line A431. however, these results were not as impressive as those reported previously in A431 and other cell lines, utilising cetuximab to inhibit EGFR. We therefore repeated the immunoprecipitation experiments, following EGFR inhibition with **cetuximab**, in NET and A431 cell lines.

3.4.4.1 Co-immunoprecipitation following cetuximab treatment

Figure 3.8: Exponentially growing cells were treated with cetuximab (30 or 60 µM). Cell lysates were prepared. Anti-EGFR immunoprecipitation was performed and the resultant samples were electrophoresed, transferred to membranes, and probed for EGFR (lower immunoblots). Protein transfer membranes were also probed for DNA-PK$_{CS}$ (upper immunoblots) in order to determine whether it was co-imunoprecipitated with EGFR. No such association was seen in these experiments. +C consisted of A431 cell lysate.

As can be seen from the above immunoblots (figure 3.8), EGFR inhibition with cetuximab did not lead to an increase in EGFR/DNA-PK$_{CS}$ interactions. These findings are in stark contrast to previously published data (Bandyopadhyay D et al 1998).

3.4.5 Immunofluorescence

These co-immunoprecipitation experiments thus demonstrated mixed results for direct EGFR/DNA-PK$_{CS}$ interaction in the NET cell-lines tested, under the stated conditions. However, EGFR/DNA-PK$_{CS}$ relationship has been shown to be a complex one having multiple components. For instance, EGFR inhibition has been shown to affect not only DNA-PK$_{CS}$ activity but also its intracellular translocation, between the nucleus and the cytosol (Friedmann BJ et al 2006). One very powerful and informative way of observing these events is through the use of confocal microscopy. Utilising this technique, we repeated the EGFR inhibition experiments to determine the effect on DNA-PK$_{CS}$ localisation in NET cell-lines (figure 3.11).

EGFR inhibition was shown to influence the localisation of DNA-PK$_{CS}$ in SHP cell-line (figure 3.10) and possibly BON cell-line (incomplete data only, therefore not shown) with DNA-PK$_{CS}$ translocation from the nucleus to the cytoplasm, but no effect was seen in NCI, CRI, and RIN cell lines. Thus, it appears that in some NET cell-lines EGFR inhibition leads to translocation of DNA-PK$_{CS}$ from the nucleus to the cytoplasm. This translocation may (as in the case of BON) or may not (as in the case of SHP) be due to increase in direct binding of EGFR to DNA-PK$_{CS}$ thereby leading to sequestration of DNA-PK$_{CS}$ in the cytoplasm.
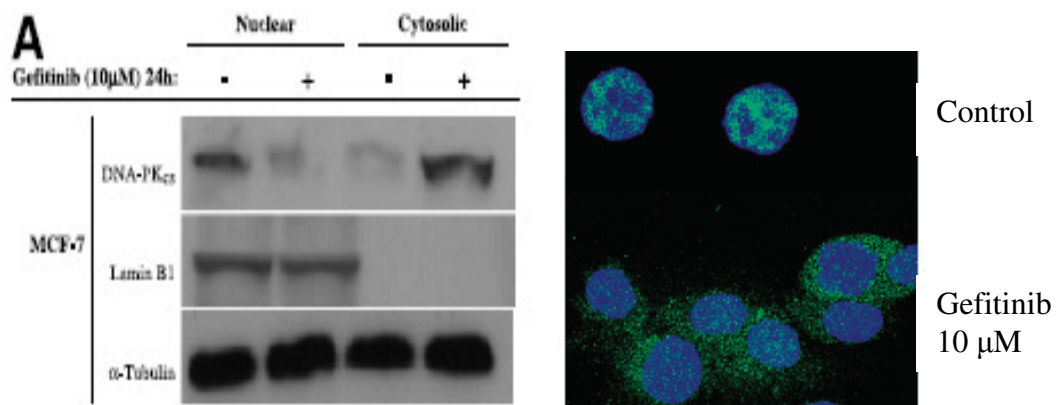
Figure 3.9: Nuclear separation and immunofluorescence experiments in mcf-7 cell line demonstrating export of nuclear into the cytoplasm upon EGFR inhibition with gefitinib (Friedmann BJ et al 2006).

Further evidence for these immunofluorescence findings was sought using a combination of cellular fractionation, to separate out the nuclear and cytosolic compartments, followed by western blotting to determine the relative concentrations of DNA-PKCS in these compartments. Cells had been cultured under same conditions as previously and treated with gefitinib as described for the co-immunoprecipitation and immunofluorescence experiments.
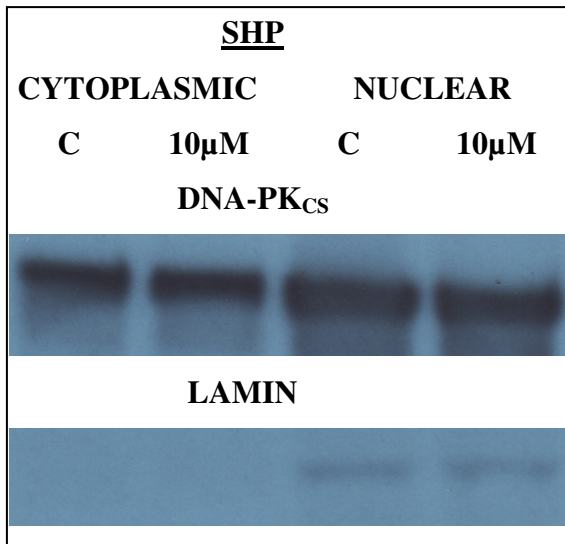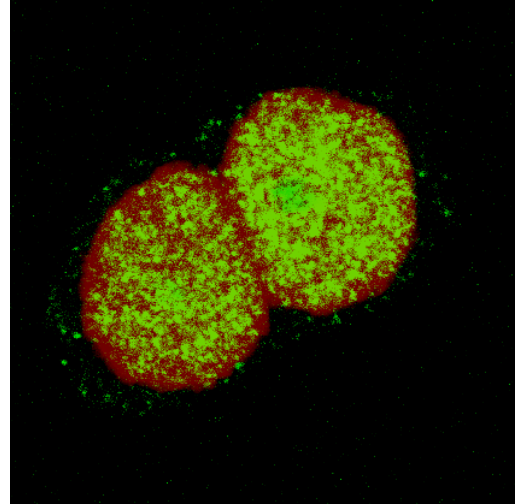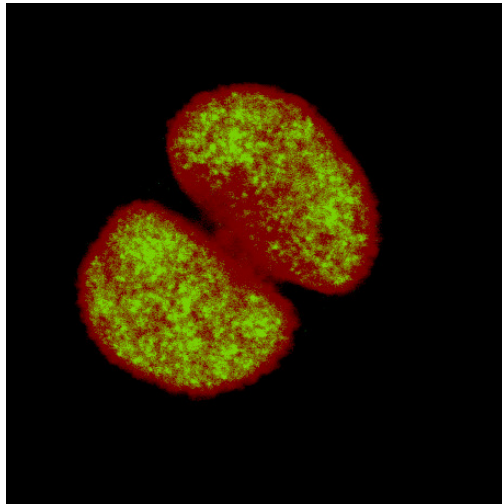
Figure 3.10 SHP cell-line: Results of immunofluorescence and cell fractionation experiments, following gefitinib treatment, to determine the effects on DNA-PK$_{CS}$ localisation. Gefitinib therapy led to a **20% increase** in cytoplasmic DNA-PK$_{CS}$ in **SHP** cells as demonstrated by the photographs above, immunoblot, left, and densitometry graph, below.

CRI

CYTOPLASMIC NUCLEAR

C   10   C   10
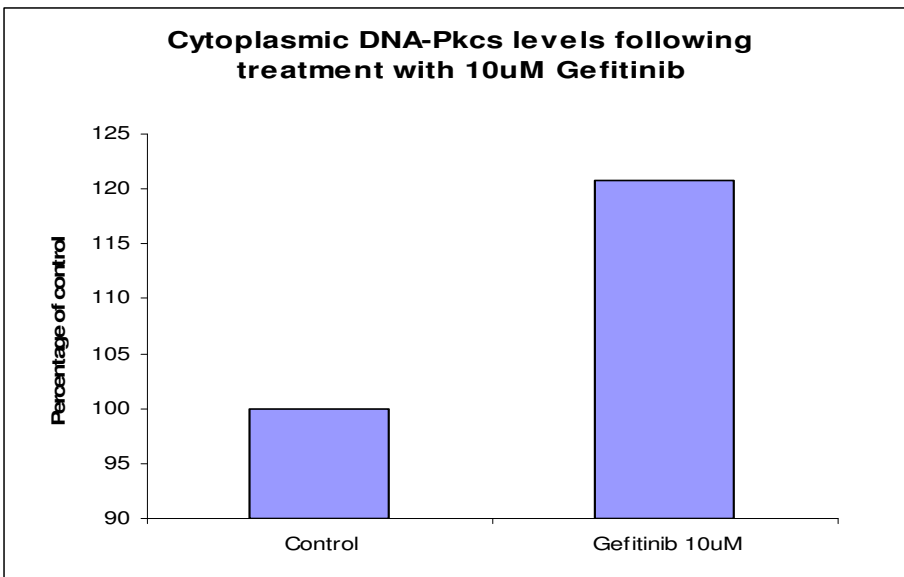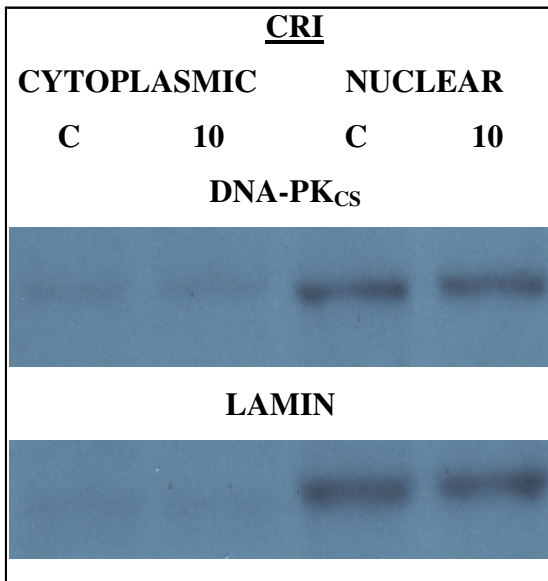
DNA-PK$_{CS}$

LAMIN

Figure 3.11A: Results of cell fractionation experiments, following gefitinib treatment, to determine the effects on DNA-PK$_{CS}$ localisation. Gefitinib therapy did not alter DNA-PK$_{CS}$ localisation in **CRI**. Lamin immunoblots are included to show efficient nuclear and cytoplasmic separation.

NCI

CYTOPLASMIC NUCLEAR

C   10   C   10

DNA-PK$_{CS}$

LAMIN
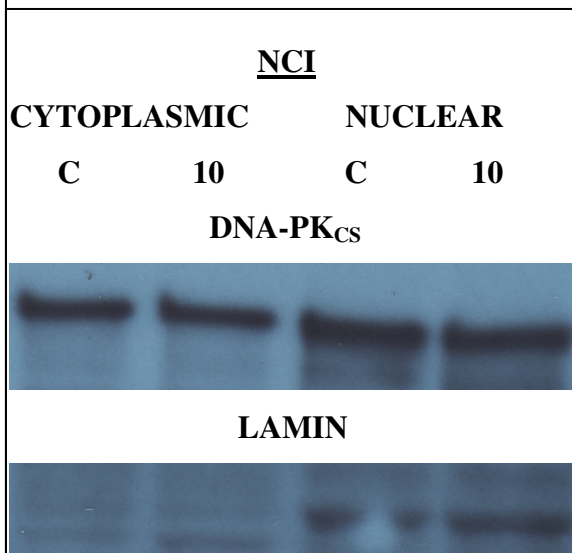
Figure 3.11B: Results of cell fractionation experiments, following gefitinib treatment, to determine the effects on DNA-PK$_{CS}$ localisation. Gefitinib therapy did not alter DNA-PK$_{CS}$ localisation in **NCI** cells.

RIN

CYTOPLASMIC NUCLEAR

C   10   C   10

DNA-PK$_{CS}$

LAMIN
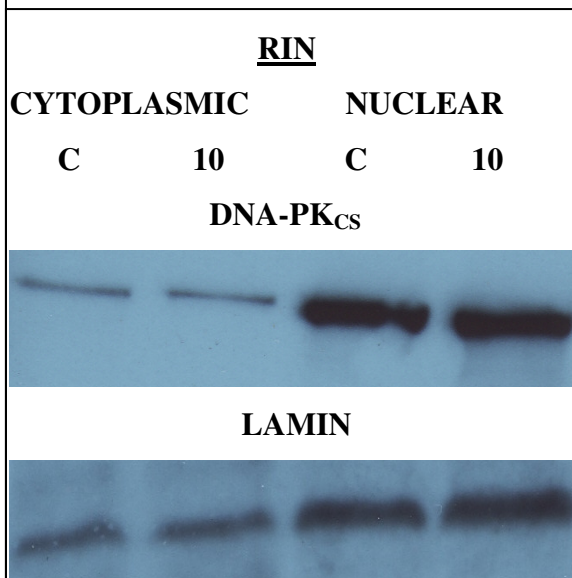
Figure 3.11C: Results of cell fractionation experiments, following gefitinib treatment, to determine the effects on DNA-PK$_{CS}$ localisation. Gefitinib therapy did not alter DNA-PK$_{CS}$ localisation in **RIN** cells.

3.5 Discussion

EGFR is a major tumour behaviour determinant, with increased EGFR expression associated with resistance to anti-tumour therapy and poorer prognosis. The mechanisms underlying these observations are the subject of intense study. EGFR has been shown to be expressed to a much higher degree in cell lines derived from highly metastasising tumours as opposed to cell lines derived from same type but poorly metastasising tumours. Furthermore, the highly metastasising tumour derived cell lines express higher concentrations of anti-apoptotic proteins such as Bcl-2, NFκB, and MDM2. They also expressed lower concentrations of pro-apoptotic proteins such as Bax and p53.

Our early experiments involving EGFR inhibition in NET cell lines had already shown promise with potentiation of chemotherapeutic effects. This work is concerned with discovering the nature of EGFR/ DNA-PK$_{CS}$ interactions, if any, in NET cell lines.

We initially tested for the expression of EGFR by NET cell lines (figure 3.3). All NET cell lines being grown in our laboratory were demonstrated to express EGFR, with RIN demonstrating the lowest, and CRI expressing the highest, concentration of the protein. All NET cell lines expressed large amounts of DNA-PK$_{CS}$ (figure 3.4).

Bandyopadhyay et al had demonstrated direct EGFR/DNA-PK$_{CS}$ interactions with their work using cetuximab to inhibit EGFR. They demonstrated a clear association of EGFR/DNA-PK$_{CS}$ upon cetuximab treatment. This work encouraged other groups to explore this modulation of double-strand DNA repair mechanism further. In particular, our group has concentrated on using gefitinib, a small molecule tyrosine kinase inhibitor of EGFR, to understand the mechanisms underlying the actions of EGFR. We had already made a number of new insights into EGFR biology using, amongst others the mcf-7 breast cancer cell line, demonstrating that EGFR inhibition with gefitinib leads to decreased overall concentration of DNA-PK$_{CS}$, physical interaction between EGFR and DNA-PK$_{CS}$ leading to movement of DNA-PK$_{CS}$ from nucleus into cytoplasm, decreased DNA-PK$_{CS}$ activity, and sensitisation of cells to ionising radiation as well as DNA damaging chemotherapy (Friedmann B 2004 & 2006). In view of the limited knowledge available regarding the biology of NET cells, and our group's major interest in these tumours, we decided to explore EGFR/DNA-PK$_{CS}$ interactions in NET cell lines.

Co-immunoprecipitation experiments were performed in NET cell lines to look for EGFR/DNA-PK$_{CS}$ association and the effect of EGFR inhibition on it. Our experiments demonstrate that there is direct EGFR/DNA-PK$_{CS}$ association, and that the degree of association between these 2 proteins can be increased in some NET cell lines, namely NCI and BON, by EGFR inhibition using gefitinib (figure 3.5-3.7). However the baseline degree of association, and its increase following gefitinib treatment, is very small compared to the overwhelmingly huge quantity of DNA-PK$_{CS}$ that is expressed by all NET cell lines. Therefore the contribution of direct EGFR/DNA-PK$_{CS}$ association as a means of reducing nuclear DNA-PK$_{CS}$ concentration, as has been previously suggested, is probably minimal. Other possible effects of this increased association, such as switching off the activity of DNA-PK$_{CS}$ or tagging it for degradation need to be further studied in NET cell lines.

This lack of a large increase in EGFR/DNA-PK$_{CS}$ interactions is in stark contrast to the initial published data on EGFR inhibition, using cetuximab, demonstrating a clear interaction between these two proteins following cetuximab treatment (Bandyopadhyay D et al 1998). We decided to repeat the immunoprecipitation experiments using cetuximab to inhibit EGFR in NET cell lines. However the results in this case were negative, that is to say there was lack of any enhancement in association between EGFR and DNA-PK$_{CS}$ following cetuximab treatment (figure 3.8). One possible explanation for this outcome may be that cetuximab induced EGFR/DNAPK$_{CS}$ interactions are cell type specific and the results of Bandyopadhyay et al are not reproducible in NET cell lines. However the results of our experiments were negative even in A453 cell-line, the same cell line as used in Bandyopadhyay et al's experiments (figure 3.8). Upon review of Bandyopadhyay et al's experiments a second, more likely explanation can be found which can attribute all the positive immunoprecipitation results to flawed experimental methodology.

Those original experiments were performed by treating cells with cetuximab, preparing a cell lysate and immunoprecipitating out DNA-PK$_{CS}$. However Western blot analysis revealed not only the 360kDa DNA-PK$_{CS}$ protein band but also a 170kDa protein band, which was confirmed to be EGFR. These experiments were taken as evidence of EGFR being co-immunoprecipitated with DNA-PK$_{CS}$ due to a direct attachment of EGFR to DNA-PK$_{CS}$. What is more likely is that cetuximab, an anti-EGFR antibody used to inhibit EGFR, was in fact acting as an immunoprecipitating antibody. Thus instead of

DNA-PK$_{CS}$ being immunoprecipitated and EGFR being **co-**immunoprecipitated, there were in fact two independent immunoprecipitation processes occurring. These same co-immunoprecipitation methods have also been employed by K Dittman et al. Since we had treated with cetuximab, a high affinity anti-EGFR antibody, immunoprecipitated using another anti-EGFR antibody and then looked for DNA-PK$_{CS}$, we showed that only EGFR on its own was pulled out of the cell lysate and that DNA-PK$_{CS}$ did not co-immunoprecipitate with it. Incidentally, immunoprecipitation of EGFR was much more efficient from samples already treated with cetuximab, despite the concentrations of EGFR being the same in the control and cetuximab treated samples, confirming the immunoprecipitating qualities of cetuximab.

Despite these negative co-immunoprecipitation results with cetuximab therapy there is ample evidence to suggest that EGFR influences DNA-PK$_{CS}$: Dote et al's data on inhibition of heat shock protein 90 (Hsp90) indicates that the attenuation of repair of radiation induced DNA double strand breaks is due to inhibition of EGFR which then leads to decreased interaction of EGFR with DNA-PK$_{CS}$ in the nucleus resulting in decreased activation of DNA-PK$_{CS}$; Jee Hyun Um et al demonstrated that EGFR and DNA-PK$_{CS}$ activity are mutually regulated by each other; Toulany M et al 2005 demonstrated decreased radiation induced DNA-PK$_{CS}$ autophosphorylation (and hence decreased activation) upon inhibition of EGFR or AKT in K-RAS mutated A549 cells, but not in tumour cells containing wild type K-RAS; K-RAS being a member of the small GTPase family and involved in EGFR activation induced cell signalling pathway; Joanne B Wedhaas et al 2006 demonstrated, using the Radelegans model of radiation induced reproductive cell death (a model of reproductive clonogen cell death in the nematode *Caenorhabditis elegan)*, the importance of EGFR/RAS/MAPK network in DNA repair post-irradiation. Dittman et al 2005 have demonstrated radiation induced translocation of EGFR to the cellular nucleus, its activation, its physical interaction with DNA-PK$_{CS}$ and the activation of DNA-PK$_{CS.}$ (Dittmann K et al 2005, Friedmann B et al 2004 & 2006, Toulany M et al 2005 ; Wedhaas JB et al 2006).

EGFR activation → ↑GRP association with SOS → ↑RAS-GTP binding → ↑activation of Raf → ↑activation of MEK → ↑activation of MAPK→ various cellular effects.

Published work from our laboratory and by others had also reported the export of DNA-PK$_{CS}$ upon EGFR inhibition and had concluded that this was due to the direct binding of EGFR to DNA-PK$_{CS}$ (Friedmann BJ et al 2006). We looked for this effect in NET cell lines using confocal microscopy techniques as well as analysis of separated cytoplasmic and nuclear fractions to determine any changes in the concentration of DNA-PK$_{CS}$ in the two compartments upon EGFR inhibition. SHP and BON cell lines demonstrated significant changes in the distribution of DNA-PK$_{CS}$ upon EGFR inhibition such that gefitinib treatment led to movement of DNA-PK$_{CS}$ from the nucleus to the cytoplasm, as observed using confocal microscopy (figure 3.10). This re-distribution was confirmed for the SHP cell lines by Western blot analysis of separated nuclear and cytoplasmic fractions to determine the relative concentration of DNA-PK$_{CS}$ with or without gefitinib treatment (figure 3.10). Similar experiments were not performed using the BON cell line due to lack of time. No redistribution of DNA-PK$_{CS}$ was observed for the remainder of NET cell lines (figure 3.11). While the discrepancy between the different cell-lines could possibly be explained by the low level of EGFR expression in the RIN cell-lines, as yet the reasons for differential outcomes observed in the other NET cell-lines is not clear. It is possible that these differences are due to differential expression of proteins which act as adaptors, such GRB2 and SHC, for interactions between EGFR and other proteins or possibly due to mutations in a range of intermediary proteins, such as Ras, Raf, MEK etc.

One possible mechanism of reduced DNA damage repair has been attributed to the ability of EGFR inhibitors to decrease DNA-PK$_{CS}$ concentration and activity. We demonstrate here that prolonged exposure of NET cells to gefitinib leads to decrease in the concentration of DNA-PK$_{CS.}$ This effect was consistently reproduced in all NET cell lines except for RIN (figure 3.6). This lack of effect in RIN cells is likely to be due to the much lower expression of EGFR by this cell line. Reduction in DNA-PK$_{CS}$ concentration, upon EGFR inhibition with cetuximab, was not observed. This is likely to be due to the much shorter treatment period with cetuximab. These are very encouraging results and confirm a very important mode of action of EGFR inhibition which is likely to impair non-homologous end joining, essential in double strand DNA break repair, for which DNA-PK$_{CS}$ is essential.

In summary EGFR inhibition in NET cell lines enhances chemotherapy related reduction in cellular proliferation. Previous studies in non-NET cell lines have demonstrated that EGFR/DNAPK$_{CS}$ interactions play a major role in sensitising cells to ionising radiation and DNA damaging radiotherapy. Analysis of the effects of EGFR inhibition with gefitinib reveals that:

i) There are direct EGFR/DNAPK$_{CS}$ interactions in NET cell lines, which can be enhanced by EGFR inhibition.

ii) EGFR inhibition leads to transfer of DNAPK$_{CS}$ from the nucleus to the cytoplasm in SHP and BON cell lines but not in CRI, RIN, or NCI cell lines. This difference in the observed outcomes may be due to the lack of or mutations in intermediary proteins, though proof is needed for this hypothesis. The re-distribution of DNAPK$_{CS}$ is likely to lead to sensitisation of NET cells to ionising radiation, which causes double-strand DNA breaks, DNAPK$_{CS}$ being crucial to their repair.

iii) Prolonged EGFR inhibition leads to reduction in DNAPK$_{CS}$ concentration in all tested NET cell lines except RIN, which displays the lowest levels of EGFR expression. This reduction in DNAPK$_{CS}$ is likely to lead to sensitisation of NET cells to ionising radiation, which causes double-strand DNA breaks, DNAPK$_{CS}$ being crucial to their repair.

Further work is being performed to discover the mechanisms involved in the outcomes observed following EGFR inhibition. In particular, the role of EGFR inhibition in sensitising NET cell lines to ionising radiation; the reasons for differences in DNAPK$_{CS}$ re-distribution following EGFR inhibition, in varying NET cell lines; the role of EGFR as a transcription factor etc are under study.

3.5.1 APPENDIX 1
The Immunoprecipitation (IP) Principle

The principle of an IP is very simple (Figure 3.12). An antibody (monoclonal or polyclonal) against a specific target antigen is allowed to form an immune complex with that target in a sample, such as a cell lysate. The immune complex is then captured on a solid support to which either Protein A or Protein G has been immobilized (Protein A or G binds to the antibody, which is bound to its antigen). The process of capturing this

complex from the solution is referred to as precipitation. Any proteins not "precipitated" by the immobilized Protein A or G support are washed away. Finally, components of the bound immune complex (both antigen and antibody) are eluted from the support and analyzed by SDS-PAGE (gel electrophoresis), often followed by Western blot detection to verify the identity of the antigen.

Traditional immunoprecipitation involves the following steps:

1. Form the antigen-antibody complex (immune complex) by incubating specific antibody with the antigen-containing sample for 1 hour to several hours.
2. Capture the immune complex on an immobilized Protein A or Protein G agarose gel support by incubation for ≈16 hours.
3. Remove any non-bound protein (non-immune complex sample components) from the precipitated complex by washing gel support with additional sample buffer.
4. Boil gel support in reducing SDS-PAGE sample loading buffer.
5. Recover sample eluted in loading buffer from gel support and analyze by SDS-PAGE.
6. Perform Western blot analysis, probing with antigen-specific antibody.
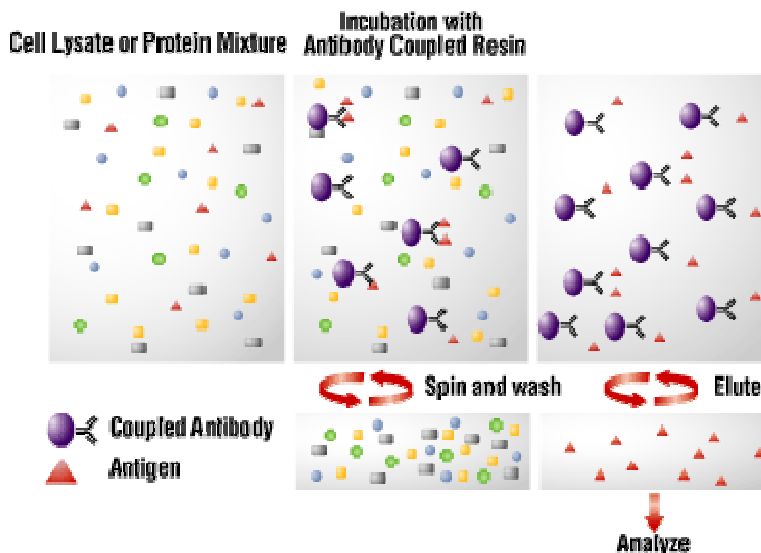
Figure 3.12. Summary of a traditional immunoprecipitation procedure.

Co-IP vs. IP

Co-immunoprecipitation (Co-IP) is a popular technique for protein interaction discovery. Co-IP is conducted in essentially the same manner as an IP. However, in a co-IP (Figure 3.13) the target antigen precipitated by the antibody "co-precipitates" a binding partner/protein complex from a lysate, i.e., the interacting protein is bound to the target antigen, which becomes bound by the antibody that becomes captured on the Protein A or G gel support. The assumption that is usually made when associated proteins are co-precipitated is that these proteins are related to the function of the target antigen at the cellular level. This is only an assumption, however, that is subject to further verification.
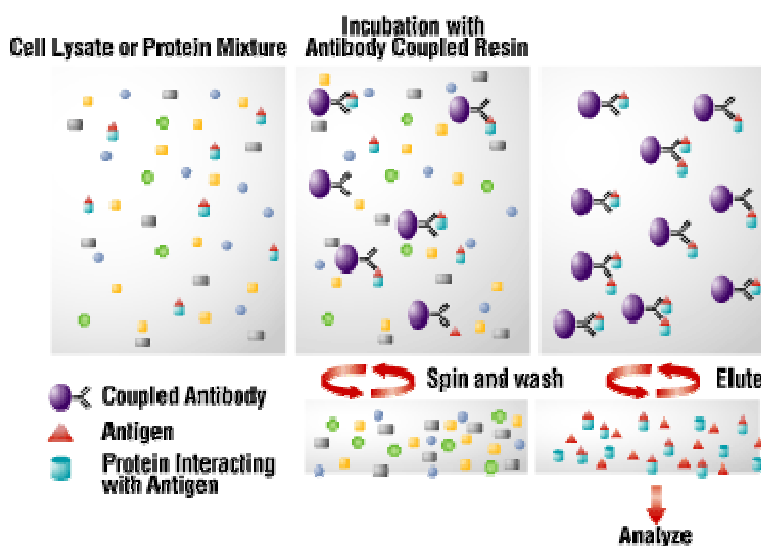
Figure 3.13. Summary of a traditional co-immunoprecipitation.

Thus an immunoprecipitation allows for the partial purification of a specific protein from a complex protein mixture that is present in a total cell lysate. In addition, co-immunoprecipitations may identify any protein-protein associations that exist in any given circumstance.

Chapter 4

The role of [99m]Technetium-depreotide in the management of neuroendocrine tumours

The role of [99m]Technetium-depreotide in the management of neuroendocrine tumours.

Tahir Shah, Ilona Kulakiene, Ann-Marie Quigley, Victoria S Warbey, Rajaventhan Srirajaskanthan, Christos Toumpanakis, Daniel Hochhauser, John Buscombe, Martyn E Caplin.

Study previously presented at:

American Gastroenterological Association annual meeting

Digestive Diseases Week Los Angeles 2006

British Society of Gastroenterology annual meeting

Birmingham 2006

4.1   Introduction:

Somatostatin is a hormone with multiple physiological effects including inhibition of secretion of other hormones and peptides. Somatostatin binds and acts through cell surface somatostatin receptors, of which there are 5 subtypes (SSTRs 1-5) (Chen C 1992, Buscail L et al 1994, Buscail L et al 1995, Liebmann C 2001). The majority of NETs express SSTRs, which can be utilised not only for tumour imaging but also for tumour targeted radiotherapy. ^{111}In-pentetreotide (OctreoScan®) binds to SSTR2 with high affinity and SSTR3/5 with lower affinity (table 4.1). It is widely used for localisation and staging of NETs with a reported sensitivity of 60-100% (De Herder WW et al 2005). It may also identify lesions not clinically suspected or apparent on planar radiology.

Those patients displaying moderate to strong uptake with ^{111}In-pentetreotide (Krennig score $\geq$ 2 i.e. uptake greater than normal liver tissue [De Herder WW et al 2005) are deemed suitable for treatment with SSTR2 targeting agents such as ^{90}Y-[DOTA]^0-Tyr^3-octreotide or ^{177}Lu-[DOTA]^0-Tyr^3-octreotate. However, some lesions may not be OctreoScan® positive while other lesions may potentially become OctreoScan® negative with time due to tumour dedifferentiation. Although a study directly comparing ^{111}In-pentetreotide and ^{99}mTechnetium-depreotide demonstrated ^{111}In-pentetreotide to be a superior form of imaging (Lebtahi R et al 2002), we postulated that ^{99m}Tc-depreotide may be useful in the subset of NET patients who have negative or only weakly positive ^{111}In-pentetreotide scans, due to its significantly higher binding affinity for SSTR3 (table 4.1). Here we present our experience relating to this sub-group of patients.

4.2   Patients, methods, and materials

This was a prospective study of 25 patients with histologically confirmed neuroendocrine tumours. They had either negative or weakly positive ¹¹¹In-pentetreotide imaging (Krenning scale ≤ 1; measured on a scale range 0-4), and were consecutively enrolled from our NET clinic. They underwent either paired ¹¹¹In-pentetreotide and ⁹⁹ᵐTc-depreotide imaging, or just ⁹⁹ᵐTc-depreotide imaging if within 6 months of the initial ¹¹¹In-pentetreotide scan. Histology was available for 20 patients, enabling tumours to be graded as low (Ki67 <2%), intermediate (Ki67 2 – 20%), and high grade (Ki67 >20%) (Table 4.2). The results from the two imaging agents were compared and confirmed radiologically using triple-phase CT in 17 patients, MRI in 2 patients and a combination of CT and MRI imaging in 7 patients. Patients receiving long-term long-acting somatostatin analogue therapy continued with their treatment and were scanned 1 week prior to receiving their next injection. All the clinical scans were performed within the legal requirements of the UK's Administration of Radionuclide Substance Advisory Committee (ARSAC). Only patients in whom both sets of imaging had been performed at our institution were included.

¹¹¹In-PentetreotideImaging

Whole-body and tomographic imaging was performed 24 hours after administration of 220 MBq of ¹¹¹In-pentetreotide, using a double or triple-headed gamma camera fitted with medium-energy collimators (Phillips Prism 2000XP and Phillips Irix, Phillips Medical Technology, Cleveland, Ohio, USA) and the two energy windows set at 173 and 247 keV ± 10%. Tomographic imaging was performed of the chest and/or abdomen as appropriate using the following parameters: angular range 180°, steps 60,

25 second acquisition per projection on the double-headed camera or angular range 120°, steps 40, 30 second acquisition per projection on the triple-headed camera, employing a 64 x 64 matrix. The tomographic images were reconstructed using an iterative ordered-subset expectation maximization (OSEM) programme with six iterations and post-filtered with a count-optimized Butterworth filter. The images were displayed as a full data set of orthogonal slices each of 9 mm thickness.

^{99m}Tc-DepreotideImaging

Whole-body and tomographic imaging was performed at 1 and 4 hours post administration of 555 MBq of ^{99m}Tc-Depreotide, using a double or triple-headed gamma camera fitted with low-energy high resolution collimators (Phillips Prism 2000XP and Phillips Irix, Phillips Medical Technology, Cleveland, Ohio, USA) with a single energy window set at 140 keV ± 10%. Tomographic imaging was performed of the chest and/or abdomen as appropriate using the following parameters: angular range 180°, steps 60, 25 second acquisition per projection on the double-headed camera or angular range 120°, steps 40, 30 second acquisition per projection on the triple-headed camera, employing a 128 x 128 matrix. The tomographic images were reconstructed using an iterative ordered-subset expectation maximization (OSEM) programme with six iterations and post-filtered with a count-optimized Butterworth filter. The images were displayed as a full data set of orthogonal slices each of 9 mm thickness.

Scintigraphy reporting

All images were read from the computer reporting station by at least two trained readers. The images obtained from the two modalities were read on different days as a means of blinding the readers to the results from the alternate imaging agent. Any site of focal uptake of either radiopharmaceutical outside of the expected physiological distribution of tracer was identified and noted as abnormal. In addition any areas of focal increased uptake within the liver, spleen, thyroid or colon was also recorded as abnormal. For the ^{111}In-pentreotide imaging any lesions in the liver were assessed using the Krenning grading system (De Herder WW et al 2005).

A direct lesion-by-lesion comparison was then made between the two radiopharmaceuticals. Any site of abnormal uptake was also compared with any sites of abnormality seen with anatomical imaging (normally triple phase CT or MRI).

4.3   Results:

20 of 25 patients with Krenning score $\leq$ 1, for ^{111}In-pentetreotide imaging, had histology available for further detailed analysis: of these 40% had high grade tumours, a further 35% had intermediate tumours, with the remainder 25% being low grade tumours (table 4.3). 13 of the 25 patients had completely negative ^{111}In-pentetreotide scans whereas the other 12 patients had weakly positive (Krenning score = 1) ^{111}In-pentetreotide scans (table 4.3). The same patients, when imaged with ^{99m}Tc-depreotide, had strongly positive scans (Krenning score $\geq$ 2) in 8 cases (figure 4.1), with the majority of these patients having intermediate or high-grade tumours. 6 of 25 patients had weakly positive ^{99m}Tc-depreotide scans (Krenning score = 1). The remainder 11 of 25 patients had completely negative ^{99m}Tc-depreotide scans

(Krenning score = 0) despite the clinical, radiological, and histological confirmation of neuroendocrine tumours (table 4.2). Wilcoxon Signed Ranks Test confirmed a statistically significant difference between the two scintigraphy modalities, with ^{99m}Tc-depreotide scan providing better imaging in this selected group of neuroendocrine patients (Z = –2.311; Asymp. Sig. [2-tailed] 0.021).

Correlations were sought between the tumour grade and scintigraphy results. These revealed a negative correlation between tumour grade and Krenning score for ^{111}In-pentetreotide scans (Spearman's rho: –0.446; Sig (2-tailed) 0.049), i.e. the higher the tumour grade the lower the Krenning score, whereas no statistically significant correlation was found between tumour grade and the Krenning scores for ^{99m}Tc-depreotide imaging.

The ability of the three imaging modalities to highlight tumour lesions was compared (table 4.4). This revealed the two scintigraphic techniques had the ability to highlight different lesions within same patients (table 4.4).

4.4   Discussion:

[111]In-pentetreotide is a well-established scintigraphic agent with high sensitivity and specificity in NETs. Further advances in functional molecular imaging are being achieved through the development of positron emission tomography (PET) scanning, in particular ^{18}F-dopa PET/CT and ^{68}Ga PET/CT, although its use is severely limited by availability at present (Ambrosini V et al 2007, Win Z et al 2007). Additional information can also be gleaned from detailed analysis of currently available imaging techniques. Indeed a large-scale study comparing ^{111}In-pentetreotide to ^{123}I-MIBG scintigraphy demonstrated that some lesions express appropriate receptors for ^{111}In-pentetreotide but not for MIBG whilst others have uptake for MIBG but not for ^{111}In-pentreotide (Quigley AM et al 2005). The information thus gained helps individualise treatment with the most appropriate receptor targeted radio-therapeutic agent, and helps justify the increased costs associated with molecular imaging.

This study compares ^{99m}Tc-depreotide, an imaging agent with higher affinity for SSTR3 than ^{111}In-pentetreotide, in patients with negative or weakly positive ^{111}In-pentetreotide scans. Radiological imaging is also included as an independent means of confirming scintigraphy findings. High-resolution triple-phase-contrast CT was the preferred imaging modality, as it is readily available and has high sensitivity and specificity for NET lesions. MRI was used, in selected cases, either because of the need for repeated imaging in young patients or in order to visualise suspected tumour lesions not visible on CT.

Our experience with ^{99m}Tc-depreotide in this subset of NET patients demonstrated that a significant proportion (8 of 25; 32%) of OctreoScan®-negative patients were significantly positive (Krenning score $\geq$ 2) when imaged using ^{99m}Tc-depreotide. We also demonstrated a negative correlation between tumour grade and ^{111}In-pentreotide

scan Krenning scores, i.e. high tumour grade was linked to weaker images. Lack of correlation between tumour grade and ^{99m}Tc-depreotide scans highlights the fact that ^{99m}Tc-depreotide imaging is not SSTR2 dependent, as well as indicating that loss of SSTR2/5 does not imply loss of other SSTRs.

These findings imply that:

i) ^{99m}Tc-depreotide may be able to follow changes in tumour phenotype of NET patients, i.e. loss of SSTR subtypes in conjunction with tumour progression from low grade to high grade.

ii) ^{99m}Tc-depreotide may improve the sensitivity of SSTR targeted scintigraphy for highlighting tumours which do not express SSTR2/5.

iii) ^{99m}Tc-depreotide may have the ability to highlight tumours suitable for treatment with agents with an expanded SSTR subtype affinity, such as SOM-230.

In conclusion, ^{111}In-pentetreotide is highly sensitive for detecting NETs. However some tumours are ^{111}In-pentetreotide negative at presentation or become negative with time. This study demonstrated that ^{99m}Tc-depreotide, is a significantly better imaging agent for detecting NETs in this subgroup of patients, and provides a theoretical basis for targeted therapy to be performed with agents possessing an expanded SSTR subtype affinity such as SOM230 or ^{90}Y-DOTA-lanreotide. Other experimental imaging techniques based on either newer somatostatin analogues or imaging modalities, e.g. PET scanning, may also be useful for imaging the higher grade NETs.

Radioligand	SSTR1	SSTR2	SSTR3	SSTR4	SSTR5
[111]In-pentetreotide	>10,000	1.5	30	>1000	1.0
[99m]Tc-depreotide	>1000	1.0	1.5	>1000	2
^{90}Y-DOTA-lanreotide	215	4.3	5.1	3.8	10
SOM230	9.3	1.0	1.5	>1000	0.16

Table 4.1: Affinity of radiolabelled ligands for SSTR subtypes. Values are listed in nmol/l and indicate the binding affinity in terms of the inhibitory constant causing 50% inhibition of specific somatostatin receptor binding (IC_{50}). [Virgolini I et al 2002, Schmid HA2004].

Grade	Mitotic count [a](10 HPF)	Ki-67 index [b](%)
G1	<2	≤2
G2	2 – 20	3 – 20
G3	>20	>20

Table 4.2: Grading proposal for foregut neuroendocrine tumours (Rindi G et al 2006)
[a]10 HPF: high powered field = 2mm^2, at least 40 field (at 40x magnification) evaluated in areas of high mitotic density
[b]MIB1 antibody: % of 2,000 tumour cells in area of highest nuclear labelling

Patient	Diagnosis	^{111}In-pentetreotide (strength)	^{99m}Tc-depreotide (strength)	Histology grade
1	MTC	1	2	Intermediate
2	MTC	1	3	-
3	Hindgut	1	0	Low
4	Pancreatic	0	1	Intermediate
5	Hindgut	0	0	High
6	Bronchial	1	1	Intermediate
7	Midgut	0	0	High
8	MTC	1	2	Intermediate
9	Unknown primary	0	2	High
10	Midgut	1	2	Intermediate
11	Hindgut	1	0	Low
12	Midgut	0	0	Low
13	Bronchial	0	0	High
14	Pancreatic	0	0	High
15	Pancreatic	1	0	Low
16	MTC	1	1	High
17	Midgut	0	1	-
18	Unknown primary	0	2	High
19	Pancreatic	0	0	Low
20	Pancreatic	0	0	-
21	Midgut	0	0	Intermediate
22	Midgut	0	1	high
23	Pancreatic	1	1	Intermediate
24	Thymic	1	3	-
25	MTC	1	3	-

Table 4.3: Data on the 25 patients assessed. The imaging strength was measured using the Krenning scale [range 0-4]. Tumour grade was assigned using the criteria set out in the ENETS consensus document (Rindi G et al 2006). MTC = medullary thyroid carcinoma

Pt	Neck			Chest			Spine			Right arm			Left arm			Liver			Abdomen			Pelvis			Right leg			Left leg			Total		
	d	o	ct	d	o	ct	d	o	ct	d	o	ct	d	o	ct	d	o	ct	d	o	ct	d	o	ct	d	o	ct	d	o	ct	d	o	ct
1	0	0	0	4	5	0	0	0	0	0	0	0	0	0	0	0	0	0	0	0	0	0	0	0	0	0	0	0	0	0	4	5	0
2	0	0	0	10	3	10	3	0	10	0	0	0	0	0	0	0	0	3	0	0	0	0	0	10	0	0	0	0	0	0	13	3	33
3	0	0	0	0	0	0	0	0	0	0	0	0	0	0	0	0	0	1	0	1	0	0	0	0	0	0	0	0	0	0	0	1	1
4	0	0	0	0	0	0	0	0	0	0	0	0	0	0	0	0	0	3	2	0	0	0	0	0	0	0	0	0	0	0	2	0	3
5	0	0	0	0	0	0	0	0	0	0	0	0	0	0	0	0	0	0	0	0	0	0	0	0	0	0	0	0	0	0	0	0	0
6	0	0	0	1	1	0	0	2	10	1	0	0	1	0	0	0	0	0	0	0	0	0	0	10	1	0	2	1	0	3	5	3	25
7	0	0	0	0	0	10	0	0	0	0	0	0	0	0	0	0	0	1	0	0	10	0	0	0	0	0	0	0	0	0	0	0	21
8	1	0	0	2	0	10	1	0	10	0	0	0	0	0	0	3	3	10	0	0	10	0	0	0	0	0	0	0	0	0	7	3	40
9	0	0	0	0	0	10	5	0	10	3	0	3	3	0	3	0	0	2	0	0	0	0	0	0	3	0	3	3	0	3	17	0	34
10	0	0	0	0	0	0	0	0	0	0	0	0	0	0	0	0	0	0	1	1	2	1	1	1	0	0	0	0	0	0	2	2	3
11	0	0	0	0	0	0	0	0	2	0	0	0	0	0	0	0	1	6	0	0	0	0	1	0	0	0	0	0	0	0	0	2	8
12	0	0	0	0	0	1	0	0	0	0	0	0	0	0	0	0	0	10	0	0	4	0	0	0	0	0	0	0	0	0	0	0	15
13	0	0	0	1	2	2	0	0	0	0	0	0	0	0	0	0	0	10	1	1	0	0	0	0	0	0	0	0	0	0	2	2	0
14	0	0	0	0	0	0	0	0	0	0	0	0	0	0	0	0	0	0	0	0	1	0	0	0	0	0	0	0	0	0	0	0	1
15	0	3	0	0	0	10	0	0	0	0	0	0	0	0	0	0	2	10	0	0	10	0	0	0	0	0	0	0	0	0	0	5	30
16	0	0		2	1		0	0		0	0		0	0		0	0		0	0		0	0		0	0		0	0		2	2	
17	0	0		0	0		0	0		0	0		0	0		1	0	9	0	0		0	0		0	0		0	0		1	0	
18	0	0	0	0	0	1	0	0	0	0	0	0	0	0	0	0	0	0	1	0	1	1	0	1	0	0	0	0	0	0	2	0	3
19	0	0	1	0	0	1	0	0	0	0	0	0	0	0	0	0	0	3	0	0	2	0	0	0	0	0	0	0	0	0	0	0	7
20	0	0	0	0	0	0	0	0	0	0	0	0	0	0	0	0	0	0	0	0	2	0	0	0	0	0	0	0	0	0	0	0	2
21	0	0	0	0	0	1	0	0	0	0	0	0	0	0	0	0	0	10	0	0	1	0	0	0	0	0	0	0	0	0	0	0	12
22	0	0	0	0	0	2	0	0	0	0	0	0	0	0	0	2	0	6	0	0	3	0	0	1	0	0	0	0	0	0	2	0	12
23	0	0	0	0	0	2	0	0	0	0	0	0	0	0	0	0	1	10	0	1	1	1	1	0	0	0	0	0	0	0	1	3	13
24	0	0	0	1	1	1	0	0	0	0	0	0	0	0	0	0	0	0	0	0	0	0	0	0	0	0	0	0	0	0	1	1	1
25	3	3	0	0	0	10	0	0	0	0	0	0	0	0	0	0	0	3	0	0	0	0	0	0	0	0	0	0	0	0	3	3	13

Table 4.4: Site based comparison of lesions detected by each imaging modality.
d – depreotide; o – octreotide; ct – CT or MRI scan; Pt – patient number.
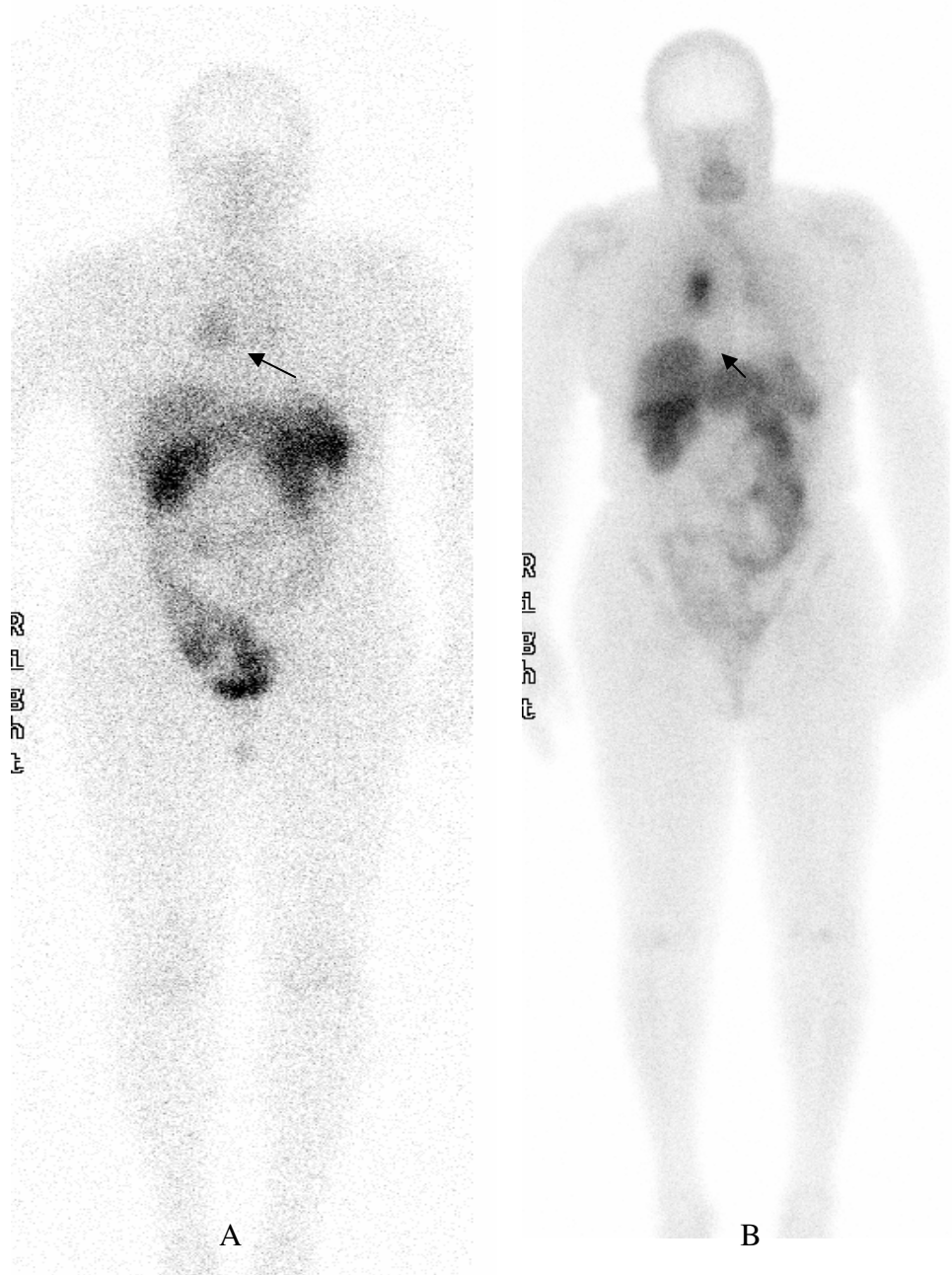
Figure 4.1: 71-year old female patient with thymic carcinoid tumour. The ^{111}In-pentetreotide scan (A) demonstrating low-grade uptake in the mediastinum (arrow) with intensity lower than that in the liver. The patient went on to have a ^{99m}Tc-Depreotide scan (B) illustrating high grade uptake in the mediastinum (arrows) with intensity greater than that in the liver.

CHAPTER 5
Alpha-fetoprotein and human chorionic gonadotrophin-β as prognostic markers in neuroendocrine tumour patients

The role of alpha fetoprotein and β-human chorionic gonadotrophin as tumour markers in neuroendocrine tumours.

T. Shah, M. E. Caplin. Br J Cancer. 2008; 99: 72-7.

Study previously presented at:
American Gastroenterological Association annual meeting
Digestive Diseases Week Los Angeles 2006

British Society of Gastroenterology annual meeting
Birmingham 2006

5.1   Introduction

Neuroendocrine tumours (NETs) comprise a heterogeneous group of tumours classified as being either functional, with symptoms due to hormone secretion, or non-functional due to an apparent lack of hormone-associated symptoms (Solcia et al 2000). The functional tumours may produce specific hormones the measurement of which can aid diagnosis and management; for example serotonin with midgut carcinoid tumours, insulin with insulinoma, and gastrin in gastrinoma. Currently, the most useful "general" NET marker is plasma CgA and recent guidelines recommending that all patients with NETs should have CgA measured (Ramage et al 2005, Rindi et al 2006b).

Tumour markers can provide valuable information on tumour functionality and presumed tumour burden in relation to anti-tumour therapy. For example an indolent non-functioning NET may produce increased amounts of CgA as the first sign of a switch to a more progressive course. Alternatively, anti-tumour therapy may not display tumour response as determined radiologically, using the RECIST criteria, since tumour cells may be replaced by fibrosis with a resultant lack of change in overall tumour size; However, there may be a significant decline in the level of circulating tumour markers together with significant symptomatic improvement. Additionally, tumour markers can have prognostic value: plasma neurokinin-A has been shown to be an accurate marker of prognosis in midgut NETs, with rising neurokinin-A levels despite somatostatin analogue therapy, shown to be associated with poorer prognosis (Turner et al 2006); patients with CgA greater than 5000µg/l have a 5 year survival of only 22% as opposed to 63% for patients with serum chromogranin-A levels of less than 5000µg/l (Janson et al 1997). Absolute plasma CgA levels may also help to differentiate between localised and diffuse NET spread, as well as between chronic active gastritis and NETs (Campana et al 2007).

There is a continuing need for tumour markers that can provide further diagnostic and prognostic information in NET patients. AFP and hCGβ have previously been reported as being elevated in some NET patients, however, the utility of these markers in NET patients has not been determined (Ramage et al 2005). Lokich reported, in a small series, that AFP may be raised in a small proportion of NET patients and that it may provide some useful information

117

(Lokich et al 1987). However this initial report has not been further explored. AFP is reactivated in numerous cancers, including hepatocellular carcinoma and teratocarcinomas. The basis of this reactivation is not well understood, but may involve changes in the level or activity of transcriptional regulators (Spear et al 1999).

hCGβ belongs to the glycoprotein hormone family that also comprises luteinizing hormone (LH), follicle-stimulating hormone (FSH), and thyroid-stimulating hormone (TSH). All members are heterodimers consisting of an α and a β subunit. The α-subunit, which is common to all glycoprotein hormones, contains 92 amino acids. The β chains determine the biological activity and display extensive homology, with that between hCGβ and LHβ being about 80%. Human chorionic gonadotropin (hCG) is mainly used for detection and monitoring of pregnancy, pregnancy-related disorders and as an extremely sensitive and specific marker for trophoblastic tumours of placental and germ cell origin (Stenman et al 2006).

The aims of this study were to determine the role of AFP and hCGβ as diagnostic and prognostic markers, their relationship to other tumour markers, as well as their value in predicting disease progression in NET patients.

5.2   Patients and methods

We have developed a database of neuroendocrine tumour patients, containing biochemical, radiological, histological and survival data available for 360 patients. Patients had been consented for approval of utilisation of blood and tissue results for research purposes. Pre-treatment biochemical data included tumour markers α-fetoprotein, hCGβ, and CgA. Histology data was collected in order to determine tumour grade. NET histological grading was assessed according to the new TNM classification, including differentiation of tumour and proliferation index Ki-67 (MIB-1): thus classified as low grade (G1) mitotic count <2 / 10 high powered fields (HPF) or Ki-67 $\leq$2%; intermediate grade (G2) mitotic count 2 - 20 / 10 HPF or Ki-67 3 - 20%; and high grade (G3) mitotic count >20 / 10 HPF or Ki-67 >20% (Rindi et al 2006). Of the 360 patients in the database,

294 had been tested for α-fetoprotein. Of these 294 patients a subset of 28 patients was identified with serum α-fetoprotein levels at least 1.5x the upper limit of normal. A further 40 patients with normal α-fetoprotein were randomly chosen from the database to act as an age and sex matched control for the α-fetoprotein-high patients. 268 patients had been tested for hCGβ, of which 33 patients had hCGβ levels at least 1.5x the upper limit of normal. A further 33 patients with normal hCGβ were randomly chosen from the database to act as an age and sex matched control for the hCGβ-high patients.

A subset of 21 patients was derived from the AFP and hCGβ groups that had raised AFP and hCGβ in combination. This subset comprised 9.1% of patients in whom the 2 markers had been measured. Control group had normal serum AFP and hCGβ levels.

Statistical Package for the Social Sciences (SPSS) was utilised in order to determine any differences between the two tumour marker groups and their respective controls [Mann-Whitney U test for non-parametric samples; table 5.1, 5.3 & 5.5]; to discover any correlations between the parameters recorded [Spearman's rho; tables 5.2, 5.4 & 5.6]; and to look for survival differences [Kaplan-Meier survival curves; figures 5.1, 5.2 & 5.3].

5.3   Results

5.3.1 AFP group:

28 of 294 patients (9.5%) had elevated AFP. The AFP-high and control groups were compared using Mann-Whitney-U test, for 2 non-parametric samples, in order to look for significant differences in age and gender make-up of the 2 groups. This confirmed the 2 groups to be evenly matched for age and sex (table 5.1). There were significant differences between the two groups for the measured tumour markers AFP, hCGβ, CgA, MIB-1 (table 5.1), and survival as measured from the time of diagnosis (figure 5.1; table 5.1).

The data from the 2 groups was then combined for further statistical analysis in order to determine possible correlations between the 5 parameters studied: absolute levels of AFP, MIB-1, hCGβ, CgA, and patient survival. Spearman's rho test was applied to the data (table 5.2). Serum AFP levels were discovered

to correlate with the 4 parameters measured. Thus, rising serum AFP levels strongly and positively correlated with rising hCGβ, CgA levels, and MIB-1 scores. There was an additional strongly negative correlation with survival from the time of diagnosis (significant at the 0.01 level) (table 5.2).

5.3.2 hCGβ group:

33 of 268 patients (12.3%) had elevated hCGβ. The hCGβ-high and control groups were compared using Mann-Whitney-U test, for 2 non-parametric samples, in order to look for significant differences in age and gender make-up of the 2 groups. This confirmed the 2 groups to be evenly matched for age and sex (table 5.3). There were significant differences between the two groups for the measured levels of tumour markers hCGβ, AFP, CgA, and survival as measured from the time of diagnosis (table 5.3; figure 5.2); but not MIB-1 scores (table 5.3).

The data from the 2 groups was then combined for further statistical analysis in order to determine possible correlations between the 5 parameters studied: absolute levels of hCGβ, AFP, MIB-1, CgA, and survival from time of diagnosis. Spearman's rho test was applied to the data (table 5.4).

Serum hCGβ levels were discovered to be correlated with 3 of 4 other parameters measured. That is: rising serum hCGβ levels strongly and positively correlated with rising AFP, and CgA, levels. Rising hCGβ levels negatively correlated with survival from the time of diagnosis. (significant at the 0.01 level) [table 5.4]. No correlation was found between hCGβ levels and MIB-1 score.

5.3.3 Combined AFP/hCGβ group:

21 of 230 patients (9.1%) had combined elevation of serum AFP and hCGβ. The combined AFP/hCGβ-high and control groups were compared using Mann-Whitney-U test, for 2 non-parametric samples, in order to look for significant differences in age and gender make-up of the 2 groups. This confirmed the 2 groups to be evenly matched for age and sex (table 5.5). There were significant differences between the two groups for the measured levels of tumour markers hCGβ, AFP, CgA, and survival as measured from the time of diagnosis (table 5.5; figure 3); but not MIB-1 scores (table 5.5).

The data from the 2 groups was then combined for further statistical analysis in order to determine possible correlations between the 5 parameters studied: absolute levels of hCGβ, AFP, MIB-1, CgA, and survival from time of diagnosis. Spearman's rho test was applied to the data (table 5.6).

These statistical tests discovered the serum AFP levels to correlate with the 4 parameters measured. That is: rising serum AFP levels strongly and positively correlated with rising hCGβ, CgA levels, and MIB-1 scores; Rising serum AFP strongly and negatively correlated with survival from the time of diagnosis (significant at the 0.01 level) (table 5.6). Serum hCGβ levels correlated with 3 of 4 other parameters measured. That is: rising serum hCGβ levels strongly and positively correlated with rising AFP, and CgA, levels. Rising hCGβ levels negatively correlated with survival from the time of diagnosis. (significant at the 0.01 level) [table 5.6]. No correlation was found between hCGβ levels and MIB-1 score (table 5.6).

5.4 Discussion:

A number of putative tumour markers are measured in NET patients, with CgA having the highest expression in NETs and being considered the most useful diagnostic and prognostic marker (Turner et al 2006, Janson et al 1997, Campana et al 2007). Tumour markers are measured at regular intervals and may be useful for monitoring disease progression. Often a rise in tumour marker levels may precede clinical indicators of disease progression such as worsening diarrhoea, facial flushing, and weight loss, as well as objective indicators of disease progression as determined radiologically. Furthermore, an increase in the number of expressed tumour markers is associated with worsening prognosis (Ardill & Erikkson 2003).

To date there are only limited data on most tumour markers measured in NET patients, which has thus created uncertainty about their role. Clinical impression of a linkage between high-grade, aggressive tumours and a rise in serum AFP and hCGβ levels led us to perform a systematic review of the utility of AFP and hCGβ measurement in our NET patients. Although, very little is known about AFP in NETs, some useful data already exists on the expression and value of alpha and beta subunits of hCG (Nobels et al 1997, Heitz et al 1987, Grossmann et al 1994, and Eriksson et al 1989). These subunits have been shown to be raised in a significant proportion of NET patients and to have the ability to differentiate between benign and malignant gastroenteropancreatic tumours (Grossmann et al 1994, Eriksson et al 1989, and Heitz et al 1987). However, neither AFP nor sub-units of hCG are able to differentiate between NETs and other tumours (Nobels et al 1997, Yuen & Lai 2005).

This analysis of a large NET patient database demonstrates, for the first time, the ability of two easily measurable agents to prognosticate in NET patients. Both AFP and hCGβ are shown to be related to poorer survival, with the clearest difference being seen between the group of patients with combined rise in AFP and hCGβ in comparison to controls matched for age at diagnosis and sex. However, only AFP associated with Ki-67. This can be explained by the fact that there are significant differences in the disease stage between the AFP-

high group and its control group, whereas no significant differences in the disease stage existed between the hCGβ-high group and its control group (tables 5.1 & 5.3).

Although overall AFP is only elevated in a minority of NET patient, this data analysis demonstrates the ability of AFP to highlight a group of NET patients with aggressive, high-grade tumours and poor prognosis. Interestingly, four patients with raised AFP did not have liver metastases but did have large volume disease elsewhere (neck, peritoneum, and chest). Thus AFP is likely to be a marker of tumour cell de-differentiation rather than a marker of hepatic metastases from NETs.

hCGβ also provides prognostic information with its demonstrated correlation with impaired survival and other markers of a poor outcome, namely CgA and AFP. When hCGβ is high, as defined by levels > 1.5 x upper limit of normal, the Mann Witney U test applied to these values demonstrates a clear difference in survival between the 2 groups (table 5.3). On determining a correlation between the absolute hCGβ level and degree of impairment of survival, although there is a trend to impaired survival this is not a statistically significant (table 5.4). The results of these analyses demonstrate that an abnormally high hCGβ is more informative than the absolute level itself. Thus hCGβ, when raised, is a marker of poor prognosis (table 5.3, figure 5.2).

The clearest predictions, however, can be made for those patients with a combined rise in both serum AFP and hCGβ levels. These are strongly associated with high CgA levels and worsening prognosis. Conversely, patients with normal AFP and hCGβ levels have low serum CgA levels and an excellent 5 year prognosis (figure 5.3).

Most NET patients have extensive metastases at the time of diagnosis. The indolent nature of these tumours means that even in the presence of liver metastases, the 5 year survival rates are surprisingly good. However, a proportion of patients have rapidly progressive disease, at diagnosis, which

requires aggressive management with cytoreductive therapies, hopefully resulting in better symptom control and improved survival. Predicting the behaviour of NETs in individual cases has to date relied on tumour histology, serum CgA levels and serial radiology imaging. This data clearly demonstrates the utility of AFP, hCGβ, CgA, and possibly Ki-67 index in highlighting those patients, with WHO stage IV disease, that are going to require intensive monitoring and possibly early and aggressive therapy. Conversely, patients with favourable results can be re-assured about their medium to long-term survival, and monitored less intensely with confidence, perhaps six monthly as opposed to three to four monthly for those patients with for example elevated AFP and hCGβ.

This is a retrospective study and the results highlight the worth of performing a prospective study to assess these markers.

In conclusion, this study has identified AFP and hCGβ to be capable of providing significant prognostic information relevant to the management of NET patients.

	High AFP	Control	P value (Mann-Whitney-U test)
Age at diagnosis	51	48	.597
Sex (M/F)	15/13	18/22	.495
DIAGNOSIS:			
Metastatic NET (of uknown primary)	9	13	
Pancreatic NET	11	16	
Gastrinoma	1	2	
Bronchial	2	4	
Midgut NET	1	3	
Hindgut NET	1	0	
MTC	1	1	
Thymic NET	1	1	
Pelvic NET	1	0	
Mean AFP (0-11.3ng/ml)	273.8	3.5	0.001
Mean hCGβ (<2.5mIU/ml)	21.3	1.6	0.001
Mean CgA (0-60U/L)	423	113	0.002
Mean Ki-67 (MIB-1)	21	10	0.009
Mean survival (months)	37.6	69	0.001
Stage IV disease (WHO classification)	24 of 28 (86%)	25 of 40 (63%)	0.037

Table 5.1: Comparison of demographic and tumour markers data for the raised-AFP and control groups demonstrating the two groups to be evenly matched for age, gender, and diagnosis. Significant differences between the two groups are apparent for the expression of tumour markers AFP, hCGβ, CgA, Ki-67 score, and survival from the time of diagnosis.

			Ki-67 (MIB1)	hCGβ	CgA	Survival in months
Spearman's rho	**AFP**	Correlation Coefficient	.381(**)	.558(**)	.451(**)	-.419(**)
		Sig. (2-tailed)	.007	.000	.000	.001

** Correlation is significant at the 0.01 level (2-tailed).
Table 5.2: Correlation of AFP levels with Ki-67 score, serum hCGβ and CgA levels, as well as survival in NET patient.

	High hCGβ	Control	P value (Mann-Whitney-U test)
Age at diagnosis	55	54	.891
Sex (M/F)	16/17	16/17	
DIAGNOSIS:			
Metastatic NET (of uknown primary)	8	7	
Pancreatic NET	15	11	
Gastrinoma	2	1	
Bronchial	4	5	
Midgut NET	1	6	
Hindgut NET	1	1	
MTC	1	1	
Thymic NET	1	1	
Mean hCGβ (<2.5mIU/ml)	198.7	2.0	0.001
Mean AFP (0-11.3ng/ml)	238.1	7.9	0.001
Mean CgA (0-60U/L)	414.2	180.3	0.02
Mean Ki-67 (MIB-1)	13	14	0.63
Mean survival (months)	48	57.3	0.037
Stage IV disease (WHO classification)	27 of 33 (82%)	24 0f 33 (73%)	0.382

Table 5.3: Comparison of demographic and tumour markers data for the raised-hCGβ and control groups demonstrating the two groups to be evenly matched for age, gender, and diagnosis. Significant differences between the two groups are apparent for the expression of tumour markers AFP, hCGβ, CgA and survival from the time of diagnosis.

			Ki-67 (MIB1)	AFP	CgA	Survival in months
Spearman's rho	**hCGβ**	Correlation Coefficient	.012	.634 (**)	.291(*)	-.229
		Sig. (2-tailed)	.931	.000	.019	.074

** Correlation is significant at the 0.01 level (2-tailed).
* Correlation is significant at the 0.05 level (2-tailed).
Table 5.4: Correlation of hCGβ levels with AFP and CgA levels. There is also a trend towards a statistically significant correlation between hCGβ levels and survival, but clear absence of linkage between hCGβ levels and Ki-67 score.

	Combined raised AFP and hCGβ	Control	P value (Mann-Whitney-U test)
Age at diagnosis	55.4	55.4	0.691
Sex (M/F)	13/8	15/13	
DIAGNOSIS:			
Metastatic NET (of uknown primary)	6	6	
Pancreatic NET	10	10	
Gastrinoma	0	0	
Bronchial	2	5	
Midgut NET	0	5	
Hindgut NET	1	1	
MTC	1	2	
Thymic NET	1	1	
Mean AFP (0-11.3ng/ml)	371.7	35.4	0.001
Mean hCGβ (<2.5mIU/ml)	283.6	2.2	0.001
Mean CgA (0-60U/L)	511	210	0.014
Mean Ki-67 (MIB-1)	15.6	11.9	0.283
Mean survival (months)	29.9	61.2	0.001
Stage IV disease (WHO classification)	18 of 21 (86%)	20 of 28 (71%)	0.240

Table 5.5: Comparison of demographic and tumour markers data for the combined raised serum hCGβ/AFP levels and control groups demonstrating the two groups to be evenly matched for age, gender, and diagnosis. Significant differences between the two groups are apparent for the expression of tumour markers AFP, hCGβ, CgA and survival from the time of diagnosis.

			Ki-67 (MIB1)	AFP	hCGb	CgA	Survival in months
Spearman's rho	**AFP**	Correlation Coefficient	.330(*)	1.000	.778(**)	.413(**)	-.486(**)
		Sig. (2-tailed)	.035	.	.000	.004	.001
Spearman's rho	**hCGb**	Correlation Coefficient	.090	.778(**)	1.000	.310(*)	-.410(**)
		Sig. (2-tailed)	.575	.000	.	.032	.005

** Correlation is significant at the 0.01 level (2-tailed).

* Correlation is significant at the 0.05 level (2-tailed).

Table 5.6: Correlation of AFP levels with Ki-67 score, serum hCGβ and CgA levels, as well as survival in NET patient.

Figure 5.1: Kaplan-Meier graph comparison of 5-year survival between the high-AFP and control (normal-AFP) groups (p=0.001).
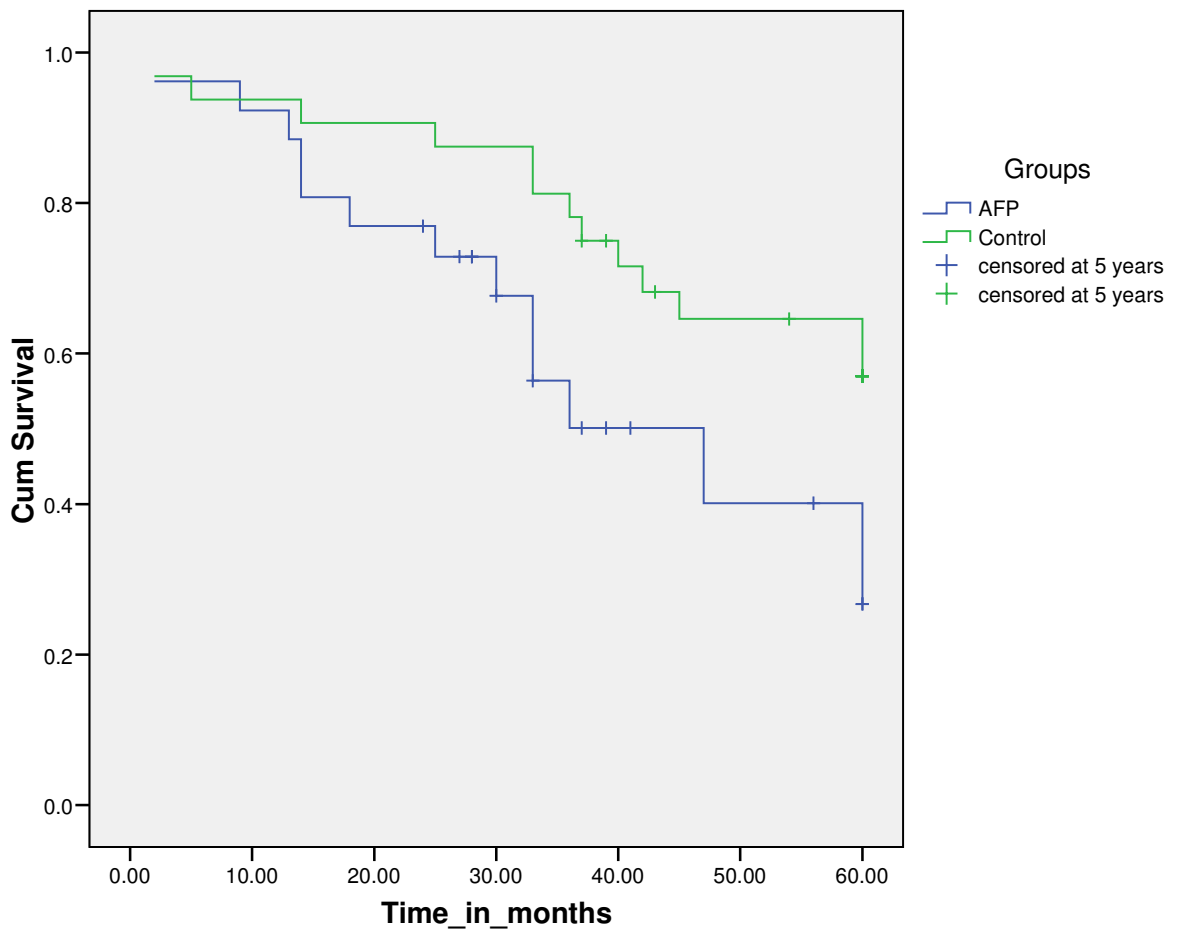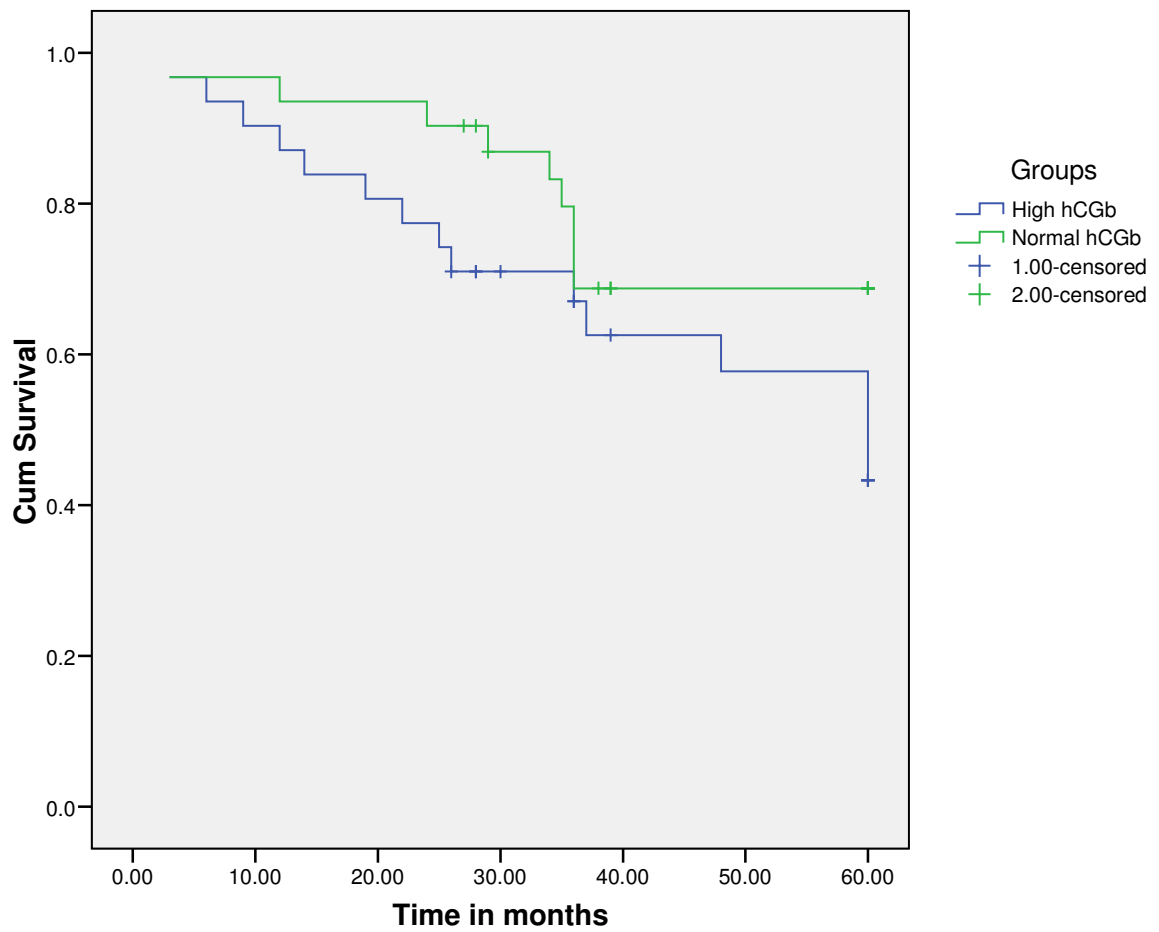
Figure 5.2: Kaplan-Meier graph comparison of 5-year survival between the high-hCGb and control (normal-hCGb) groups (p=0.037)
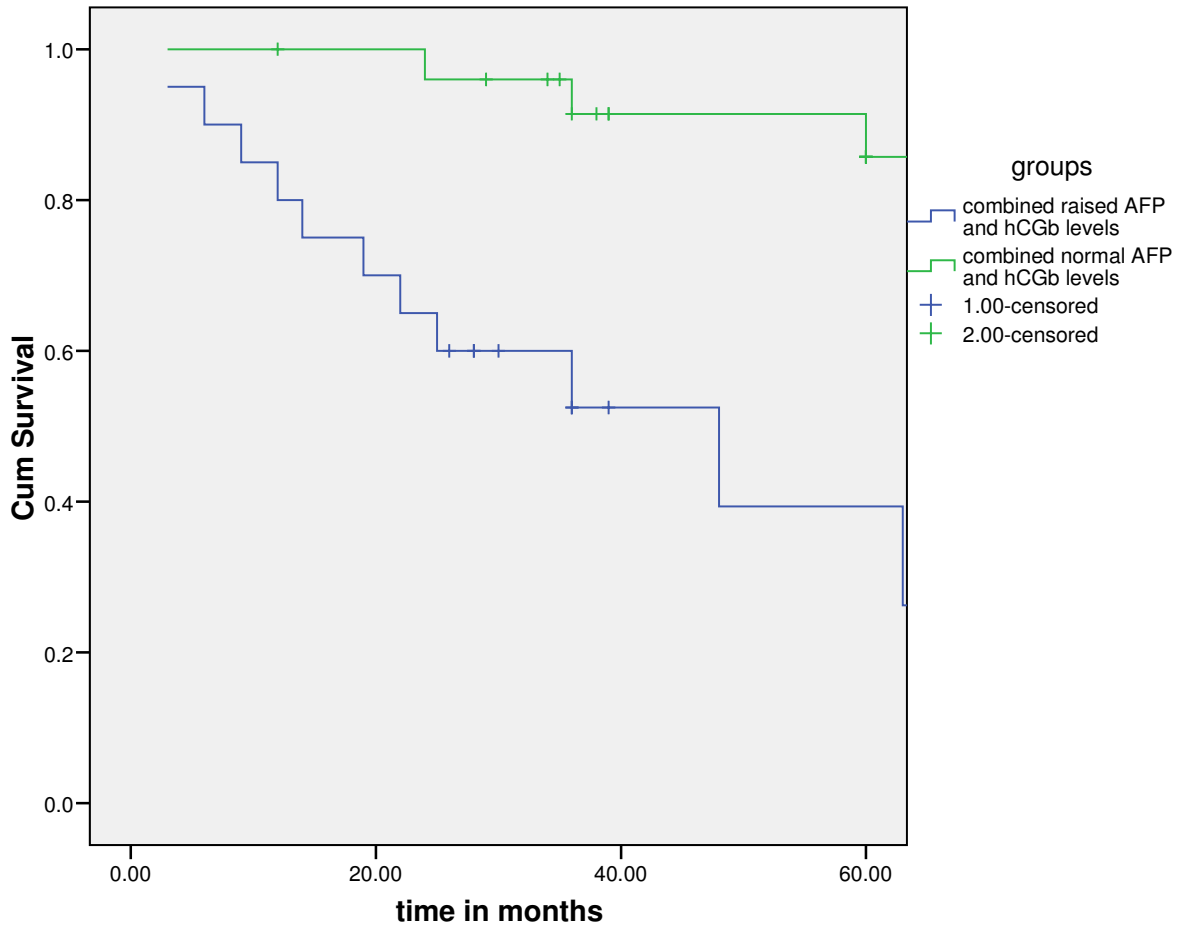
Figure 5.3: Kaplan-Meier graph comparison of 5-year survival between the combined high-AFP/hCGb and control (normal-AFP/hCGb) groups (p=0.001).

CHAPTER 6

CONCLUSIONS AND FUTURE WORK

Neuroendocrine tumours are rare cancers therefore there have been major logistical difficulties in studying them. Recently the care of these patients has started to be centralised which is providing the basis for the evaluation and development of diagnostic techniques, the study of neuroendocrine tumour biology as well as the assessment of novel therapeutic approaches.

This thesis provides new insights into: the diagnostic and prognostic value of biochemical tumour markers; the role of scintigraphic agent depreotide for tumour staging and determining suitability for targeted radiotherapy; as well as tumour biology and novel targets for therapy in neuroendocrine tumours.

Chapter 2: The traditional DNA-damaging cytotoxic agents are of limited efficacy in the treatment of neuroendocrine tumours of the gastrointestinal tract (NETs). Characterization of specific molecular features of various cancer types has prompted a new era of molecular therapeutics with the development of more selective targeted agents. Within this new setting, there is a great, as yet unexploited, therapeutic potential in the field of NETs. One possible new therapeutic target showing promise in various common tumour types, including head and neck and colon cancer, is epidermal growth factor receptor (EGFR). This cell surface receptor is over-expressed in most tumour types and is associated with resistance to anti-tumour therapy and poor prognosis. Study of EGFR activation and signalling in various cell types has demonstrated the activation of downstream pathways that ultimately lead to enhanced cell-survival, proliferation, and tumour metastases. This work had been applied to the NET field with demonstration of activation of ERK1/2 and Akt/PKB (2 tyrosine kinases which are important components of EGFR-related intra-cellular signalling pathways) in NET cell lines.

This chapter details a large-scale immunohistochemical study performed on tumour tissue obtained from 98 NET patients. The expression of EGFR and its activated form, pEGFR, was studied using specific high affinity antibodies raised against these two forms. The expression of phosphorylated forms of ERK1/2 and Akt/PKB was also studied. This large scale study of EGFR expression, activation and activation of member enzymes of downstream pathways is the first such study in NET tissue samples. We demonstrated not only the presence of these signalling molecules in their activated forms in NET tissue but also a correlation between EGFR activation and the activation of ERK1/2 and Akt/PKB.

This study provides strong scientific basis for the testing of available EGFR inhibitors, such as cetuximab and gefitinib, in patients with NETs. It also invites further research into the mechanisms underlying the observed effects of EGFR, particularly in NET tissue and NET cell-lines.

Chapter 3: In several cancers, EGFR is an important determinant of treatment response to anti-tumour therapy. Thus, it is imperative to understand how EGFR mediates these responses. There is evidence that ionising radiation-induced activation of EGFR increases tumour cell proliferation through the activation of the EGFR/RAS/mitogen-activated protein kinase/extracellular signal-regulated kinase kinase pathway (Reardon DB et al 1999, Suy S et al 1997), which is thought to result in rapid repopulation after radiation exposure (Withers HR et al 1988, Dent P et al 2003, Schmidt-Ullrich RK et al 1997). EGFR may also promote survival through the activation of the phosphatidylinositol 3-kinase and protein kinase B/AKT kinase (Contessa JN et al 2002, Toulany M et al 2005). A third mechanism implicates a direct role of EGFR as a mediator in the repair of IR-induced DNA damage. Recent evidence demonstrates ionising radiation induced rapid EGFR translocation to the nucleus and subsequent binding to both the catalytic and regulatory subunits of the DNA-dependent protein kinase (DNA-PK) (Dittmann K[b] et al 2005). DNA-PK is a critical component of the nonhomologous end-joining (NHEJ) repair pathway that plays a dominant role in repair of IR-induced DNA damage in higher eukaryotes. DNA-PK comprises three subunits, the 465-kDa catalytic subunit, DNA-PKcs, and two regulatory subunits, Ku70 (70-kDa) and Ku80 (80-kDa), which associate with XRCC4, DNA ligase IV, and Artemis at sites of double-strand breaks (DSB) to bring about the physical rejoining of DSB ends. Thus, EGFR interactions with DNA-PKcs seem crucial to the repair of DNA damage induced by DNA-damaging anti-tumour therapy.

EGFR/DNA-PKcs interactions are only partially understood in general and have not been studied in relation to neuroendocrine tumours.

Initial work on EGFR/DNA-PK$_{CS}$ interactions was carried out by Bandyopadhay et al who showed a direct interation between EGFR and DNA-PK$_{CS}$ upon EGFR inhibition with the anti-EGFR antibody 'cetuximab'. Further work performed by Friedmann et al confirmed increased associations between EGFR and DNA-PK$_{CS}$ upon EGFR inhibition with small-molecule tyrosine kinase inhibitor 'gefitinib'. EGFR inhibition

by gefitinib led to delayed repair of cisplatin and etoposide induced DNA damage. This was felt to be at least partly due to the sequestration of DNA-PK$_{CS}$ in the cytoplasm due to its direct binding to EGFR upon EGFR inhibition with gefitinib. Reduction in DNA-PK$_{CS}$ activity has also been noted in conjunction with EGFR inhibition. Other mechanisms likely to play a role in sensitising to DNA damaging therapy are the attenuation of signalling through the EGFR/RAS/mitogen-activated protein kinase and Akt pathways.

This chapter details work carried out to determine EGFR/DNA-PK$_{CS}$ interactions, and the effects of EGFR inhibition on these interactions, in NET cell-lines. Five cell lines with neuroendocrine features were used to assess the expression of EGFR and DNA-PK$_{CS,}$ direct EGFR/DNA-PK$_{CS}$ interactions and their modulation by EGFR inhibition, the effects of EGFR inhibition on DNA-PK$_{CS}$ sub-cellular localisation.

It was demonstrated that:

1. EGFR is expressed by all NET cell lines, though to various extent.
2. DNA-PK$_{CS}$ is expressed in very large quantities by all NET cell lines.
3. There are baseline EGFR/DNA-PK$_{CS}$ interactions seen in all cell lines, which can be increased by EGFR inhibition in NCI and BON cell lines.
4. EGFR inhibition with gefitinib led to redistribution of DNA-PK$_{CS}$ from the nucleus to the cytoplasm in SHP and BON cell lines.
5. EGFR inhibition led to a marked decrease in DNA-PK$_{CS}$ expression in all but the RIN cells.
6. No increase in EGFR/DNA-PK$_{CS}$ interactions was observed upon EGFR inhibition with cetuximab.

Thus it is apparent that EGFR inhibition has a role to play in NETs. This work has uncovered some of the mechanisms of EGFR/DNA-PK$_{CS}$ interactions and their modulation by EGFR inhibition. The work outlined in chapters 2 and 3 provides a strong scientific basis for the trial of EGFR inhibitors in NET patients. In view of the synergistic effects of EGFR inhibition with DNA-damaging therapy, as observed in-vitro as well as in-vivo, it makes sense to use EGFR inhibition in combination with a DNA-damaging agent.

A successful mode of DNA-damaging treatment given to NET patients is SSTR-targeted radiotherapy. However, its efficacy is limited by repopulation of tumour by radio-resistant cells. We postulate that combining EGFR inhibition with SSTR-

targeted radiotherapy will sensitise these tumours to radiotherapy treatment, leading to enhanced responses and hopefully prolonged survival in NET patients. For these reasons a phase II clinical trial of combined EGFR inhibitor therapy and SSTR-targeted radiotherapy is planned.

Further in-vitro work is also being performed in order to determine the effects of EGFR inhibition on irradiated NET cell-lines and to understand the various actions of EGFR on intra-cellular cell survival pathways, as well as its translocation within the cell and its interactions with DNA-PK$_{CS}$.

Chapter 4: Somatostatin is a peptide hormone which binds and acts through cell surface somatostatin receptors, of which there are 5 subtypes (SSTRs 1-5) (Chen C 1992, Buscail L et al 1994, Buscail L et al 1995, Liebmann C 2001). Majority of NETs express SSTRs, particularly SSTR 2 and 5, which can be utilised not only for tumour imaging but also for tumour targeted radiotherapy. ^{111}In-pentetreotide (OctreoScan®), based on a somatostatin analogue, binds to somatostatin receptor subtype 2 (SSTR2) with high affinity and is the most widely used as well as being the most sensitive scintigraphic agent for localisation and staging of NETs, with a reported sensitivity of 60-100% (De Herder WW et al 2005). However, not all NETs express SSTR2 while others may express it initially while becoming SSTR2 negative through the course of disease, either due to SSTR2 targeted radiotherapy or in conjunction with transformation of tumour grade from low to high. Unfortunately, the lack of SSTR2 expression not only lowers the sensitivity of somatostatin receptor scintigraphy, but since a strongly positive scan is a pre-requisite for SSTR-targeted radiotherapy it also deprives some patients of a valuable treatment modality.

This chapter provides evidence for the usefulness of ^{99m}Tc-depreotide, a scintigraphic agent with an expanded SSTR-subtype affinity, in improving the sensitivity of scintigraphic imaging. ^{99m}Tc-depreotide had previously been compared, head to head, with OctreoScan® and found to be less sensitive. We therefore opted to concentrate on patients with negative or weakly positive OctreoScan® and performed ^{99m}Tc-depreotide scans in this subgroup of NET patients.

It was discovered that:

1) OctreoScan® negativity correlated with increasing tumour grade.
2) 1/3rd of OctreoScan®-negative patients were significantly positive when imaged using ^{99m}Tc-depreotide.

This study demonstrates the feasibility of improving the sensitivity of SSTR-targeted scintigraphy using agents with an expanded spectrum of SSTR-subtype affinities. This not only improves NET diagnosis and staging but will lead to better treatment options for NET patients.

Chapter 5: Extensive use is made of a battery of tumour markers for diagnosis and follow-up in NET patients. However, the evidence to define the usefulness and role has been lacking for some of these markers, including for AFP and hCGβ. This chapter details the prognostic values of biochemical tumour markers AFP and hCGβ in neuroendocrine tumour patients. Data was extracted from the NET patient database and analysed to determine any relationships between these markers and clinically significant outcomes such as patient survival.

This study reveals AFP and hCGβ to be elevated in high-grade neuroendocrine tumours with a rapidly progressive course and poorer survival. They are also found to correlate with chromogranin-A, which is known to be a marker of tumour burden and to have prognostic value. Thus AFP and hCGβ are clinically important in NETs and should be routinely measured. They are also likely to be useful in helping to plan treatment and in determining prognosis.

In conclusion, NETs are rare cancers that are difficult to diagnose, prognosticate on or treat. Because of the rare nature of these tumours their pathophysiology is not well studied. Their relative chemo-resistance means that innovative methods of treatment have been applied in order to control symptoms and prolong survival. This research contributes significantly to diagnostic sensitivity, prognostic ability, and is likely to lead to improved treatment options in the mode of combined EGFR inhibition and targeted radiotherapy. Furthermore, it contributes to the better understanding of NET pathophysiology, through the discovery of activated EGFR signalling pathways, and contributes to a better understanding of the effects of EGFR inhibition on EGFR/DNA-PK$_{CS}$ interactions which are important in cellular repair and survival.

Abdelmohsen K, Gerber PA, von Montfort C, Sies H, Klotz LO. Epidermal growth factor receptor is a common mediator of quinone-induced signaling leading to phosphorylation of connexin-43: role of glutathione and tyrosine phosphatases. J Biol Chem 2003: 278; 38360-7. Epub 2003 Jul 21.

Ambrosini V, Tomassetti P, Rubello D, Campana D, Nanni C et. al. Role of 18F-dopa PET/CT imaging in the management of patients with 111In-pentetreotide negative GEP tumours. Nucl Med Commun. 2007 Jun;28(6):473-7

Ang KK, B.A. Berkey and X. Tu *et al.*, Impact of epidermal growth factor receptor expression on survival and pattern of relapse in patients with advanced head and neck carcinoma, *Cancer Res* **62** (2002) (24), pp. 7350–7356.

Ardill JE and Erikkson B. The importance of the measurement of circulating markers in patients with neuroendocrine tumours of the pancreas and gut. Endocrine-Related Cancer 2003*: **10**; 459-462

Arnold R[a]. Introduction: Definition, historical aspects, classification, staging, prognosis and therapeutic options Best Practice & Research Clinical Gastroenterology 2005:19; 491–505

Arnold R[b], Trautmann ME, Creutzfeldt W, Benning R et al. Somatostatin analogue octreotide and inhibition of tumour growth in metastatic endocrine gastroenteropancreatic tumours. Gut 1996; 38: 430 – 8.

Arnold R[c], Rinke A, Schmidt Ch, Hofbauer L. Chemotherapy 2005. Best Practice & Research Clinical Gastroenterology: 19; 649–656

Arteaga CL, Epidermal growth factor receptor dependence in human tumors: more than just expression? *Oncologist* **7** (2002) (Suppl. 4), pp. 31–39.

Bandyopadhyay D, Mandal M, Adam L et al. Physical Interaction between Epidermal Growth Factor Receptor and DNA-dependent Protein Kinase in Mammalian Cells THE JOURNAL OF BIOLOGICAL CHEMISTRY 1998: 273; 1568–1573.

Barker FG 2nd, Simmons ML, Chang SM et al. EGFR overexpression and radiation response in glioblastoma multiforme. Int J Radiat Oncol Biol Phys 2001: 51; 410-8.

Baselga J, Norton L, Masui H et al. Antitumor Effects of Doxorubicin in Combination With Anti-epidermal Growth Factor Receptor Monoclonal Antibodies. Journal of the National Cancer Institute 1993: 85; 1327-1333.

Baulida J, Kraus M. H, Alimandi M, Di Fiore PP & Carpenter G. All ErbB receptors other than the epidermal growth factor receptor are endocytosis impaired. J. Biol. Chem 1996: 271; 5251–5257.

Benali N, Ferjoux G, Puente E et al. Somatostatin receptors. Digestion 2000; 62(suppl 1): 27 – 32.

Benedetti F, Campori E, Colombo C, Smeraldi E. Fluvoxamine treatment of major depression associated with multiple sclerosis. J Neuropsychiatry Clin Neurosci. 2004 Summer;16(3):364-6.

Berset TA, Hoier EF & Hajnal A. The *C. elegans* homolog of the mammalian tumor suppressor Dep-1/Scc1 inhibits EGFR signaling to regulate binary cell fate decisions. Genes Dev 2005: 19; 1328–1340.

Bianco C, Tortora G, Bianco R, Caputo R, Veneziani BM, Caputo R, Damiano V, Troiani T, Fontanini G, Raben D, Pepe S, Bianco AR, Ciardiello F. Enhancement of antitumor activity of ionizing radiation by combined treatment with the selective epidermal growth factor receptor-tyrosine kinase inhibitor ZD1839 (Iressa). Clin Cancer Res. 2002; 8: 3250-8.

Bonner JA, Giralt J, Harari PM, Cohen R, Jones C, Sur RK, Rabin D, Azarnia N, Needle MN, Ang KK. Cetuximab prolongs survival in patients with locoregionally advanced squamous cell carcinoma of head and neck: A phase III study of high dose radiation therapy with or without cetuximab. J Clin Oncol 2004: 22(14S); 5507

Boskovic, J., Rivera-Calzada, A., Maman, J.D., Chaco´n, P., Willison, K.R., Pearl,   L.H., Llorca, O. Visualization of DNA-induced conformational changes in the   DNA   repair   kinase DNA-PKcs. The EMBO Journal.2003; 22, 5875-5882.

Brewerton, S.C., Dore, A.S., Drake, A.C.B., Leuther, K.K., Blundell, T.L. Structural analysis of DNA-PKcs: modelling of the repeat units and insights into the detailed molecular architecture. Journal of Structural Biology. 2004; 145: 295–306.

Buscail L, Delesque N, Esteve JP, Saint-Laurent N, Clerc P et al. Stimulation of tyrosine phosphatase and inhibition of proliferation by Somatostatin analogues: mediation by human ssTR1 and ssTR2. Proc Natl Acad Sci USA 1994; 91:2315 – 2319.

Buscail L[b], Esteve JP, Saint-Laurent N, Bertrand V, Reisine T et al. Inhibition of cell proliferation by the Somatostatin analogue RC-160 is mediated by Somatostatin receptor subtypes ssTR2 and ssTR5 through different mechanism. Proc Natl Acad Sci USA 1995; 92: 1580 – 1584.

Buscail L[c], Vernejoul F, Faure P, Torrisani J, Susini C. Regulation of cell proliferation by somatostatin. Ann Endocrinol (Paris) 2002; 63(2 Pt 3):2S13-8.

Campana D, Nori F, Piscitelli L, Morselli-Labate AM, Pezzilli R, Corinaldesi R, Tomassetti P. Chromogranin A. is it a useful marker of neuroendocrine tumors? J Clin Oncol 2007; **25**:1967-73.

Carter T, I Vancurová, I Sun, W Lou and S DeLeon. A DNA-activated protein kinase from HeLa cell nuclei. Mol Cell Biol. 1990; 10: 6460-6471

Chen C, Clarke IJ. Ion channels in the regulation of growth hormone secretion from somatotrophs by somatostatin.Growth Regul. 1992 Dec; 2(4):167-74.

Chiarugi P, Cirri P. Redox regulation of protein tyrosine phosphatases during receptor tyrosine kinase signal transduction. Trends Biochem Sci. 2003: 28; 509-14.

Chinnaiyan P, Huang S, Vallabhaneni G et al. Mechanisms of enhanced radiation response following epidermal growth factor receptor signaling inhibition by erlotinib (Tarceva). Cancer Res 2005: 65; 3328-35.

Citri A., Skaria K.B. and Yarden Y. The deaf and the dumb: the biology of ErbB-2 and ErbB-3. *Exp. Cell Res 200:* **284**; 54–65.

Citri A, and Yarden Y. EGF–ERBB signalling: towards the systems level
Nature Reviews Molecular Cell Biology 2006: 7; 505-516

Citri A *et al*. Drug-induced ubiquitylation and degradation of ErbB receptor tyrosine kinases: implications for cancer therapy. EMBO J 2002: 21; 2407–2417.

Clynes RA, Towers TL, Presta LG & Ravetch JV. Inhibitory Fc receptors modulate *in vivo* cytoxicity against tumor targets. Nature Med 2000: 6; 443–446.

Cochet C, Kashles O, Chambaz EM, Borrello I, King CR, Schlessinger J. Demonstration of epidermal growth factor receptor dimerization in living cells using a chemical covalent cross-linking agent. J Biol Chem 1988: 263; 3290 – 3295.

Cohen S. Isolation of a mouse submaxillary gland protein accelerating incisor eruption and eyelid opening in the newborn animal. J. Biol. Chem1960. **237**, pp. 1555–1562.

Collis SJ, DeWeese TL, Jeggo PA and Parker AR. The life and death of DNA-PK. Oncogene. 2005; 24: 949-961.

Contessa JN, Hampton J, Lammering G, et al. Ionizing radiation activates Erb-B receptor dependent Akt and p70 S6 kinase signaling in carcinoma cells. Oncogene 2002; 21: 4032–41.

Cunningham D, Humblet Y, Siena S, Khayat D, Bleiberg H, Santoro A, Bets D, Mueser M, Harstrick A, Verslype C, Chau I, Van Cutsem E. Cetuximab monotherapy and cetuximab plus irinotecan in irinotecan-refractory metastatic colorectal cancer. N Engl J Med. 2004; 351(4): 337-45

DeFazio LG, Stansel RM, Griffith JD, Chu G. Synapsis of DNA ends by DNA-   dependent protein kinase. EMBO J. 2002; 21: 3192-200.

De Herder WW, Kwekkeboom DJ, Valkema R, Feelders RA, van Aken MO, et al. Neuroendocrine tumors and somatostatin: imaging techniques**.** J Endocrinol Invest2005;28(11 Suppl):132-6.

Dent P, Yacoub A, Contessa J, Caron R et al. Stress and radiation-induced activation of multiple intracellular signaling pathways. Radiat Res 2003: 159; 283-300.

Dittmann K, Mayer C, Rodemann HP. Inhibition of radiation-induced EGFR nuclear import by C225 (Cetuximab) suppresses DNA-PK activity. Radiother Oncol. 2005: 76; 157-61.

Dittmann K[b], Mayer C, Fehrenbacher B, Schaller M, Raju U, Milas L, Chen DJ, Kehlbach R, Rodemann HP. Radiation-induced EGFR nuclear transport is linked to activation of DNA-dependent protein kinase. J Biol Chem. 2005 Jul 5; [Epub ahead of print]

Ekstrand A J, Sugawa N, James CD & Collins VP. Amplified and rearranged epidermal growth factor receptor genes in human glioblastomas reveal deletions of sequences encoding portions of the N- and/or C-terminal tails. Proc. Natl Acad. Sci. USA 1992: 89; 4309–4313.

Ekstrand AJ *et al*. Genes for epidermal growth factor receptor, transforming growth factor, and epidermal growth factor and their expression in human gliomas *in vivo*. Cancer Res 1991: 51; 2164–2172.

Engelman JA *et al*. ErbB-3 mediates phosphoinositide 3-kinase activity in gefitinib-sensitive non-small cell lung cancer cell lines. Proc. Natl Acad. Sci. 2005: USA 102; 3788–3793.

Eriksson B, Oberg K. An update of the medical treatment of malignant endocrine pancreatic tumours. Acta Oncol 1993; 32: 203 – 208.

Eriksson B, Oberg K, Skogseid B. Neuroendocrine pancreatic tumors. Clinical findings in a prospective study of 84 patients. Acta Oncol 1989. **28**: 373-7.

Espejel S, Martin M, Klatt P, Martin-Caballero J, Flores JM, Blasco MA. Shorter telomeres, accelerated ageing and increased lymphoma in DNA-PKcs-deficient mice. EMBO Rep. 2004; 5: 503-9.

Evans JS, Gerritsen GC, Mann KM et al. Antitumor and hyperglycemic activity of streptozocin (NSC-37917) and its cofactor, U-15 774. Cancer Chemother Rep 1965; 48: 1–6.

Falls D.L. Neuregulins: functions, forms, and signaling strategies. *Exp. Cell Res 2003:* **284**; 14–30.

Ford AC & Grandis JR. Targeting epidermal growth factor receptor in head and neck cancer. Head Neck 2003: 25; 67–73.

Friedman LM *et al*. Synergistic down-regulation of receptor tyrosine kinases by combinations of mAbs: implications for cancer immunotherapy. Proc. Natl Acad. Sci. USA 2005: 102; 1915–1920.

Friedmann B, Caplin M, Hartley JA, Hochhauser D. Modulation of DNA repair in-vitro after treatment with chemotherapeutic agents by the epidermal growth factor receptor gefitinib (ZD 1839). Clinical Cancer Research 2004: 10; 6476 – 6486.

Friedmann BJ, Caplin M, Savic B, Shah T, Lord CJ et al. Interaction of the epidermal growth factor receptor and the DNA-dependent protein kinase pathway following gefitinib treatment. Mol Cancer Ther. 2006: 5; 209-18.

Gibril F, Doppman JL, Jensen RT. Recent advances in the treatment of metastatic pancreatic endocrine tumours. Semin Gastrointest Dis 1995; 6: 114 – 21.

Gilbert JA, Lloyd RV, Ames MM. Lack of mutations in EGFR in Gastroenteropancreatic Neuroendocrine Tumours. N Eng J Med 2005: 353; 209-210

Giocanti N, Hennequin C, Rouillard D, Defrance R, Favaudon V. Additive interaction of gefitinib ('Iressa', ZD1839) and ionising radiation in human tumour cells in vitro. Br J Cancer. 2004; 91: 2026-33.

Goldie JH & Coldman AJ. A mathematic model for relating the drug sensitivity of tumors to their spontaneous mutation rate. Cancer Treat. Rep 1979: 63; 1727–1733.

Goldstein NS and M. Armin, Epidermal growth factor receptor immunohistochemical reactivity in patients with American Joint Committee on Cancer Stage IV colon adenocarcinoma: implications for a standardized scoring system, *Cancer* **92** (2001) (5), pp. 1331–1346.

Grandis JR, M.F. Melhem and E.L. Barnes *et al.*, Quantitative immunohistochemical analysis of transforming growth factor-alpha and epidermal growth factor receptor in patients with squamous cell carcinoma of the head and neck, *Cancer* **78** (1996), pp. 1284–1292

Groenen L.C., Nice, E.C. and Burgess A.W., 1994. Structure-function relationships for the EGF/TGF-alpha family of mitogens. *Growth Factors* 1994: **11**; 235–257.

Grossmann M, Trautmann ME, Poertl S, Hoermann R, Berger P, Arnold R, Mann K. Alpha-subunit and human chorionic gonadotropin-beta immunoreactivity in patients with malignant endocrine gastroenteropancreatic tumours.Eur J Clin Invest 1994. **24**: 131-6.

Guy P.M., Platko J.V. Cantley L.C., Cerione R.A. and Carraway III K.L.. Insect cell-expressed p180erbB3 possesses an impaired tyrosine kinase activity. *Proc. Natl. Acad. Sci. USA* 1991: **91;** 8132–8136.

Haimovitz-Friedman A, Vlodavsky I et al. Autocrine Effects of Fibroblast Growth Factor in Repair of Radiation Damage in Endothelial Cells. *Cancer Research* 1991: 51; 2552-2558.

Haj FG, Verveer PJ, Squire A, Neel BG & Bastiaens PI. Imaging sites of receptor dephosphorylation by PTP1B on the surface of the endoplasmic reticulum. Science 2002: 295; 1708–1711.

Harari PM and Huang SM. Clin. Cancer Res 2000: **6**; 323.

Harari PM and Huang SM. Int. J. Radiat. Oncol. Biol. Phys. 2001: **49**; p. 427.

Harari PM, Huang SM. Combining EGFR inhibitors with radiation or chemotherapy: will preclinical studies predict clinical results?Int J Radiat Oncol Biol Phys. 2004: 58; 976-83.

Harlow E, Lane D. Using Antibodies: A Laboratory Manual. 1999; Cold Spring Harbour Press, New York.

Harris R.C., Chung E. and Coffey R.J. EGF receptor ligands. *Exp. Cell Res 2003*. **284**, pp. 2–13.

Heitz PU, von Herbay G, Klöppel G, Komminoth P, Kasper M, Höfler H, Müller KM, Oberholzer M. The expression of subunits of human chorionic gonadotropin (hCG) by nontrophoblastic, nonendocrine, and endocrine tumors. Am J Clin Pathol 1987. **88**: 467-72.

Heldin CH. Dimerization of cell surface receptors in signal transduction. Cell 1995: 80; 213 – 225.

Hirai T *et al*. Clinical results of transhiatal esophagectomy for carcinoma of the lower thoracic esophagus according to biological markers. Dis. Esophagus 1998: 11; 221–225.

Hirono Y, Tsugawa K, Fushida S, Kaji M, Miwa K, Miyazaki I, Yamamoto H. Amplification of epidermal growth factor receptor gene and its relationship to survival in human gastric cancer. Oncology 1995: 52; 182 – 188.

Hoeijmakers JH. Genome maintenance mechanisms for preventing cancer. Nature. 2001; 411(6835): 366-74.

Hofsli E (2006). Genes involved in neuroendocrine tumor biology. Pituitary 2006; 9: 165-178

Holbro T., Civenni G. and Hynes N.E. The ErbB receptors and their role in cancer progression. *Exp. Cell Res 2003:* **284**; 99–110.

Höpfner M, Sutter AP, Gerst B, Zeitz M, Scherübl H. A novel approach in the treatment of neuroendocrine gastrointestinal tumours. Targeting the epidermal growth factor receptor by gefitinib (ZD1839). Br J Cancer 2003: 89; 1766-75.

Huang HS *et al*. The enhanced tumorigenic activity of a mutant epidermal growth factor receptor common in human cancers is mediated by threshold levels of constitutive tyrosine phosphorylation and unattenuated signaling. J. Biol. Chem. 1997: 272; 2927–2935.

Hunter A, Hendrikse A, Renan M, Abratt R. Does the tumor microenvironment influence radiation-induced apoptosis? Apoptosis (2006) 11:1727–1735

Hurley LH. DNA and its associated processes as targets for cancer therapy. Nature Reviews Cancer. 2002; 2, 188-200.

Iddon J, Bundred NJ, Hoyland J, Downey SE, Baird P, Salter D, McMahon R, Freemont AJ. Expression of parathyroid hormone-related protein and its receptor in bone metastases from prostate cancer. J Pathol. 2000: 191(2); 170 – 4

Igney FH and Krammer PH. Death and anti-death: Tumour resistance to apoptosis. Nat Rev Cancer. 2002; 2: 277-288.

Jackson SP, Jeggo PA. DNA double-strand break repair and V(D)J recombination: involvement of DNA-PK. Trends Biochem Sci. 1995 Oct;20(10):412-5.

Janson ET, Holmberg L, Stridsberg M, Eriksson B, Theodorsson E, Wilander E, Oberg K. Carcinoid tumors: Analysis of prognostic factors and survival in 301 patients from a referral center. Annals of Oncology 1997; **8**: 685-90.

Jensen RT & Doherty GM. Carcinoid tumors and the carcinoid syndrome. In Devita VT, Hellmann S & Rosenberg SA (eds.) Principles and Practice of Oncology, 6th edn. Philadelphia: Lippincott Williams & Wilkins, 2001.

Jonas S, John M, Boese-Landgraf J, Häring R, Prevost G, Thomas F et al. Somatostatin receptor subtypes in tumour cell lines and tumour tissue. Langenbecks Arch Chir 1995; 380: 90 – 95.

Kario E *et al*. Suppressors of cytokine signaling 4 and 5 regulate epidermal growth factor receptor signaling. J. Biol. Chem 2005: 280; 7038–7048.

Knebel A, Rahmsdorf HJ, Ullrich A, Herrlich P. Dephosphorylation of receptor tyrosine kinases as target of regulation by radiation, oxidants or alkylating agents. EMBO J 1996:15; 5314-25.

Lammering G, Hewit TH, Valerie K, Lin PS, Contessa JN, Schmidt-Ullrich RK. Anti-erbB receptor strategy as a gene therapeutic intervention to improve radiotherapy in malignant human tumours. Int J Radiat Biol. 2003: 79;561-8.

Lazarides E, Moon RT. Assembly and topogenesis of the spectrin-based membrane skeleton in the erythroid development. Cell 1984: 37; 354 – 356.

Lebtahi R, Le Cloirec J, Daou D, Sobhani I, Sassolas G et al. Detection of neuroendocrine tumors: 99mTc-P829 scintigraphy compared with 111In-pentetreotide scintigraphy. J NUcl Med 2002; 43: 889 – 895.

Lei W, Mayotte J, Levitt M. Enhancement of chemosensitivity and programmed cell death by tyrosine kinase inhibitors correlates with EGFR expression in non-small cell lung cancer cells. Anticancer Res 1999: 19; 221 – 228.

Lenferink AE et al. Differential endocytic routing of homo- and hetero-dimeric ErbB tyrosine kinases confers signaling superiority to receptor heterodimers. EMBO J 1998: 17; 3385–3397.

Lieber MR, Ma Y, Pannicke U, Schwarz K. Mechanism and regulation of human non-homologous DNA end-joining. Nat Rev Mol Cell Biol. 2003; 4: 712-20.

Liebmann C. Regulation of MAP kinase activity by peptide receptor signalling pathway: paradigms of multiplicity. Cellular Signalling 2001; 13: 777-785.

Liu L *et al*. Clinical significance of EGFR amplification and the aberrant EGFRvIII transcript in conventionally treated astrocytic gliomas. J. Mol. Med 2005: 83; 917–926.

Llorca O and Pearl LH. Electron microscopy studies on DNA recognition by DNA-PK. Micron. 2004; 35: 625-633.

Lokich JJ, Ganda OP, O'Hara CJ, Warren KW, Moertel CG, Klee G. Alpha-fetoprotein associated with islet cell tumors. Am J Clin Oncol 1987; **10**:133-5.

Lynch TJ *et al*. Activating mutations in the epidermal growth factor receptor underlying responsiveness of non-small-cell lung cancer to gefitinib. N. Engl. J. Med 2004: 350; 2129–2139.

Martensson, S., Hammarsten, O. DNA-dependent protein kinase catalytic subunit. Journal of Biological Chemistry. 2002; 277: 3020–3029.

John Mendelsohn, Zhen Fan. Epidermal Growth Factor Receptor Family and Chemosensitization. Journal of the National Cancer Institute 1997: 89; 341 – 343.

Modlin IM, Sandor A. an analysis of 8305 cases of carcinoid tumours. Cancer1997; 79: 813 – 829.

Moertel CG, Rubin J, Kvols LK. Therapy of metastatic carcinoid tumour and the malignant carcinoid syndrome with recombibant leukocyte A interferon. J Clin Oncol 1989: 865 – 868.

15. Moertel CG[b], Hanley JA & Johnson LA. Streptozocin alone compared with streptozocin plus fluorouracil in the treatment of advanced islet-cell carcinoma. N Engl J Med 1980; 303: 1189–1194.

Moertel CG[c], Lefkopoulo M, Lipsitz S et al. Streptozocin–doxorubicin, streptozocin–fluorouracil, or chlorozotocin in the treatment of advanced islet cell carcinoma. N Engl J Med 1992; 326(8): 519–523.

Moertel CG[d], Ribin J, O'Connell MJ & Rubin J. Phase II study of cisplatin therapy in patients with metastatic carcinoid tumor and the malignant carcinoid syndrome. Cancer Treat Rep 1986; 70: 1459–1460.

Nagane M, Lin H, Cavenee WK, Huang HJ. Aberrant receptor signaling in human malignant gliomas: mechanisms and therapeutic implications. *Cancer Lett* 2001*:* 162*;* Suppl:S17-S21.

Nagata Y *et al*. PTEN activation contributes to tumor inhibition by trastuzumab, and loss of PTEN predicts trastuzumab resistance in patients. Cancer Cell 2004: 6; 117–127.

Neckers L & Ivy SP. Heat shock protein 90. Curr. Opin. Oncol 2003: 15; 419–424.

Neskovic-Konstantinovic Z, D. Nikolic-Vukosavljevic and M. Brankovic-Magic *et al.*, Expression of epidermal growth factor receptor in breast cancer, from early stages to advanced disease, *J Exp Clin Cancer Res* **18** (1999), pp. 347–355.

Nicholson RI, Gee JM & Harper ME. EGFR and cancer prognosis. Eur. J. Cancer 2001: 37 (Suppl. 4), S9–S15.

Nilsson O, Kolby L, Wangberg B et al. Comparative studies on the expression of somatostatin receptor subtypes, outcome of octreotide scintigraphy and response to octreotide treatment in patients with carcinoid tumours. Br J Cancer 1998; 77(4): 632 – 7.

Norbury CJ and Zhivotovsky B. DNA damage-induced apoptosis. Oncogene. 2004;   23: 2797-2808.

Oberg K, Eriksson B. The role of interferons in the management of carcinoid tumours. Br J Haematol 1991; 79(suppl 1): 74 – 77.

Oberg K. The action of interferon on human carcinoid tumours. Semin Cancer Biol 1992; 3: 35 – 41.

Oberg K. Interferon in the management of neuroendocrine GEP-tumours. Digestion 2000; 62(suppl 1): 92 – 97.

Oberg K, Norheim I, Lundqvist G, Wide L. Cytotoxic treatment in patients with malignant carcinoid tumours: response to streptozocin – alone or in combination with 5-FU . Acta Oncol 1987; 26: 429 – 32.

Ohgaki H. Genetic pathways to glioblastomas. Neuropathology. 2005: 25; 1-7.

O'Toole D, Ruszniewski P. Chemoembolization and other ablative therapies for liver metastases of gastrointestinal endocrine tumours 2005. Best Practice & Research Clinical Gastroenterology: 19; 585–594

Paez JG *et al*. EGFR mutations in lung cancer: correlation with clinical response to gefitinib therapy. Science 2004: 304; 1497–1500.

Pao W. *et al*. EGF receptor gene mutations are common in lung cancers from 'never smokers' and are associated with sensitivity of tumors to gefitinib and erlotinib. Proc. Natl Acad. Sci 2004. USA 101, 13306–13311.

Papouchado B, LA Erickson, AL Rohlinger, TJ Hobday, C Erlichman, MM Ames and RV Lloyd. Epidermal growth factor receptor and activated epidermal growth factor receptor

expression in gastrointestinal carcinoids and pancreatic endocrine carcinomas. Modern Pathology 2005: **18;** 1329–1335.

Pazin MJ, Williams T. Triggering signal cascades by receptor tyrosine kinases. Trend Biochem Sci 1992: 17; 374 – 378.

Peghini PL, Iwamoto M, Raffeld M, Chen YJ, Goebel SU. Overexpression of epidermal growth factor receptor and hepatocyte growth factor receptors in a proportion of gastrinomas correlates with aggressive growth and lower curability. Clinical Cancer Research 2002: 8; 2273 – 2285.

Perry RR, Vinik AI. Clinical review 72. Diagnosis and management of functioning islet cell tumours. J Clin Endocrinol Metab 1995: 80: 2273 – 8.

Prise KM, Schettino G, Folkard M, Held KD. New insights on cell death from radiation exposure. Lancet Oncol. 2005 Jul;6; 520-8.

Quigley AM, Buscombe JR, Shah T, Gnanasegaran G, et al. Intertumoural variability in functional imaging within patients suffering from neuroendocrine tumours. An observational, cross-sectional study. Neuroendocrinology 2005; 82(3-4): 215-20.

Raben D, Bianco C, Damiano V et al. Antitumor activity of ZD6126, a novel vascular-targeting agent, is enhanced when combined with ZD1839, an epidermal growth factor receptor tyrosine kinase inhibitor, and potentiates the effects of radiation in a human non-small cell lung cancer xenograft model. Mol Cancer Ther 2004: 3; 977-83.

Rakieten N, Rakieten ML & Nadkarni MV. Studies on the diabetogenic action of streptozocin (NSC-37917). Cancer Chemother Rep 1963; 29: 91–98.

Ramage JK, Davies AH, Ardill J, Bax N, Caplin M, Grossman A, Hawkins R, McNicol AM, Reed N, Sutton R, Thakker R, Aylwin S, Breen D, Britton K, Buchanan K, Corrie P, Gillams A, Lewington V, McCance D, Meeran K, Watkinson A; UKNETwork for Neuroendocrine

Tumours. Guidelines for the management of gastroenteropancreatic neuroendocrine (including carcinoid) tumours. *Gut 2005*; **54**: iv1-iv16

Reardon DB, Contessa JN, Mikkelsen RB, et al. Dominant negative EGFR-CD533 and inhibition of MAPK modify JNK1 activation and enhance radiation toxicity of human mammary carcinoma cells. Oncogene 1999; 18: 4756–66.

Rebuzzini P, Lisa A, Giulotto E, Mondello C. Chromosomal end-to-end fusions in immortalized mouse embryonic fibroblasts deficient in the DNA-dependent protein kinase catalytic subunit. Cancer Lett. 2004; 203: 79-86.

Reeves WH, Wang J, Ajmani AK, Stojanov L, Satoh M. (1997) in *The Antibodies* (Zanetti, M., and Capra, J. D., eds), Vol. 3, pp. 33-84, Harwood Academy Publishers, Amsterdam, Netherlands

Reubi JC, Hacki WH, Lamberts SW. Hormone-producing gastrointestinal tumours contain a high density of somatostatin receptors. J Clin Endocrinol Metab 1987; 65: 1127 – 34.

Rindi G, Villanacci V, Ubiali A, Scarpa A. Endocrine tumours of the digestive tract and pancreas: histogenesis, diagnosis and molecular basis. Expert review mol diagn 2001; 1: 323 – 333.

Rindi G, Kloppel G, Alhman H, Caplin M, Couvelard A, et al. TNM staging of foregut (neuro)endocrine tumors: a consensus proposal including a grading system. Virchows Arch 2006 Oct; 449: 395 – 401.

Rindi G[b], de Herder WW, O'Toole D, Wiedenmann B (2206). Consensus Guidelines for the Management of Patients with Digestive Neuroendocrine Tumors: Why Such Guidelines and How We Went about It. Neuroendocrinology; **84**:155-157

Ross JS *et al*. The *Her-2/neu* gene and protein in breast cancer 2003: biomarker and target of therapy. Oncologist 2003: 8; 307–325.

Rusch V, Medelsohn J, Dmitrovsky E. The epidermal growth factor receptor and its ligands as therapeutic targets in human tumours. Cytokine Growth Factor Rev 1996: 7; 133 – 141.

Rusch VW, Klimstra DS, Venkatraman ES. Molecular markers help characterize neuroendocrine lung tumors. Ann Thorac Surg. 1996; 62(3): 798-809

Rusch V, D. Klimstra and E. Venkatraman *et al.*, Overexpression of the epidermal growth factor receptor and its ligand transforming growth factor alpha is frequent in resectable non-small cell lung cancer but does not predict tumor progression, *Clin Cancer Res* **3** (1997), pp. 515–522.

Shi W, Buchanan D, Johnson F et al. The octreotide suppression test and [111In-DTPA-D-Phel]-Octreotide scintigraphy in neuroendocrine tumours correlate with responsiveness to somatostatin analogue treatment. Clin Endocrinol 1998; 48: 303 – 9.

Saltz L, Trochanowski B, Buckley M et al. Octreotide as an anti-neoplastic agent in the treatment of functional and non-functional neuroendocrine tumours. Cancer 1993; 72: 244 – 8.

Schafer B, Gschwind A. & Ullrich A. Multiple G-protein-coupled receptor signals converge on the epidermal growth factor receptor to promote migration and invasion. Oncogene 2004: 23; 991–999.

Schlessinger J. Cell signaling by receptor tyrosine kinases. *Cell* 2000: **103**; 211–225

Schlessinger J. The epidermal growth factor receptor as a multifunctional allosteric protein. Biochemistry 1998: 27; 3119 – 3123.

Schlessinger J, Ullrich A. Growth factor signalling by receptor tyrosine kinases. Neuron 1992: 9; 383 – 391.

Schulze A, Lehmann K, Jefferies, HB, McMahon M & Downward J. Analysis of the transcriptional program induced by Raf in epithelial cells. Genes Dev 2001: 15; 981–994.

Schmidt-Ullrich RK, Dent P, Grant S, Mikkelsen RB, Valerie K. Signal transduction and cellular radiation responses. Radiat Res 2000: 153; 245-57.

Schmid HA, Schoeffter P. Functional activity of the multiligand analog SOM230 at human recombinant somatostatin receptor subtypes supports its usefulness in neuroendocrine tumors. Neuroendocrinology2004; 80 Suppl 1:47-50.

Schmidt-Ullrich RK, Mikkelsen RB, Dent P, et al. Radiation-induced proliferation of the human A431 squamous carcinoma cells is dependent on EGFR tyrosine phosphorylation. Oncogene 1997; 15: 1191–7.

Shah T, Hochhauser D, Frow R, Quaglia A, Dhillon AP, Caplin ME. Epidermal growth factor receptor expression and activation in neuroendocrine tumours. J Neuroendocrinol. 2006: 18; 355-60.

Shigematsu H *et al*. Somatic mutations of the HER2 kinase domain in lung adenocarcinomas. Cancer Res 2005: 65; 1642–1646.

Shintani S, Li C, Mihara M, Terakado N, Yano J, Nakashiro K, Hamakawa H. Enhancement of tumour radioresponce by combined treatment with gefitinib (iressa, ZD1839), an epidermal growth factor receptor tyrosine kinase inhibitor, is accompanied by inhibition of DNA damage repair and cell growth in oral cancer. Int J Cancer 2003: 107; 1030 – 1037.

Shou J et al. Mechanisms of tamoxifen resistance: increased estrogen receptor-HER2/neu cross-talk in ER/HER2-positive breast cancer. J. Natl Cancer Inst. 96, 926–935 (2004).

Shvartsman SY, Hagan MP, Yacoub A, Dent P, Wiley HS, Lauffenburger DA. Autocrine loops with positive feedback enable context-dependent cell signaling. Am J Physiol Cell Physiol 2002: 282; C545-59.

Singh AB, Harris RC. Autocrine, paracrine, and juxtacrine signalling by EGFR ligands. Cellular Signalling 2005: 17; 1183 – 1193

Slamon D J *et al*. Studies of the *HER-2/neu* proto-oncogene in human breast and ovarian cancer. Science 1989: 244; 707–712.

Slamon DJ *et al*. Use of chemotherapy plus a monoclonal antibody against HER2 for metastatic breast cancer that overexpresses HER2. N. Engl. J. Med 2001: 344; 783–792.

Smith GC, Jackson SP. The DNA-dependent protein kinase. Genes Dev. 1999; 13: 916-   34.

Solcia E, Kloppel G, Sobin LH et al. Histologic typing of endocrine tumours**.** WHO International Histological Classification of Tumours 2000**.** Heidelberg: Springer Verlag.

Song C, Perides G, Liu YF. Expression of full-length polyglutamine-expanded huntingtin disrupts growth factor receptor signalling in rat phaeochromocytoma (PC12 cells). The J Biol Chem 2002: 277; 6703 – 6707.

Solomon B, Hagekyriakou J, Trivett MK, Stacker SA, McArthur GA, Cullinane C.   EGFR blockade with ZD1839 ("Iressa") potentiates the antitumor effects of   single and multiple fractions of ionizing radiation in human A431 squamous cell carcinoma. Epidermal growth factor receptor. Int J Radiat Oncol Biol Phys.   2003; 55: 713-23.

Sordella R, Bell DW, Haber DA & Settleman J. Gefitinib-sensitizing EGFR mutations in lung cancer activate anti-apoptotic pathways. Science 2004: 305; 1163–1167.

Spear BT. Alpha-fetoprotein gene regulation: lessons from transgenic mice. Cancer Biology 1999: **9**; 109-116.

Spiridon CI *et al*. Targeting multiple Her-2 epitopes with monoclonal antibodies results in improved antigrowth activity of a human breast cancer cell line *in vitro* and *in vivo*. Clin. Cancer Res 2002: 8; 1720–1730.

Stenman U-H, Aila Tiitinen, Alfthan H and Valmu L. The classification, functions and clinical use of different isoforms of HCG. Human Reproduction Update 2006; **12**: 769-784.

Suy S, Anderson WB, Dent P, Chang E, Kasid U. Association of Grb2 with Sos and Ras with Raf-1 upon irradiation of breast cancer cells. Oncogene 1997; 15: 53–61.

Szumiel I. Epidermal growth factor receptor and DNA double strand break repair: The cell's self-defence. Cellular Signalling 2006: 18; 1537–1548

Taal BG, Visser O. Epidemiology of Neuroendocrine Tumours Neuroendocrinology 2004;80 (Suppl. 1):3-7)

Tateishi M, Ishida T, Mitsudomi T, Kaneko S & Sugimachi K. Immunohistochemical evidence of autocrine growth factors in adenocarcinoma of the human lung. Cancer Res 1990: 12; 1183–1188.

Teunissen JJM, Kwekkeboom DJ, de Jong M, Esser JP, Valkema R, Krenning EP Peptide receptor radionuclide therapy Best Practice & Research Clinical Gastroenterology 2005:19; 595–616

Thulin L, Samnegard H, Tyden G et al. Efficacy of somatostatin in a patient with carcinoid syndrome. Lancet 1978; 2: 43.

Toulany M, Dittmann K, Kruger M, Baumann M, Rodemann HP. Radioresistance of K-Ras mutated human tumor cells is mediated through EGFR-dependent activation of PI3K-AKT pathway. Radiother Oncol 2005; 76: 143–50.

Tracy S *et al*. Gefitinib induces apoptosis in the EGFRL858R non-small-cell lung cancer cell line H3255. Cancer Res 2004: 64; 7241–7244.

Turner GB, Johnston BT, McCance DR, McGinty A, Watson RG, Patterson CC, Ardill JE. Circulating markers of prognosis and response to treatment in patients with midgut carcinoid tumours. Gut 2006; **55**: 1586-91.

Ullrich A. and Schlessinger, J. Signal transduction by receptors with tyrosine kinase activity. *Cell* 1990: **61**; 203–212.

Ullrich A, Coussens L, Hayflick JS, Dull TJ, Gray A, Tam AW, Lee J, Yarden Y, Libermann TA, Schlessinger J, Downward J, Mayes ELV, Whittle N, Waterfield MD, Seeburg PH. Human epidermal growth factor receptor cDNA sequence and aberrant expression of the amplified gene in A431 epidermal carcinoma cells. Nature 1984: 309; 418 – 425.

Varva JJ, DeBoer C, Dietz A et al. Streptozocin, a new antibacterial antibiotic. Antibiot Annu 1959–60; 7:230–235.

Vinik1 AI, O'Dorisio TM, Woltering EA, Go VLW. A. Neuroendocrine Tumors: Comprehensive Guide to Diagnosis and Management. Interscience Institute

Virgolini I, Britton K, Buscombe J, Moncayo R, Paganelli G, Riva P. In- and Y-DOTA-lanreotide: results and implications of the MAURITIUS trial. Semin Nucl Med. 2002: 32: 148-55.

Weaver DT. What to do at an end: DNA double-strand-break repair. Trends Genet. 1995; 11:388-92.

Weidhaas JB, Eisenmann DM, Holub JM and Nallur SV. A Conserved RAS/Mitogen-Activated Protein Kinase Pathway Regulates DNA Damage-Induced Cell Death Postirradiation in Radelegans: Cell, Tumor, and Stem Cell Biology 2006.

Wiley HS. Trafficking of the ErbB receptors and its influence on signaling. Exp. Cell Res 2003: 284; 78–88.

Win Z, Al-Nahhas A, Rubello D, Gross MD. Somatostatin receptor PET imaging with Gallium-68 labeled peptides. Q J Nucl Med Mol Imaging. 2007 Sep;51(3):244-50.

Withers HR, Taylor JM, Maciejewski B. The hazard of accelerated tumor clonogen repopulation during radiotherapy. Acta Oncol 1988; 27: 131–46.

Worthylake R, Opresko LK & Wiley HS. ErbB-2 amplification inhibits down-regulation and induces constitutive activation of both ErbB-2 and epidermal growth factor receptors. J. Biol. Chem 1999: 274; 8865–8874.

Xia W *et al.* Anti-tumor activity of GW572016: a dual tyrosine kinase inhibitor blocks EGF activation of EGFR/erbB2 and downstream Erk1/2 and AKT pathways. Oncogene 2002: 21; 6255–6263.

Yarden Y. and Sliwkowski M.X. Untangling the erbB signalling network. *Nature Reviews (Mol. Cell. Biol 2001:* **2**; 127–137.

Ye D, Mendelsohn J & Fan Z. Augmentation of a humanized anti-HER2 mAb 4D5 induced growth inhibition by a human–mouse chimeric anti-EGF receptor mAb C225. Oncogene 1999: 18; 731–738.

Yuen MF, Lai CL. Serological markers of liver cancer. Best Pract Res Clin Gastroenterol 2005.**19**:91-9.

Zhou BB and Elledge SJ. The DNA damage response: putting checkpoints in   perspective. Nature 2000 408, 433–439.